

2012

## INFLAMMATORY INTERACTIONS AND SECRETION IN CARDIAC REMODELING

Fanmuyi Yang

University of Kentucky, [fyang3@uky.edu](mailto:fyang3@uky.edu)

[Right click to open a feedback form in a new tab to let us know how this document benefits you.](#)

### Recommended Citation

Yang, Fanmuyi, "INFLAMMATORY INTERACTIONS AND SECRETION IN CARDIAC REMODELING" (2012).  
*Theses and Dissertations--Physiology*. 4.  
[https://uknowledge.uky.edu/physiology\\_etds/4](https://uknowledge.uky.edu/physiology_etds/4)

This Doctoral Dissertation is brought to you for free and open access by the Physiology at UKnowledge. It has been accepted for inclusion in Theses and Dissertations--Physiology by an authorized administrator of UKnowledge. For more information, please contact [UKnowledge@lsv.uky.edu](mailto:UKnowledge@lsv.uky.edu).

## **STUDENT AGREEMENT:**

I represent that my thesis or dissertation and abstract are my original work. Proper attribution has been given to all outside sources. I understand that I am solely responsible for obtaining any needed copyright permissions. I have obtained and attached hereto needed written permission statements(s) from the owner(s) of each third-party copyrighted matter to be included in my work, allowing electronic distribution (if such use is not permitted by the fair use doctrine).

I hereby grant to The University of Kentucky and its agents the non-exclusive license to archive and make accessible my work in whole or in part in all forms of media, now or hereafter known. I agree that the document mentioned above may be made available immediately for worldwide access unless a preapproved embargo applies.

I retain all other ownership rights to the copyright of my work. I also retain the right to use in future works (such as articles or books) all or part of my work. I understand that I am free to register the copyright to my work.

## **REVIEW, APPROVAL AND ACCEPTANCE**

The document mentioned above has been reviewed and accepted by the student's advisor, on behalf of the advisory committee, and by the Director of Graduate Studies (DGS), on behalf of the program; we verify that this is the final, approved version of the student's dissertation including all changes required by the advisory committee. The undersigned agree to abide by the statements above.

Fanmuyi Yang, Student

Dr. Susan S. Smyth, Major Professor

Dr. Bret Smith, Director of Graduate Studies

INFLAMMATORY INTERACTIONS AND SECRETION  
IN CARDIAC REMODELING

---

DISSERTATION

---

A dissertation submitted in partial fulfillment  
of the requirements for the degree of Doctor of Philosophy in the  
College of Medicine  
at the University of Kentucky

By  
Fanmuyi Yang

Lexington, Kentucky

Co-Director: Dr. Susan S. Smyth, Professor of Internal Medicine  
and Dr. David Randall, Professor of Physiology

Lexington, Kentucky

2012

Copyright © Fanmuyi Yang 2012

## ABSTRACT OF DISSERTATION

### INFLAMMATORY INTERACTIONS AND SECRETION

#### IN CARDIAC REMODELING

Heart failure contributes to nearly 60,000 deaths per year in the USA and is often caused by hypertension and preceded by the development of left ventricular hypertrophy (LVH). LVH is usually accompanied by intensive interstitial and perivascular fibrosis which may contribute to arrhythmogenic sudden cardiac death. Emerging evidence indicates that LV dysfunction in patients and animal models of cardiac hypertrophy is closely associated with perivascular inflammation.

To investigate the role of perivascular inflammation in coronary artery remodeling and cardiac fibrosis during hypertrophic ventricular remodeling, we used a well-established mouse model of pressure-overload-induced LVH: transverse aortic constriction (TAC). Early perivascular inflammation was indicated by accumulation of macrophages and T lymphocytes 24 hours post-TAC and which peaked at day 7. Coronary luminal platelet deposition was observed along with macrophages and lymphocytes at day 3. Also, LV protein levels of VEGF and MCP-1 were significantly increased. Consistent with lymphocyte accumulation, cardiac expression of IL-10 mRNA was elevated. Furthermore, circulating platelet-leukocyte aggregates tended to be higher after TAC, compared to sham controls. Platelets have been shown to modulate perivascular inflammation and may facilitate leukocyte recruitment at sites of inflamed endothelium. Therefore, we investigated the impact of thrombocytopenia in the response to TAC. Immunodepletion of platelets decreased early perivascular accumulation of T lymphocytes and IL-10 mRNA expression, and altered subsequent coronary artery remodeling. The contribution of lymphocytes was examined in *Rag1*<sup>-/-</sup> mice, which displayed significantly more intimal hyperplasia and perivascular fibrosis compared to wild-type mice following TAC. Collectively, our studies support a role of early perivascular accumulation of platelets and T lymphocytes in pressure overload-induced inflammation which will contribute to long-term LV remodeling.

One potential mechanism for inflammatory cells to modulate their environment and affect surrounding cells is through release of cargo stored in granules. To determine the contribution of granule release from inflammatory cells in the development of LVH, we used *Unc13d*<sup>*Jinx*</sup> (*Jinx*) mice, which contain a single point mutation in *Unc13d* gene resulting in defects in Munc13-4. Munc13-4 is a limiting factor in vesicular priming and fusion during granule secretion. Therefore, *Jinx* mice have defects in degranulation of platelets, NK cells, cytotoxic T lymphocytes, neutrophils, mast and other cells. With the use of bone marrow transplantation, *Jinx* chimeric mice were created to determine whether the ability of hematopoietic cells to secrete granule contents affects the development of LVH. Wild-type mice (WT) that were transplanted with WT bone marrow (WT>WT) and WT mice that received *Jinx* bone marrow (*Jinx*>WT) developed

LVH and a classic fetal reprogramming response early after TAC (7 days), but at later times (5 weeks), Jinx>WT mice failed to sustain the cardiac hypertrophic response observed in WT>WT mice. No difference in cardiac fibrosis was observed at early or late times. Repetitive injection of WT platelets or platelet releasate restored cardiac hypertrophy in Jinx>WT mice. These results suggest that sustained LVH in the setting of pressure overload depends on factor(s) secreted, likely from platelets.

In conclusion, our studies demonstrate that platelets and lymphocytes are involved in early perivascular inflammation post-TAC, which may contribute to later remodeling in the setting of LVH. Factors released from hematopoietic cells, including platelets, in a Munc13-4-dependent manner are required to promote cardiac hypertrophy. These findings focus attention on modulating perivascular inflammation and targeting granule cargo release to prevent the development and consequences of LVH.

Fanmuyi Yang

August 30<sup>th</sup>, 2012

INFLAMMATORY INTERACTIONS AND SECRETION  
IN CARDIAC REMODELING

By  
Fanmuyi Yang

Dr. Susan S. Smyth  
Co-Director of Dissertation

Dr. David C. Randall  
Co-Director of Dissertation

Dr. Bret N. Smith  
Director of Graduate Studies

Date: August 30<sup>th</sup>, 2012

To my beloved mother Yu Fang, my father Jiemin Yang, my husband Yunjie Huang and my son Francis Letianyang Huang.

## ACKNOWLEDGEMENT

During the past 6 years of my Ph.D studies, I have had incredible help and support from many individuals whom I would like to thank and express my appreciation.

I would love to first express my appreciation to my mentor Dr. Susan Smyth for all her sincere help and guidance in my Ph.D study. She brought me into this field and helped me grow, enabling me to think and design experiments independently. She has shown her incredible patience with my work and is always there to offer support. Her intelligence and enthusiasm towards research has made her a fantastic role-model.

I would also love to thank all my committee members, Dr. Randall, Dr. Esser, Dr. Daugherty and Dr. Whiteheart, who help me in various aspects. Along the way, their comments and suggestions have been very helpful in my research progress and growing as a scientist.

In terms of cooperation, I really appreciate the great help of Dr. Anping Dong from the Smyth lab who has been performing the transverse aortic constriction surgery over the past years. My work could not be fulfilled without his technical support. I also thank him for training me on performing echocardiography and the Doppler measurement. I would like to express my appreciation to all the Smyth/Morris present lab members for their support, especially my sincere friends Liping Yang and Tao Wu, who consistently help me in work. I would also wish to thank the previous lab members Hsin, Lorenzo, Zachary for their friendship and help in work.

I am really indebted to our wonderful collaborators: Dr. Daugherty's lab (University of Kentucky, KY) for providing the assistance and facility on frozen IHC (immunohistochemistry), Dr. Whiteheart's lab (University of Kentucky, KY) for providing the Jinx mice and insight on data interpretation, Dr. Latif's lab (University of Kentucky, KY) for the help on cardiac fibroblast culturing, Dr. Li's lab (University of Kentucky, KY) for the assistance on platelet experiments and insight on experimental design, Dr. Morris' lab (University of Kentucky, KY) for the performance of lipid mass spectrometry, and Dr. Collier's lab (Rockefeller University, NY) for the help on TGF $\beta$ -1 measurement. I would also like to thank Matt Hazzard (University of Kentucky, TASC) for his contribution of artwork.

I would express my sincere appreciation to Yuri, Deepa, Travis and Megan for their intelligent comments and great help on proof-reading of my dissertation.

I am also indebted to all my friends for their friendship and support.



Finally, I would also like to thank my whole family, especially my mother Yu Fang, my father Jiemin Yang, my husband Yunjie and my son Francis who are always supporting and encouraging me with their great love, making me optimistic whenever. Above all, I would thank God for giving me a joyful life and walking with me through each and every day.

## TABLE OF CONTENTS

ACKNOWLEDGMENT.....	III
LIST OF TABLES.....	IX
LIST OF FIGURES.....	X
CHAPTER 1: INTRODUCTION.....	1
SECTION 1: Cardiac Hypertrophy and Perivascular Inflammation .....	1
Left Ventricular Hypertrophy (LVH) .....	1
Pathological Changes that Occur During Development of LVH.....	1
Myocardial Hypertrophy.....	2
Myocardial Fibrosis .....	3
Clinical Treatment for LVH .....	5
Perivascular Inflammation Contributes to Cardiac fibrosis .....	6
Role of Platelets in Vascular Inflammation.....	6
Pro .....	7
Anti.....	8
Platelet Function in Hypertensive Cardiac Diseases.....	9
Lymphocyte Function in cardiovascular Diseases .....	10
T Lymphocytes in Hypertension.....	10
Platelet-Lymphocyte Interaction in Vascular Inflammation.....	11
Transverse Aortic Constriction (TAC).....	12
SECTION 2: Platelet Granular Secretion.....	14
Exocytosis.....	14
Platelet Granule Components and Development.....	15
$\alpha$ -Granules.....	15
$\alpha$ -Granules Deficiency.....	15
Dense Granules .....	16

Dense Granule Deficiency .....	16
Lysosomes .....	17
The Key Step of Platelet Secretion: Membrane Fusion .....	21
Significance and Involvement of Lipid Components.....	21
Phosphatidic Acid (PA) .....	21
Phosphatidylinositol 4, 5-Bisphosphate (PIP2) .....	21
Soluble NSF Attachment Protein Receptor (SNARE) Complexes.....	22
Chaperone Proteins .....	24
Munc13-4 Dependent Granule Secretion and Jinx Mice.....	25
Potential Mediators from Platelets in Cardiac Hypertrophic Remodeling.....	27
Serotonin (5-hydroxytryptamine, 5-HT) .....	27
Transforming Growth Factor $\beta$ -1 (TGF $\beta$ -1) .....	29
Sphingosine 1-Phosphate (S1P) .....	31
SECTION 3: Summary .....	33

## CHAPTER 2: CORONARY ARTERY REMODELING IN A MODEL OF LEFT VENTRICULAR PRESSURE OVERLOAD IS INFLUENCED BY PLATELETS AND INFLAMMATORY CELLS .....

INTRODUCTION.....	34
MATERIALS AND METHODS .....	36
Animals.....	36
Transverse Aortic Constriction Model .....	36
Doppler Studies.....	36
Echocardiography .....	37
Histology .....	37
Quantitative PCR.....	39
Flow Cytometry.....	40
Whole Blood Aggregation.....	40

Mouse Plasma Collection.....	41
Mouse Cardiac Tissue Extraction .....	41
Luminex Assay.....	41
Culturing and Treatment of myocardial fibroblasts .....	41
Statistical Analysis.....	42
RESULTS.....	43
TAC is Accompanied by Early Pericoronary Inflammation .....	43
The Effect of Thrombocytopenia on TAC-Induced LV Remodeling .....	44
Absence of Lymphocytes Exaggerates Left Coronary Remodeling .....	47
IL-10 may Play a Protective Role in LV Remodeling.....	48
SUMMARY.....	64
 CHAPTER 3: PLATELET SECRETION CONTRIBUTES TO PRESSURE-OVERLOAD-INDUCED LEFT VENTRICULAR HYPERTROPHY (LVH) .....	 65
INTRODUCTION .....	65
MATERIALS AND METHODS.....	68
Mice .....	68
Bone Marrow Transplantation.....	68
Transverse Aortic Constriction (TAC).....	68
Washed Platelet Preparation.....	68
Platelet Aggregation .....	69
Platelet Releasate .....	69
Lipid Extraction and S1P Determinations .....	69
Statistical Analysis.....	70
RESULTS.....	71
Lack of Munc13-4 does not Alter Early Response to Pressure Overload .....	71

Attenuated Cardiac Hypertrophy 5 Weeks after TAC in Mice with Defects in Granule Cargo Release from Hematopoietic Cells .....	72
Platelet and Platelet Releasate Partially Restores Cardiac Hypertrophy after TAC in Mice Lacking Munc13-4 in Hematopoietic Cells.....	73
SUMMARY .....	90
CHAPTER 4: DISCUSSION AND FUTURE DIRECTIONS.....	91
SECTION 1 .....	91
TAC Model.....	91
Suprarenal Abdominal Constriction (AC).....	91
Shear-Stress and Perivascular Inflammation.....	92
Coronary Flow Regulation.....	93
Platelets and Leukocyte Interaction .....	94
Induced-Thrombocytopenia .....	94
The Role of T lymphocytes in Cardiac Remodeling.....	95
The Role of IL-10 in TAC .....	96
SECTION 2 .....	99
Cardiac Endogenous Negative Regulators of Hypertrophy .....	99
Platelet-Derived Potential Mediators of Cardiac Hypertrophy .....	100
Reprogramming of Fetal Genes .....	101
Future Directions .....	102
BIBLIOGRAPHY .....	105
VITA.....	133

## LIST OF TABLES

Table 2.1 Organ and body weight in WT and Rag1 <sup>-/-</sup> mice five weeks after TAC or sham surgery .....	50
Table 2.2 Echocardiographic analysis of heart size and function in WT and Rag1 <sup>-/-</sup> mice five weeks after TAC or sham surgery.....	51
Table 3.1 Echocardiography parameters in before surgery.....	76
Table 3.2 Complete blood count (CBC) 7-day after surgery .....	77
Table 3.3 Complete blood count (CBC) data of chimeric mice 5-week after surgery.....	78
Table 3.4 WT mice with Jinx marrow are partially protected from LVH at five weeks after TAC .....	79
Table 3.5 Plasma TGF $\beta$ -1 in chimeric mice .....	80

## LIST OF FIGURES

Figure 2.1 TAC-induced LV pressure overload stimulates left coronary remodeling and dysfunction in wild-type C57BL/6 male mice .....	52
Figure 2.2 TAC elicits an early inflammatory response in wild-type (C57BL/6) male mice... ..	54
Figure 2.3 Endothelial disruption at three and seven days after TAC surgery .....	56
Figure 2.4 Upregulation of inflammatory markers after TAC in wild-type mice .....	57
Figure 2.5 Platelet accumulation and effects on perivascular inflammation .....	58
Figure 2.5 Thrombocytopenia promotes coronary vessel remodeling and perivascular fibrosis after TAC .....	59
Figure 2.7 The effects of platelet releasate on myocardial fibroblasts .....	60
Figure 2.8 Enhanced TAC-induced coronary remodeling in the absence of lymphocytes.... ..	61
Figure 2.9 TAC-induced coronary remodeling in the absence of IL-10 .....	62
Figure 2.10 Model of TAC-induced early inflammatory responses in which platelets and inflammatory cells are recruited and contribute to the subsequent development of intimal hyperplasia and fibrosis .....	63
Figure 3.1 Lack of Munc13-4 in irradiated B6 WT mice reconstituted with Jinx marrow cells .....	81
Figure 3.2 TAC-induced cardiac hypertrophy and perivascular inflammation 7 days after surgery .....	82
Figure 3.3 Jinx chimeric mice are protected from cardiac hypertrophy 5 weeks after TAC . .....	84
Figure 3.4 Cardiac fibrosis 5 weeks after TAC .....	86
Figure 3.5 TGF- $\beta$ 1 plasma and serum levels in Jinx and B6 WT mice .....	87
Figure 3.6 Plasma S1P levels in 7 days after TAC .....	88
Figure 3.7 TGF $\beta$ -1 signaling 7 days after TAC .....	89

## **CHAPTER 1: INTRODUCTION**

### **SECTION 1: Cardiac Hypertrophy and Perivascular Inflammation**

**Left Ventricular Hypertrophy (LVH):** LVH is a compensatory mechanism for the heart to work more effectively when greater workloads are required in the setting of mechanical or oxidized stress, overactive sympathetic drive, or as a consequence of genetic abnormalities. Physiological LVH can happen in the short-term during pregnancy and exercise, and is reversible when the physical demands disappear [1]. In the presence of pathological signals, compensatory increase of cardiomyocyte size and number cannot preserve cardiac contractility persistently and might proceed to dilated hypertrophy [2,3]. The latter impaired contractility and chamber dilation might be due to other remodeling (i.e.. Imbalance of extracellular matrix (ECM) turnover and fibrosis formation) and myocyte apoptosis. LVH can also be influenced by other factors, such as age and gender [4].

The major cause of LVH is systemic hypertension and application of anti-hypertensive medication may reverse LVH and improve the clinical outcomes [3-6]. Nearly one-third of American adults have hypertension, of which 20% – 60% will develop LVH and may progress to heart failure. Heart failure contributes to nearly 60,000 deaths per year in the USA. Given that LVH is a strong risk factor of heart failure and an independent predictor of cardiovascular death [7,8], a better understanding of the underlying mechanisms is needed for prevention and treatment.

#### **Pathological Changes that Occur During Development of LVH**



**Myocardial Hypertrophy** Myocardial hypertrophy is described as the increase of the cardiomyocyte size and number in response to stresses, such as the increase of intracavitary pressure and mechanical stretch. Typically, LVH has two subtypes: concentric hypertrophy and eccentric hypertrophy. Concentric hypertrophy is usually induced by pressure-overload and is characterized by significant increase of LV wall thickness and force generation, and impaired filling state due to stiffness (diastolic dysfunction). Eccentric hypertrophy is mainly caused by volume-overload and is characterized by moderate increase of wall thickness with impressive chamber dilation (systolic dysfunction). In the compensated state, an increase in diameter of cardiomyocytes and number of sarcomeres in parallel elevates the contractile force generated per cell to meet the required cardiac output. However, the compensatory increase of cardiac output cannot last indefinitely and will gradually precede to life-threatening cardiac episodes, such as myocardial infarction (MI), arrhythmia, and heart failure. The decompensation could be due to (1) inadequate oxygen and nutrition supply (2) reduced myocardial capillary density, (3) reduced space for coronary artery vasodilatation and (4) capillary compression, which together contribute to myocardial ischemia and make the hypertrophic cardiomyocytes more vulnerable [9,10]. Also, cardiomyocytes add in series in the decompensated state which contributes to chamber dilation, reduced myocyte contractility and cardiac output. The molecular mechanisms of cardiac hypertrophy have been widely studied in the context of membrane-bound receptor activation in response to mechanical stress, oxidative stress, and other neurohormonal factors. The resulting downstream signaling will induce myocardial re-expression of a fetal gene program (i.e. atrial natriuretic peptide, brain natriuretic peptide,  $\beta$ -myosin heavy chain and  $\alpha$ -skeletal muscle actin) and abnormal increase in synthesis of myocardial proteins, which will

ultimately leads to pathological growth and proliferation of cardiomyocytes [5,11].

**Myocardial Fibrosis:** Apart from myocardial hypertrophy, hypertensive LV remodeling is also associated with a disproportionate contribution of cardiac fibroblasts. Under normal conditions, cardiac fibroblasts secrete the major components of the extracellular matrix (ECM), such as collagen, elastin, fibronectin, vitronectin, laminin and proteoglycan which together contribute to the microenvironment favorable to cardiomyocytes. However, in the setting of pressure overload, enhanced angiotensin II signaling by mechanical stretch increases the production of TGF $\beta$ -1 in cardiac fibroblasts which contributes to the cardiac remodeling [12]. TGF $\beta$ -1 can upregulate the function of fibroblasts through autocrine signaling which leads to enlarged fibroblast population and increased deposition of ECM components [12]. TGF $\beta$ -1 can also upregulate the expression of cardiomyocyte  $\beta$ -adrenergic receptors through paracrine signaling and result in myocyte hypertrophy [12]. Likewise, TGF $\beta$ -1 derived from cardiomyocytes modulates functions of both myocytes and cardiac fibroblasts [12]. The importance of such regulation is evident during cardiac hypertrophic remodeling, since dysfunction of cardiac fibroblasts leads to excessive production of fibrillar collagen [13,14]. In addition, maladaptive collagen turnover contributes to inappropriate collagen deposition. Collagen turnover is mainly regulated by matrix metalloproteinases (MMPs) and their inhibitors – tissue inhibitors of metalloproteinases (TIMPs) in ECM [14]. Studies have emphasized the significance of the abnormal transition from cardiac fibroblasts to myofibroblasts, the major contributors to cardiac fibrotic remodeling, in hypertensive cardiac diseases. Myofibroblasts have been shown to play an important role in arrhythmogenic remodeling by (1) generating more fibrotic ECM which separates muscle bundles, reduces gap junctional coupling between cardiomyocytes

and impairs electrical uniform conduction; and (2) forming gap junctional coupling to cardiomyocytes which induces slow conduction and abnormal automaticity [13]. Myofibroblasts also generate extracellular matrix (ECM) with an imbalanced composition of MMPs and their inhibitors which promotes fibrosis formation [14]. Until recently, cardiac fibrosis was thought to occur as a secondary response to systemic changes in the renin - angiotensin II - aldosterone system (RAAS). It is also thought to be the response to primary changes in cardiomyocytes by mechanical stretch or local release of growth or inflammatory factors, such as transforming growth factor  $\beta$ -1 (TGF $\beta$ -1), endothelin-1 (ET-1), tissue necrosis factor- $\alpha$  (TNF- $\alpha$ ), etc. [6,14,15]. Two patterns of fibrosis formation have been revealed in hypertensive hearts: reactive fibrosis and reparative fibrosis [15]. Reactive fibrosis refers to the initial accumulation of collagen I and III in the pericoronary areas which subsequently extends to interstitial spaces [15]. The impaired diffusion of oxygen and nutrients, which is caused by reactive fibrosis, results in cardiomyocyte apoptosis or necrosis, and consequently leads to reparative fibrosis [15]. Extensive interstitial fibrosis formation leads to increase of ventricular stiffness, which impairs normal LV diastolic function and results in inadequate filling [16-18]. Over time, the hypertrophic heart progresses to LV failure (congestive heart failure; CHF), characterized by ventricular dilation, decreased contractile force, pulmonary congestion, and an increase of cardiomyocyte length-to-width ratio. Cardiac interstitial fibrosis not only diminishes LV elasticity and contractility, but also limits oxygen diffusion and increases oxidative stress which has been recognized as a crucial factor for LV dysfunction [15]. Taking the advantage of delayed hyper-enhancement magnetic resonance imaging, recent clinical studies have found a strong correlation between potentially fatal ventricular arrhythmias and

myocardial fibrosis in patients with hypertrophic cardiomyopathy [19]. In addition to interstitial fibrosis, cardiac perivascular fibrosis occurs in the setting of LVH and congestive heart failure, which impairs the vasodilation function of coronary arteries, causing increased susceptibility to myocardial hypoperfusion and ischemia [20-25].

**Clinical Treatment for LVH** Hypertension is the major contributor to LVH, so reducing blood pressure by diuretic medication (i.e. indapamide, HCTZ) and vascular smooth muscle cell relaxers ( $\alpha$ -blockers, i.e. prazosin, doxazosin) is commonly seen in hypertensive patients. The RAAS system is considered to be critical in regulating blood pressure. In addition, the RAAS system can lead to myocyte hypertrophy and cardiac fibrosis in LVH. Thus, the medication targeting renin (i.e. aliskiren), angiotensin II converting enzyme (i.e. perindopril, enalapril), aldosterone (i.e. eplerenone) and angiotensin II receptors (i.e. losartan) are also applied in clinical treatments. Activation of the  $\beta_1$ -adrenergic receptors contributes to enhanced myocyte contraction and increased conduction velocity in the heart. It also increases the renin production in the kidney. Therefore,  $\beta_1$ -blockers (i.e. atenolol) are also common treatments of LVH. Also, calcium channel blockers (i.e. nifedipine) are used to reduce myocyte contractility in heart. In practical conditions, inhibitors of RAAS system or  $\beta_1$ -blockers are usually combined with diuretic drugs to be more effective in regression of LVH. Recently, targeting other signaling pathways (i.e. MAPK pathways, JAK-STAT Pathways, TGF $\beta$  signaling, oxidant signaling), which have been shown important in progression of LVH, has been more extensively explored in terms of the side effects of the traditional treatments.

**Perivascular Inflammation Contributes to Cardiac fibrosis** LVH is also associated with inflammatory changes in the peripheral blood and myocardium, which have been proposed to influence myocardial fibrosis. Inflammatory cells have been considered indispensable in hypertension, which is the major trigger of LVH [26]. Inflammatory cells, especially macrophages, have been shown to accumulate in the organs involved in hypertension, in particular the kidney [26]. Hypertension was ameliorated in both patients and animal models with inhibition of T lymphocytes [26]. Other hypertensive triggers, such as neurohormonal factors, can also enhance the pro-fibrotic effect of the immune system. Studies have shown that inhibition of inflammatory responses may attenuate cardiac fibrosis [17,18,27-29]. In DOCA/salt-induced hypertensive rats, pharmacologically targeting monocyte/macrophage accumulation attenuated cardiac perivascular and interstitial fibrosis and reduced expression of inflammatory markers, such as interleukin 6 (IL-6) and monocyte chemoattractant protein-1 (MCP-1) [27,30]. In a rat model of suprarenal aortic constriction, antibody blockade of either intercellular adhesion molecule - 1 (ICAM-1) or MCP-1 reduced early macrophage recruitment as well as later myocardial fibrosis [17,28]. Moreover it has been shown that LV remodeling after myocardial ischemia in rats is attenuated by reducing inflammation-induced cardiac fibrosis using a P38 mitogen-activated protein kinase (MAPK) inhibitor [31]. However, the triggers responsible for initiation of perivascular inflammation in the setting of LVH are poorly understood.

**Role of Platelets in Vascular Inflammation** Platelets are small anucleated cytoplasmic bodies in circulation which are generated by megakaryocytes in bone marrow. In settings of vascular

injury, platelets adhere to the exposed subendothelial matrix via GPIb – vWF and GPVI – collagen interaction which are substituted later by integrins [32]. Subsequent platelet activation maintains hemostasis through platelet-platelet interactions ( $\alpha_{IIb}\beta_3$  – fibrinogen), which contribute to the primary platelet clot. In addition to their essential role in hemostasis, platelets are important mediators of vascular inflammation in a variety of settings [33-40]. Activated platelets express and release granule contents. Stimulated platelets deposit and adhere to inflamed endothelium through activation-dependent surface expression of adhesive molecules, such as P-selectin, serving to recruit and interact with leukocytes. Inflammatory mediators released by platelets, such as IL-8, PF4, RANTES, TNF $\alpha$ , CD40L, may recruit and modulate leukocyte responses at sites of vascular inflammation or injury [32,35,37,41-43]. Studies have also shown that instead of their individual effect, interaction between platelet-derived cytokines( i.e. platelet factor 4 (PF4) and RANTES) may facilitate leukocyte recruitment and adhesion to the inflamed endothelium [44]. The same group reported later that blocking the interaction between PF4 and RANTES reduced the size of atherosclerosis lesion [45].

Due to the complicated platelet function as well as interactions between platelets and leukocytes, it has been debated for a long time and is still not quite clear whether platelets play a pro- or anti-inflammatory role in vascular diseases.

**Pro:** Initially it was believed that platelets promoted inflammation since their activation and upregulation of platelet-induced cytokines were observed in cardiac hypertrophy and heart failure [46,47]. Platelets were also activated during myocardial ischemic reperfusion, contributing to the neutrophil recruitment and myocardial infarction in a P-selectin

dependent manner [48]. Platelet-derived P-selectin has been shown to be important for intimal hyperplasia in a mouse model of carotid artery injury [49]. Using an experimental arthritis mouse model, Cloutier et al discovered that platelets can enhance vascular permeability by promoting formation of endothelial gaps, possibly through their serotonin secretion [50]. Specific inhibition of platelet activation or knockout of platelet serotonin has been shown to decrease bleomycin-induced tissue fibrosis [51]. Furthermore, platelet depletion by neuraminidase or inhibition by clopidogrel benefited the mice which were suffering from acute hemolysis-associated fatal pulmonary arterial hypertension (PAH) [52]. In another animal model of autoimmune encephalomyelitis, platelet depletion by GPIIb/IIIa antibody reduced leukocyte recruitment, local inflammation and the CNS lesion [53]. In the clinical studies, application of anti-thrombotic therapy, such as clopidogrel (P<sub>2</sub>Y<sub>12</sub> receptor inhibitor), is suggested to decrease the mortality due to heart failure or acute myocardial infarction [54,55]. Cilostazol is a phosphodiesterase 3 (PDE3) inhibitor and inhibits platelet aggregation by upregulating cAMP-mediated PKA activation. Serving as an alternative anti-platelet therapy, application of cilostazol has been shown to decrease the restenosis after percutaneous transluminal coronary angioplasty (PTCA) [56]. A cohort study also showed that anti-platelet therapy could reduce the probability of acute lung injury (ALI) [57].

**Anti:** Denisa Wagner's group has recently shown that in inflammatory diseases, including tumors, platelets and their secretion are critical for maintenance of vascular integrity, loss of which tends to cause severe hemorrhage [58,59]. The benefits of platelet gel for endogenous myocardial repair and preserved cardiac function in a myocardial infarction

model have also been reported by Cheng et al [60]. In terms of more complicated roles of platelets in different settings of vascular inflammation, anti – platelet therapy should be carefully applied with consideration of the potential adverse effects on cardiac function and more efforts should be put to elucidate the underlying mechanisms of the role of platelets in cardiac diseases.

**Platelet Function in Hypertensive Cardiac Diseases** Forty-five years ago, scientists first discovered that platelet adhesion to vessel wall was dramatically increased in hypertensive cardiac diseases [61]. Indices of Platelet activation, such as mean platelet volume (MPV), platelet mass, P-selectin per platelet (pP-sel), soluble P-selectin (sP-sel), lower platelet granularity, are upregulated in hypertensive patients [62]. Even for prehypertension patients, mean platelet volume (MPV), an indicator of platelet activation, is significantly increased [63,64]. Mechanisms of pathological platelet activation in hypertensive diseases include (1) upregulation in sympathetic nerve system (SNS) and renin-angiotensin-aldosterone system (RAAS) activity which contribute to enhanced platelet aggregation; (2) damaged or inflamed endothelium and therefore decreased nitric oxide (NO) which promotes platelet adhesion and aggregation; (3) decreased platelet-derived NO which causes increase in circulating levels of monocyte-platelet aggregates (MPAs); (4) increased shear stress which triggers platelet secretion and activation [65]. Interestingly, reducing blood pressure by anti-hypertensive medication – quinapril ( angiotensin-converting enzyme (ACE) inhibitor) and/or nifedipine ( calcium-channel blockers) could significantly inhibit platelet hyperactivity [66]. Furthermore, combination of angiotensin II receptor antagonist (losartan) and anti-dyslipidemia medication



(simvastatin) reduced platelet activation in patients with hypertension, hyperlipidemia and diabetes [67]. Recently, anti-platelet therapies, such as aspirin, clopidogrel and cilostazol, have been shown to reduce the risk of cardiovascular events and improve the outcome of patients with hypertension [65] [68].

**Lymphocyte Function in Cardiovascular Diseases** As inflammatory cells, lymphocytes have been shown to be involved in cardiovascular diseases in animal models. In mice with carotid collar injury, intimal hyperplasia is positively correlated with increased number of CD1d-restricted natural killer T lymphocytes in spleen and peri-carotid adventitia [69]. T lymphocytes also regulate cardiac diastolic function and contribute to hypertension-related cardiac ECM fibrotic remodeling by regulating collagen production and MMPs activity [70,71]. On the other hand, different lymphocyte subsets and lymphocyte signaling might play a protective role in cardiac pathological development [72-77]. For instance, injection of CD4<sup>+</sup>CD25<sup>+</sup> regulatory T cells (Tregs) attenuated Angiotensin II-induced cardiac hypertrophic and fibrotic responses, and maintained the normal distribution of gap junctions [74]. Furthermore, adoptive transfer of B cells to Rag1<sup>-/-</sup> mice decreased intimal hyperplasia in carotid artery in response to periadventitial cuff injury [78]. Furthermore, lymphocyte antigens (DR3 and DR4) are detected in patients suffering from systemic sclerosis and rheumatoid arthritis coexistent with cardiac hypertrophy [79,80].

**T Lymphocytes in Hypertension** Lymphocytes, especially T cells, are important in regulating blood pressure and contributing to hypertensive cardiac remodeling. David Harrison's group

reported in 2007 that angiotensin II and DOCA-salt-induced hypertension were significantly attenuated in Rag1<sup>-/-</sup> mice which are deficient of T and B lymphocytes. Interestingly, T lymphocyte transfer completely restored the hypertension and vascular dysfunction which was hypothesized to be mediated by TNF- $\alpha$  [81]. Apart from responding to exogenous Angiotensin II, T lymphocytes can produce Angiotensin II endogenously which modulates their function in hypertension [82]. Central nervous system (CNS) has also been shown to independently influence Angiotensin II-induced hypertension and T lymphocyte activation [83]. The contribution of lymphocytes to Angiotensin II-induced hypertension was confirmed by another group using a SCID mouse model [84].

**Platelet-Lymphocyte Interaction in Vascular Inflammation** Activated platelets stick to the vascular wall to facilitate lymphocyte tethering, rolling and adhering to inflamed endothelium or exposed subendothelial matrix. This is first initiated mainly through P-selectin (platelet) – PSGL-1 (lymphocyte) interaction and is substituted by integrins for later firm adhesion [85]. Platelet-lymphocyte conjunction through P-selectin – PSGL-1 interaction will also promote lymphocyte recruitment to sites of vascular inflammation in animal models [86,87]. Secreted or surface-expressed cytokines from platelets, such as platelet factor 4 (PF4) and CD154, have been shown to regulate T lymphocyte function [85]. Using a CD40 ligand (CD40L) deficient mouse model, platelet-derived CD40Ls have been shown to play an important role in production and maturation of IgG in B lymphocytes [85,88,89]. Another study suggested that CD40Ls on platelet-derived micro vesicles (PDMVs) might be the biologically active form [88]. Platelet-derived CD40Ls are also shown to mediate transfusion-induced inflammatory responses, such as [90]. On the other hand, lymphocytes influence platelet function through

direct interaction or secreted contents. Platelet deposition observed in ischemia/reperfusion was significantly reduced in mice deficient of T cells and was recovered in mice reconstituted with WT splenocytes [91]. T cell-derived CD40L contributes to platelet activation thereby causing platelets to secrete RANTES which further aids in T-cell recruitment and activation [92]. In addition, T cells can regulate platelet cytotoxicity through antibodies (IgE and IgG) or cytokines (IFN- $\gamma$ , TNF- $\alpha$ ) [85].

**Transverse Aortic Constriction (TAC)** is an established model to study pressure-overload-induced cardiac remodeling, in which a constriction of the lumen is formed by suture of the aortic arch between the right and left carotid arteries (Figure 10). TAC creates a pressure-difference across the constricted jet, which mimics the similar effect caused by hypertension or aortic stenosis in patients. It has been suggested that after TAC the LV function is impaired abruptly (within 1 day), but gradually returns to a normal level (around day 10) which will last for a while before the onset of decompensation and heart failure [93]. TAC induces LV remodeling, including myocardial hypertrophy and fibrosis. Studies also show that TAC-induced LV remodeling could be reversed by removing the constriction 2 weeks after TAC [94]. Our data corroborates that of the Hartley group which suggests a reduction of coronary flow reserve (CFR) following TAC [95-97], indicating coronary artery dysfunction. We previously reported that pressure overload in mice created by TAC is associated with a marked perivascular inflammation, reactive myocardial fibrosis, and medial thickening of intramyocardial coronary arteries [98]. Xia et al also characterized the inflammatory responses in TAC model and detected the increased proinflammatory cytokines and inflammatory cell myocardial infiltration

[99]. Together this evidence suggests that acute perivascular inflammation plays a role in remodeling of intramyocardial arteries during LVH.

## SECTION 2: Platelet Granule Secretion

**Exocytosis** (secretion) by inflammatory cells is one of the major routes whereby cytokines or molecules are released or expressed on the outer surfaces to maintain cell function during vascular physiological or pathological events. Three different patterns of exocytosis have been identified, including 1) classical exocytosis: single granule forming, fusing with membrane and releasing cargo; 2) compound exocytosis: multiple granules integrating into one secretory vesicle before secretion 3) piecemeal degranulation (PMD): partial loss of secretory contents in the focal area of granules, a common observation in mast cells, eosinophils and basophils [100]. Most of the inflammatory cells bear classical and compound secretory patterns (macrophages only have the classical one). PMD secretion is often observed in mast cells, eosinophils and basophils.

In general, the secretion process includes vesicle transport, tethering, docking, priming and fusing to the plasma membrane of the secreted sites. Insertion of newly synthesized plasma membrane proteins and secretion of extracellular matrix components are fulfilled through the constitutive exocytosis pathway; while release of other granule contents or membrane proteins, which require a specific signal trigger is through strictly regulated exocytosis [101]. Recent breakthroughs in characterization of the platelet secretory machinery suggest that platelets play a critical role in vascular inflammation.

**Platelet Granule Components and Development** platelets contain three types of granules:  $\alpha$ -granules, dense granules and lysosomes. These granules have distinct morphology, contents, and respond differently to secretory stimuli.

**$\alpha$ -Granules** are the largest granules (diameter: 200 nm) and are present within a range of 50-80 per platelet [102]. Platelet  $\alpha$ -granules are budded from the trans-Golgi compartment of megakaryocytes [103] and contain a variety of coagulation factors (i.e. factor V, XI), growth factors (i.e. TGF $\beta$ -1, PDGF), angiogenic factors (i.e. VEGF, PF4), membrane-born proteins (i.e. P-selectin, GPIb,  $\alpha_{IIb}\beta_3$ ), cytokines and chemokines (IL-1 $\beta$ , RANTES, IL-8), and adhesion molecules (i.e. fibrinogen, vWF) (Table 144-2) [102]. The above-mentioned proteins can also be categorized into (1) platelet-specific proteins, such as PF4 and  $\beta$ -thromboglobulin family, which are derived only from megakaryocytes; (2) platelet-selective molecules, such as thrombospondin, P-selectin and vWF, which are highly concentrated in platelet compared to blood; (3) proteins taken up by platelets through endocytosis, such as fibrinogen [103]. Inside the  $\alpha$ -granules, there are 4 morphologic zones: granular peripheral membrane, tubular and vesicular part, electron-lucent area and electron-dense nucleoid; each of which contains different types of molecules [103]. Some of the  $\alpha$ -granules have the ultrastructure of exosomes, which are characterized by smaller size (40-100 nm) and expression of CD63 and can be secreted upon thrombin stimulation [104].

While the underlying mechanisms of  **$\alpha$ -granule deficiency** have not been fully elucidated, such deficiencies have been readily observed in patients with gray platelet syndrome, Medich giant platelet disorder and White platelet syndrome [105]. In a mouse model,  $\alpha$ -

granule defect or decrease in granule population appears under the following conditions: (1) absence of certain transcription factors (eg. GATA, Hzf); (2) mutation of proteins involved in vesicular trafficking (eg. VPS33B, Rab geranylgeranyl transferase, Rab27b); (3) absence of membrane composition (eg. ABCG5) [105]. Recently, mutation of *NBEAL2*, the gene encoding the neurobeachin-like 2 (NBEAL2) protein which is important in vesicular trafficking and  $\alpha$ -granule biogenesis, was identified as another cause of gray platelet syndrome [106-108].

**Dense Granules** are much smaller (20-30 nm) than  $\alpha$ -granules and are present in the range of 3 to 8 granules per platelet. Dense granules have a high concentration of calcium and phosphate which contributes to their electric density [97]. Dense granules maintain a high level of serotonin which is taken up from plasma and is trapped there due to the granule acidic pH (6.1) [109]. Dense granules also contain a high concentration of ADP/ATP and magnesium which, in addition to calcium and serotonin, creates high osmotic pressure and makes the granule opaque-looking under transmission electron microscopy [102,103]. Dense granules contain some lysosome membrane protein, such as CD63 and LAMP-2, but not LAMP-1.

**Dense Granule Deficiency** was observed in patients suffering from Hermansky-Pudlak syndrome (HPS) which is an autosomal recessive disease associated with pigmentation disorders and is caused by mutations of different *HPS* gene isoforms [103]. Due to the defects of platelet dense granules, those patients have bleeding disorders and they may also have abnormality in the lung, liver, intestine and heart. Defects of homologues of HPS

proteins cause a similar phenotype in mice (Table 1) [103]. Mutations of other genes, such as gene encoding Rab27a, a regulatory protein important in vesicular trafficking, also cause dense granule defects [103].

**Lysosomes:** Platelet lysosomes maintain the size of 175-250 nm and have the subtypes of primary and secondary lysosomes [103]. Lysosomes are derived from the endosome and contain membrane proteins CD63, LAMP-1 and LAMP-2. The stimuli required to induce lysosomal secretion *in vitro* has been indicated to be much stronger than the stimuli required to induce secretion of  $\alpha$ - and dense granules. Therefore, lysosome exocytosis may represent a high level of platelet activation [102]. Platelet lysosomes contain numerous acid hydrolases, such as elastase and collagenase, which might be involved in vascular disintegrity during thrombosis [110].

Table 114–2. Platelet Granule and Cytoplasmic Contents	
Dense granules	<a href="#">1574</a>
ADP	653 mM
ATP	436 mM
Calcium	2181 mM
Serotonin	65 mM
Pyrophosphate	326 mM
GDP	
Magnesium	
$\alpha$ Granules	<a href="#">120</a> , <a href="#">129</a> , <a href="#">132</a>



Platelet-specific proteins:
Platelet factor 4 (PF4)
$\beta$ -Thromboglobulin ( $\beta$ - <a href="#">TG</a> ) family (platelet basic protein, low-affinity PF4, $\beta$ -thromboglobulin, and $\beta$ -thromboglobulin-F)
Multimerin
Adhesive glycoproteins:
Fibrinogen
von Willebrand factor (VWF)
VWF propeptide
Fibronectin
Thrombospondin-1
Vitronectin
Coagulation factors:
Factor V
Protein S
Factor XI
Mitogenic factors:
Platelet-derived <a href="#">growth factor</a> ( <a href="#">PDGF</a> )
Transforming <a href="#">growth factor</a> - $\beta$ (TGF- $\beta$ )
Endothelial cell <a href="#">growth factor</a>
Epidermal <a href="#">growth factor</a> (EGF)
Insulin-like <a href="#">growth factor</a> I
Angiogenic factors:
Multiple inducers and inhibitors (see text)
Fibrinolytic inhibitors:
$\alpha_2$ -Plasmin inhibitor ( $\alpha_2$ -PI)

Plasminogen activator inhibitor-1 (PAI-1)
<a href="#">Albumin</a>
Immunoglobulins
Granule membrane-specific proteins:
P-selectin (CD62P)
CD63 (LAMP-3)
GMP 33
<i>Other secreted or released proteins</i> <a href="#">120,132</a>
Protease nexin I
Gas6
Amyloid $\beta$ -protein precursor (protease nexin II)
Tissue factor pathway inhibitor (TFPI)
Factor XIII
$\alpha_1$ -Protease inhibitor
CI-inhibitor
High-molecular-weight kininogen
$\alpha_2$ -Macroglobulin
Vascular permeability factor (VPF) / Vascular endothelial growth factor A (VEGF-A)
Interleukin (IL)-1 $\beta$
Histidine-rich glycoprotein
Chemokines:
MIP-1 $\alpha$ (CCL3)
RANTES (CCL5)
MCP-3 (CCL7)

To Be Continued

GRO $\alpha$ (CXCL1)
PF4 (CXCL4)
ENA-78 (CXCL5)
NAP-2 (CXCL7)
IL-8 (CXCL8)
TARC (CCL17)

Smyth SS, Whiteheart SW, Italiano JE, Collier BS (2010) Platelet Morphology, Biochemistry and Function. *Williams Hematology. 8e ed.*

**Table 1.** Granule defects associated with human and mouse platelet dense SPD

Dense SPD syndrome <sup>a</sup>	Affected protein	Lysosomes <sup>b</sup>						Dense granules		Alpha granules
		Platelet		Kidney		Liver		Granule number <sup>d</sup>		
		C	S	C	S	C	S	Whole mount <sup>f</sup>	Mepacrine staining <sup>g</sup>	
<b>HPS-1</b> <sup>114</sup>	HPS-1p							↓		
Pale ear <sup>47, 110, 115, 116</sup>	HPS-1p	N	↑	↑	↓	N		↓	N	↓
<b>HPS-2</b> <sup>75</sup>	AP-3 β3A subunit							↓		
Pearl <sup>47, 60, 110, 116</sup>	AP-3 β3A subunit	N	↓	↑	↓	N		↓↓	N	↓↓
<b>HPS-3</b> <sup>73</sup>	HPS-3p							↓		
Cocoa <sup>60, 112</sup>	HPS-3p	N	N	N	N			↓↓	N	↓↓
<b>HPS-4</b> <sup>76</sup>	HPS-4p									
Light ear <sup>47, 60, 110</sup>	HPS-4p	N	↑	↑	↓			↓↓	N	↓
<b>CHS</b> <sup>80, 117</sup>	Lyst							↓		↓
Beige <sup>47, 110, 118</sup>	Lyst		↓	↑	↓	N		↓	N	↓↓
Subtle gray <sup>60, 113</sup>	Unknown	N	N	N	N	N	N	↓		↓
Cappuccino <sup>60, 107, 119</sup>	Unknown	N		↑	↓	↑		↓↓		↓↓
Ashen <sup>77</sup>	Rab27a							↓↓		↓↓
Gunmetal <sup>94, 95</sup>	RabGGTase α	N	N	N	N	N		↓		↓
Ruby eye <sup>47, 60, 110</sup>	Unknown	N	N	↑	↓			↓↓	N	
Ruby eye-2 <sup>47, 60, 110</sup>	Unknown	N	N	↑	↓			↓↓	N	
Sandy <sup>60, 108</sup>	Unknown	N	↓	↑	↓	N		↓↓	N	↓↓
Mocha <sup>106</sup>	AP-3 δ subunit	N	↓	↑	↓	N		↓↓	N	↓↓
Muted <sup>106</sup>	Unknown	N	↓	↑	↓	N		↓↓	N	↓
Pallid <sup>47, 60, 110, 116</sup>	Palladin	N	↓	↑	↓	N		↓↓	N	↓↓

<sup>a</sup> Human diseases are in bold, mouse models in plain text.

<sup>b</sup> C, lysosomal enzyme content; S, lysosomal enzyme secretion; N, normal; ↑, increased; ↓, reduced.

<sup>c</sup> Alpha granule abnormalities have not been noted in mouse models of dense SPD with the exception of gunmetal.<sup>60</sup>

<sup>d</sup> Results vary according to method used.

<sup>e</sup> Serotonin concentration: ↓↓ highly reduced (<1  $\mu$ g per platelet).

<sup>f</sup> Whole mount: ↓↓ highly reduced (<3 granules per platelet on average).

<sup>g</sup> All dense granules stained with mepacrine exhibited reduced fluorescence intensity and reduced flashing.

King SM, Reed GL (2002) Development of Platelet Secretory Granules. *Semin Cell Dev Biol*

## **The Key Step of Platelet Secretion: Membrane Fusion**

**Significance and Involvement of Lipid Components** Membrane fusion is a highly regulated process in which fusion between lipid bilayers of vesicle and the targeted membrane occurs when energy demand is met. About 70% of platelet membrane lipid components are phospholipids [111]. Until now, it has been shown that at least two types of lipids are essential for platelet secretion.

**Phosphatidic Acid (PA)** While the significance of PA in membrane fusion is not clear, its involvement has been corroborated by numerous studies. Manipulating PA production in permeabilized platelets through activation of PKC and in the presence of GTP $\gamma$ -s can potentially increase platelet granule secretion [112]. Also, addition of PA can enhance PKC or GTP $\gamma$ -s-mediated platelet dense granule secretion [113]. In other systems, such as chromaffin and PC12 cells, inhibition of PA production reduced membrane fusion and granular release [114]. Also the same group found that exogenously adding LPC could restore the exocytosis in those cells, indicating that PA might contribute to the membrane fusion through affecting membrane curvature [114]. PA might also enhance the environment for protein-protein interactions and cell signaling thereby further contributing to membrane fusion [115].

**Phosphatidylinositol 4, 5-Bisphosphate (PIP<sub>2</sub>)** Similar to PA, PIP<sub>2</sub> is very important in granule secretion [116]. The cleavage of PIP<sub>2</sub> by addition of phosphatidylinositol-specific phospholipase C decreased Ca<sup>2+</sup>-induced platelet  $\alpha$ -granule secretion in a dose- and time-dependent manner [116]. Antibodies to type II phosphatidylinositol-phosphate kinase

reduced PIP<sub>2</sub> levels and subsequently resulted in inhibition of  $\alpha$ -granule secretion [116]. The mechanisms through which PIP<sub>2</sub> affects the secretion are not well understood. It has been indicated that PIP<sub>2</sub> interacts with secretion complex components and their regulators. Increase of PIP<sub>2</sub> level in the plasma membrane inhibited SNARE-dependent liposome fusion [117]. However, PIP<sub>2</sub>-binding-activated protein CAPS significantly increases SNARE-dependent liposome fusion in the presence of PIP<sub>2</sub>, indicating that PIP<sub>2</sub> plays a regulatory role, rather than an inhibitory role, in SNARE-dependent membrane fusion [117]. Recently, another study showed that PIP<sub>2</sub> can also regulate Munc13-4-dependent granule secretion in human natural killer (NK) cells [118]. Granule secretion, which triggers Munc13-4 membrane raft recruitment and subsequent internalization, is inhibited by RNA-silencing of PIP5K; and AP-2-dependent Munc13-4 internalization is also blocked [118].

**Soluble NSF Attachment Protein Receptor (SNARE) Complexes** are membrane proteins which have been considered essential for secretory vesicle docking and fusion. Replacement of one of the three glutamines with arginine in the highly conservative core of SNARE causes lethal effects or growth defects in yeast which can be compensated by replacement of the other arginine with glutamine in the core area [119]. Similarly genetic defects of SNAREs in other species, such as *Drosophila*, *C. elegans* and mice also cause neurotransmission dysfunction [101]. SNAREs were formerly divided into two categories: vesicular SNARE proteins (v-SNAREs), such as VAMP proteins, and targeted membrane SNARE proteins (t-SNAREs), such as syntaxin and SNAP-23. It is currently believed that v- and t-SNAREs are not solely located on vesicular or targeted membranes. One SNARE complex is generally composed by one VAMP helix, one Syntaxin helix and two helices of SNAP-23 protein. Different cell types or granules possess

different isoforms of VAMP, Syntaxin and SNAP [100]. In 1999, Flaumenhaft et al first observed a core complex in human platelets (consisting of VAMP protein, SNAP-23 and syntaxin 4) which was shown to be crucial for platelet exocytosis [120]. Lemons et al confirmed the core complex in platelet  $\alpha$ -granule secretion, further indicating that both syntaxin 2 and 4 are involved [121]. Permeabilized platelets treated with anti-syntaxin 4 antibodies or tetanus toxin (which cleaves VAMP-1,-2 and -3) had significantly less granule secretion upon stimulation, indicated by P-selectin membrane expression [120]. SNAREs were also shown to communicate with the platelet actin cytoskeleton during platelet  $\alpha$ -granule secretion [122]. The most recent data have identified four **Vesicle Associated Membrane Proteins (VAMP)** isoforms in human platelets: VAMP-2[120], VAMP-3 [123], VAMP-7 [124] and VAMP-8 [125], out of which VAMP-3 and VAMP-8 were initially thought to be required for secretion of platelet  $\alpha$ -granules and dense core granules [120,125]. However, studies on VAMP-3 null mouse platelets suggest that VAMP-3 is not necessary for normal platelet granular release [126]. Further, platelet secretions are defective in VAMP-8 deficient mice, indicating that VAMP-8 is the major v-SNARE in platelets [124]. Immuno-blocking of **SNAP-23**, a t-SNARE in the secretory core complex, inhibits  $\alpha$ -granule, dense core granule and lysosome secretion in permeabilized platelet [121,127,128]. This was further confirmed by another group, using an dominant negative SNAP-23 mutant, showing that competitive binding of the mutant to the docking site suppresses the native protein binding and subsequently inhibits platelet granule secretion [129]. In the presence of  $\text{Ca}^{2+}$ , SNAP-23 is degraded by calpain cleavage in a dose- and time-dependent manner after platelet degranulation, suggesting its role in membrane exteriorization [130,131]. It was considered that **Syntaxin** 2 and 4 were critical for platelet granule secretion by antibody

blocking studies [121,127,128]. Compared to VAMP and SNAP-23, syntaxin 2 and 4 are more equally distributed in all the membranes [116]. However, recently Ye S. et al from Whiteheart's lab found that syntaxin 11, rather than syntaxin 2 or 4, is the critical *t*-SNARE for platelet exocytosis and the previous finding about syntaxin 2 and 4 are due to the cross-reactivity of the antibody [132]. In the resting status, two SNAP-23 helices and one Syntaxin helix form the *cis*-SNARE complex located on plasma membrane. Upon activation, the *cis* SNARE complex is transformed to the four-helix *trans* SNARE complex through binding to one VAMP helix on the vesicle membrane. The structure transition from *cis* SNARE to *trans* SNARE leads to fusion between vesicle membrane and plasma membrane and the release of granular contents.

**Chaperone Proteins** many chaperone proteins interact with the secretory core complex to regulate the granule release. Binding of  $\alpha$ -SNAP to NSF, a hexameric ATPase, activates the latter which will transform the *cis* SNARE to the *trans* SNARE, facilitating the fusion between the opposed membranes. Inhibition of NSF by recombinant peptides significantly reduced platelet  $\alpha$ - and dense core granule secretion in a dose-dependent manner [133]. There are three isoforms of **Munc-18** proteins (Munc-18 a, b and c) which interact and sequester different syntaxin proteins in platelets. Phosphorylation of Munc-18 c by protein kinase C (PKC) will decrease the binding affinity of Munc-18 c to syntaxin which also facilitates the SNARE transformation from *cis* to *trans*, and therefore allows granule release [115]. The role of Munc18-b in platelet secretion is also identified recently by forming complex between syntaxin-11, SNAP-23, and VAMP-8 [134]. **Rab** proteins are the largest family within the Ras GTPase superfamily and are considered important in vesicle tethering before membrane fusion [135]. Individual Rab GTPase is located at certain cellular compartment and regulates distinct

trafficking steps when activated by GTP loading. Rab1a and 1b, 3b, 4, 6c, 8, 11, 27a and b, 31, 38 have all identified and characterized in platelets [136-139]. Rab27a mutation has been associated with Hermansky-Pudlak and Griscelli syndrome in human and it also causes murine (*ashen* mice) granular secretion defects in a variety of secretory cells, such as melanocytes, cytotoxic T lymphocytes, and platelets [140-147]. The effect of Rab27a mutation on platelet function has been debated. It was found by Wilson et al that *ashen* mice had a significantly longer bleeding time due to their dense granule number and content defects [146]. On the contrary, Seabra's group showed that *ashen* mice possess normal platelet morphology and function normally in response to high dose of agonists, and Rab27a deficiency could be compensated by Rab27b [115]. The differences in the findings of the above groups are potentially due to differing mouse genetic backgrounds and assay set-up [145]. The function of Rab27b in platelets has also been elucidated by Seabra's group suggesting that mice with Rab27b mutation have attenuated dense granule release and platelet aggregation which was not further dampened by Rab27a mutation [148].

**Munc13-4 Dependent Granule Secretion and Jinx Mice** Munc13-4 protein was first cloned and identified in rat lung and spleen tissue by Koch H. et al in 2000 [149]. It was later observed that Munc13-4 RNA was also expressed in human hematopoietic cells [150]. Munc13-4 belongs to Munc13 protein family in which Munc13-1, Munc13-2 and Munc13-3 isoforms are recognized as important regulators of synaptic exocytosis, specifically in the central nervous system (CNS) [151,152]. Encoded by *Unc13d* gene, Munc13-4 functions similarly to its homologues in CNS and is important for secretory vesicle priming and fusion in hematopoietic cells, including platelets, natural killer (NK) cells, cytotoxic T lymphocytes, neutrophils and mast cells [150,153-



158]. Munc13-4 regulates granule secretion by binding to Rab27 (Rab27a and Rab27b), the chaperone proteins responsible for tethering vesicles to the targeted membrane before membrane fusion [158,159]. Munc13-homology domains (MHDs) are present in all Munc13-like proteins and are required for proper Munc13-4 membrane location [149]. Studies have shown that platelet Munc13-4 proteins are present in the cytosol and on the plasma membrane, but not in dense core granules; whereas Rab27 proteins are exclusively present on the plasma membrane fraction, a large proportion of which are located on dense core granule [159]. In cytotoxic T lymphocytes and NK cells, Munc13-4 colocalizes and directly interacts with Rab27 and is indispensable in the interaction between Rab27a and Rab11 to fulfill the endosomal assembly [160]. Mutation of *MUNC13-4* gene is closely associated with a fatal human disease – familial haemophagocytic lymphohistiocytosis type 3 (FHL3) [150,161]. FHL3 patients suffer from aberrant granule secretion of cytotoxic T cells, which leads to the abnormal enlargement of liver and spleen, anemia and thrombocytopenia. *Unc13d*<sup>Jinx</sup> (Jinx) mice are the animal model of FHL3 [162]. Jinx mice have a point mutation in *Unc13d* gene (mouse orthologue of *MUNC13-4*) which causes a splicing defect, generating truncated Munc13-4 protein which will undergo ubiquitination leading to its subsequent degradation [162]. Interestingly, Jinx mice under normal condition do not exhibit FHL3 characteristics. It is only when they are infected with lymphocytic choriomeningitis virus that they exhibit FHL3-like phenotype [162]. Absence of Munc13-4 in platelets of Jinx mice leads to severely compromised secretion of dense core granules,  $\alpha$ -granules and lysosomes which could be recovered by adding normal Munc13-4 to permeabilized platelets [154]. Because the amount of Munc13-4 in platelets is much lower than other secretory regulators, it is suggested that Munc13-4 is a limiting factor in platelet granular

secretion [154]. The data from heterozygous mice further confirmed that platelet granule secretion is correlated with Munc13-4 level and can be recovered by titration of the recombinant human Munc13-4 [154]. Because of granular secretion defects, Jinx mice have increased bleeding time.

### **Potential Mediators from Platelets in Cardiac Hypertrophic Remodeling**

**Serotonin (5-hydroxytryptamine, 5-HT)** has been recognized for many years as an important neurotransmitter modulating brain function through universally-expressed serotonin receptor subtypes (16 identified receptors until now) in the CNS and influencing all of the human behavioral activities [163]. Defects in serotonin signaling are related to neurological and cognitive disorders [163,164]. The signaling of different serotonin receptors can regulate one behavior in an integrated pattern and one serotonin receptor may also be involved in different behavioral events [163]. For example, 5-HT<sub>1A</sub> and 5-HT<sub>2C</sub> cooperate to regulate the behavior of anxiety, but 5-HT<sub>2C</sub> is also involved in regulating locomotion and appetite [163]. Despite the undeniable importance of serotonin in the CNS, 95% of serotonin is actually stored in the peripheral vascular system, mainly in the platelet dense granules. The serotonin found within platelets is synthesized and released by the enterochromaffin cells in the intestinal wall and is taken up by platelets through 5-HT transporter (SERT) [165]. Taking the advantage of established serotonin receptor knockout animal models and serotonin receptor antagonists, studies have further revealed its influences in pulmonary, gastrointestinal (GI), and cardiovascular systems [163]. Series of studies have shown that serotonin regulates platelet function, vascular tone, heart rate, cardiac development and remodeling [163]. Serotonin has

also been shown to be involved in liver regeneration [166]. 5-HT<sub>2B</sub> receptor has been shown to be indispensable in embryonic cardiac development since the disruption of 5-HT<sub>2B</sub> gene in mice causes embryonic or neonatal death [167]. This study also indicated that cardiac development is regulated through activation of ErbB-2, a tyrosine kinase receptor [167]. Later, the same group observed prominent cardiac hypertrophic responses in transgenic mice overexpressing G<sub>q</sub>-coupled 5-HT<sub>2B</sub> receptor, indicating a role for serotonin in cardiac hypertrophy mediated by PLC activity [168]. Upregulation of 5-HT<sub>2B</sub> was observed in norepinephrine (NE)-induced and aortic constriction-induced cardiac hypertrophy [169,170]. Furthermore, cardiac hypertrophy induced by isoproterenol perfusion could be attenuated by application of 5-HT<sub>2B</sub> receptor antagonist SB206553 or in 5-HT<sub>2B</sub><sup>-/-</sup> mice probably through inhibiting secretion of IL-6, IL-1 $\beta$  and TNF- $\alpha$  from ventricular fibroblasts [171]. It was also been confirmed that blocking 5-HT<sub>2B</sub> receptor by SB215505 reduced the superoxide generation and NAD(P)H oxidase activity in both cardiomyocytes and cardiac fibroblasts during hypertrophic cardiac remodeling [172]. These studies suggested a critical role of serotonin in both physiological and pathological development of the heart with an emphasis on 5-HT<sub>2B</sub> receptor signaling. However, an *in vitro* study showed that addition of 5-HT<sub>2B</sub> antagonist SB206553 only partially inhibited serotonin-triggered hypertrophy of cultured rat ventricular myocytes, while inhibition of serotonin turnover by monoamine oxidase-A (MAO-A) inhibitor, pargyline, significantly blocked hypertrophic responses mainly through reducing production of the reactive oxygen species (ROS) [173]. The partial inhibition by 5-HT<sub>2B</sub> antagonist was confirmed by another *in vivo* study in which SB204741 partially attenuated the NE-overload-induced cardiac hypertrophy and cardiac apoptosis in rats [169]. The significance of MAO-A has been further identified in MAO-A

knockout mice in which peripheral serotonin as well as ventricular expression of 5-HT<sub>2A</sub> receptor are significantly increased [174]. Independent pathways have also been elucidated through which 5-HT<sub>2A</sub> and MAO-A contribute to serotonin-induced cardiac hypertrophy [93]. The above evidence contributed to the development of drugs designed to modulate serotonin or its receptor (i.e. ketanserin) in order to treat hypertrophic cardiomyopathy. Such novel drugs, however, are not without side effects which include QT interval prolongation and increased risk of sudden cardiac death [175].

**Transforming Growth Factor  $\beta$ -1 (TGF $\beta$ -1)** TGF $\beta$ -1 is secreted by many cell types in a latent-form sequestered by TGF $\beta$ -1 latency-associated peptide (LAP). It will be subsequently activated by stimuli such as acidic microenvironment, MMPs, shear stress and thrombospondin-1 (THP-1) which can facilitate release of LAP. TGF $\beta$ -1 signals by binding to TGF $\beta$  type II receptor and subsequently recruiting and activating the TGF $\beta$  type I receptor, which will activate its downstream effectors, such as Smad proteins. In the canonical pathway, TGF $\beta$  type I receptor phosphorylates and activates Smad 2/3, leading to the formation of Smad 2/3/4 complex which will translocate to the nuclei, bind to the promoter region of certain genes and regulate gene expression. Smad 6/7 inhibits Smad 2/3 phosphorylation by binding to TGF $\beta$  type I receptor or recruiting Smad ubiquitination-related factor 1 and 2 (Smurf 1 and 2) [176]. Alternatively, TGF $\beta$  type I receptor activates other targets, such as TGF $\beta$ -activated kinase 1 (TAK1), which will activate P38 through MKK6 and MKK3, thereby upregulating gene expression of extracellular matrix components, such as collagen [176,177]. The non-canonical pathway is more closely associated with pathological remodeling [176]. It has been universally recognized that TGF $\beta$ -1 contributes to cardiac hypertrophic and fibrotic remodeling [176,178]. TGF $\beta$ -1 can be induced

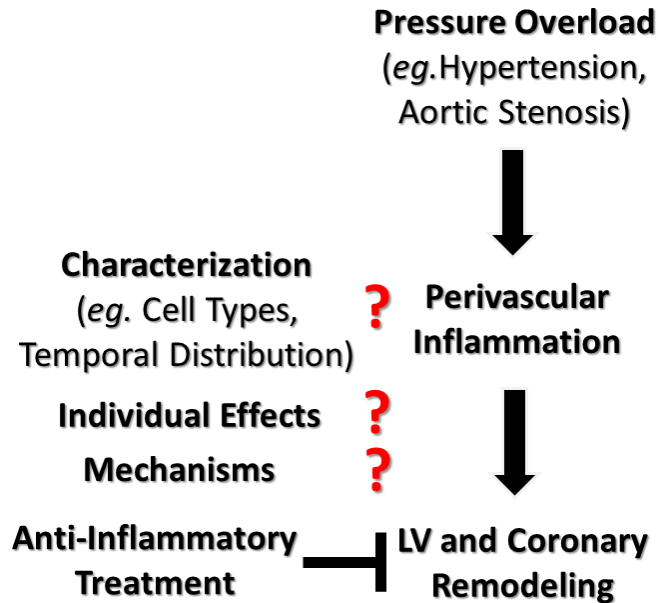
by cardiac injury and hypertrophic stimuli, such as Angiotensin II and pressure overload [177,179,180]. TGF $\beta$ -1 levels are also enhanced in myocardial hypertrophy and heart failure [176]. Both cardiomyocytes and cardiac fibroblasts produce TGF $\beta$ -1 which can modulate the function of cardiac cells through autocrine or paracrine pathways. A recent report showed that circulating platelets maintain an abundant storage of TGF $\beta$ -1 and contribute to plasma TGF $\beta$ -1 levels [179]. Depletion of platelet TGF $\beta$ -1 will partially protect the heart from pressure-overload-induced remodeling and dysfunction [179]. TGF $\beta$ -1 is important for mice embryonic hematopoiesis and vasculogenesis, since the TGF $\beta$ -1-null phenotype contributes to yolk sac defect which often leads to embryonic death [181]. Forty percent of TGF $\beta$ -1 null mice that were born alive rapidly developed multi-organ inflammatory diseases two weeks later and died by two to three weeks after birth [182]. An immuno-deficient mouse in which TGF $\beta$ -1 is genetically knocked out, was able to abolish angiotensin II-induced cardiac hypertrophy with no impact on cardiac fibrosis formation [180], while transgenic mice overexpressing TGF $\beta$ -1 showed cardiac hypertrophy and increased myocyte contractility [183]. The effect of disrupting TGF $\beta$ -1 signaling on cardiac function is still debatable. It was observed that intraperitoneal injection of a monoclonal antibody to neutralize TGF $\beta$ -1 (NAb) in rodents did not alter myocyte hypertrophy but prevented aortic-constriction-induced perivascular and myocardial fibrosis [177,184]. However, data are not consistent on whether Nabs could protect the animals from diastolic dysfunction [177,184]. Interestingly, competitive blocking of TGF $\beta$ -1 signal by expressing a dominant-negative mutant of TGF $\beta$  type II receptor in mice led to left ventricular dilation and dysfunction without affecting cardiac hypertrophy and interstitial fibrosis [185], while myocyte specific knockout of TGF $\beta$  type II receptor in mice attenuated cardiac

hypertrophy and dysfunction [177]. The differences are probably due to activation of distinct downstream pathways in different target cells. It has been shown that exacerbation of cardiac hypertrophy remodeling by NABs is mainly due to disruption of Smad3 signaling without affecting TAK1 activation in noncardiomyocytes, and inhibition of both Smad3 and TAK1 pathways in cardiomyocytes preserved cardiac function and reduced cardiac hypertrophy [177].

**Sphingosine 1-Phosphate (S1P)**, generated from sphingosine phosphorylation by sphingosine kinases, is a potent lipid ligand which can regulate cell growth, migration, contractility and intracellular calcium mobilization through binding to its receptors. The majority of S1P comes from platelets, erythrocytes and vascular endothelium. In the circulation, albumin and HDL are the major carriers of S1P. S1P receptors are G protein coupled receptors (GPCR) and to date five of them have been identified: S1P<sub>1</sub>, S1P<sub>2</sub>, S1P<sub>3</sub>, S1P<sub>4</sub> and S1P<sub>5</sub>, which are organ and cell-specifically distributed. S1P<sub>1</sub>, S1P<sub>2</sub>, S1P<sub>3</sub> are present in the heart with S1P<sub>1</sub> being the predominant S1P receptor in cardiomyocytes. The effects of S1P on the heart mainly depend on the receptor subtype it binds to and the coupled G protein signaling. S1P<sub>1</sub> mainly couples to G<sub>i/o</sub>. Upon activation, G<sub>i/o</sub> releases the G<sub>α</sub> subunit which can inhibit adenylate cyclase and reduce intracellular cAMP, decreasing the myocyte contractility. G<sub>βγ</sub> can also induce downstream signaling. S1P<sub>2</sub> and S1P<sub>3</sub> are coupled to G<sub>i/o</sub>, G<sub>q</sub> and G<sub>12/13</sub> [186]. The role of S1P on cardiac hypertrophy has been debated. Studies on cardiac remodeling in settings of myocardial hypoxia and ischemia reperfusion revealed the protective role of S1P through activating Akt pathway, which will inhibit GSK3 and activate NOS [187]. The cardiac protective role of S1P is probably mediated through S1P<sub>2</sub> and S1P<sub>3</sub> receptors because S1P-induced cardiac protection was missing in S1P<sub>2</sub> or S1P<sub>3</sub> knockout mice and was even more significant in S1P<sub>2</sub>/ S1P<sub>3</sub> double

knockout mice [188]. However, it has also been shown in an *in vitro* experiment that S1P triggered hypertrophic responses in rat neonatal myocytes in a dose-dependent manner [189]. S1P<sub>1</sub> receptor probably mediated it since specific anti-S1P<sub>1</sub> antibody inhibited the hypertrophy [189]. In an *in vivo* experiment, intraperitoneal injection of S1P for 4 weeks induced cardiac hypertrophic responses which were shown by increased HW: BW, cardiomyocyte size and ANP protein level [190]. It has been revealed that G<sub>i/o</sub> signaling through S1P<sub>1</sub> is involved cardiac hypertrophic responses. However, G<sub>q</sub>-mediated PLC activation also induces cardiac hypertrophy which suggests a role of S1P<sub>3</sub> [187].

### Section 3: Summary



Although inflammation has been observed in settings of pressure overload and anti-inflammatory procedures are associated with a better cardiac outcome, the detailed features of early perivascular inflammation, for example, the involved inflammatory cell types and their temporal distribution, have not been fully characterized. Moreover, the individual effects of those inflammatory cells on LV and coronary remodeling and the underlying mechanisms are also not clear. Therefore, my study, which will be presented in the next two chapters, is focused on characterizing the early perivascular inflammation in TAC-induced LV pressure overload and the contribution of individual inflammatory cell type (CHAPTER 2) and inflammatory secretion, granular secretion of platelets in particular, to cardiac remodeling (CHAPTER 3).



## **CHAPTER 2: CORONARY ARTERY REMODELING IN A MODEL OF LEFT VENTRICULAR PRESSURE OVERLOAD IS INFLUENCED BY PLATELETS AND INFLAMMATORY CELLS**

### **INTRODUCTION**

Left ventricular hypertrophy (LVH) is a common risk factor for the development of heart failure and an independent predictor of cardiovascular death. LVH usually develops in the setting of mechanical stress, overactive sympathetic drive, or as a consequence of genetic abnormalities. One important pathophysiologic characteristic of hypertensive LV remodeling is the production of excessive interstitial fibrillar collagen by fibroblasts [13]. Extensive fibrosis is thought to impair normal LV diastolic function and oxygen diffusion, leading to LV dysfunction [15]. Recent clinical studies have found a strong correlation between potentially fatal ventricular arrhythmias and myocardial fibrosis, as detected by delayed hyper-enhancement magnetic resonance imaging in patients with hypertrophic cardiomyopathy [19]. In addition to interstitial fibrosis, perivascular fibrosis occurs in the setting of LVH and congestive heart failure. LVH also results in susceptibility to myocardial hypoperfusion and ischemia as a result of disturbances in coronary flow physiology, that likely reflects remodeling of coronary arteries [20-25].

Perivascular inflammation has been observed in hypertensive disease and congestive heart failure (CHF) and may initiate fibrosis and coronary artery remodeling. Inhibition of inflammatory responses tends to attenuate cardiac fibrosis in experimental models [17,18,27,28]. In DOCA/salt-induced hypertensive rats, pharmacological targeting of monocyte/macrophage accumulation ameliorated cardiac perivascular and interstitial fibrosis

and reduced inflammatory marker expression, such as interleukin-6 (IL-6) and monocyte chemoattractant protein-1 (MCP-1) [17,18,27,28,30]. In a rat model of suprarenal aortic constriction, antibody blockade of either intercellular adhesion molecule-1 (ICAM-1) or MCP-1 reduced early macrophage recruitment, and prevented the development of myocardial fibrosis [17,28]. However, the triggers for initiation of perivascular inflammation in the setting of LVH are poorly understood.

Accumulating evidence implicates platelets in vascular inflammation in a variety of settings. Platelets, small cytoplasmic bodies that lack nuclei, are generated by megakaryocytes in bone marrow. In settings of vascular injury or inflammation, platelets adhere to the subendothelial matrix or endothelial cells. Subsequent platelet activation maintains hemostasis through platelet-platelet interactions that form the primary platelet clot. Activated platelets express and release granule contents. Activation-dependent surface expression of adhesive molecules, such as P-selectin, serves to recruit leukocytes; inflammatory mediators released by platelets may modulate leukocyte responses at sites of vascular injury [32,35,37,41-43]. Thus, in addition to their essential role in hemostasis, platelets have been proposed to serve as important mediators of vascular inflammation [33-40].

In this chapter, we investigated early cellular events that mediate perivascular inflammation and coronary artery remodeling. We report that platelets and T lymphocytes are recruited to coronary arteries after TAC and that both cell types may play unanticipated roles in modulating perivascular inflammation and fibrosis in the setting of LV pressure overload.

## MATERIALS AND METHODS

*Animals* All procedures conformed to the recommendations of "Guide for the Care and Use of Laboratory Animals" (Department of Health, Education, and Welfare publication number NIH 78-23, 1996) and were approved by the Institutional Animal Care and Use Committees at the University of Kentucky. The C57BL/6J (B6), RAG-1-deficient ( $Rag1^{-/-}$ ) mice, and IL-10-deficient ( $IL-10^{-/-}$ ) mice, were obtained from The Jackson Laboratory (Bar Harbor, ME). All the mice were maintained on the C57BL/6J background.

*Transverse aortic constriction Model* Pressure overload of the LV was elicited by TAC in male mice at the age of eight to 12 weeks. Sham surgery, in which a suture was passed around the aorta but removed without tying, was performed as a control [98]. Mice were euthanized at early (one day, three days, and seven days) and late (five weeks) time points after surgery. Left ventricle function and coronary flow reserve were measured by echocardiography and Doppler (Figure 2.1).

*Doppler Studies* Velocity of blood flow in the left and right carotid arteries and coronary artery was measured as described previously [96,97] using a hand-held 20 MHz Doppler probe (Indus Instruments, Houston, TX) before and after surgery, as well as the additional time points post surgery. The mice were anesthetized with isoflurane 1.5-2 %, and taped supine to a temperature-controlled board. The board included electrocardiographic electrodes placed under each limb and a heating pad under the body. Body hair was clipped and the skin was moistened with water to improve sound transmission. The Doppler probe was placed on the left and right sides of the neck at a 45° angle to detect flow velocity in the left and right carotid arteries. For coronary flow, the probe tip was placed on the left chest at the level of the cardiac

base and pointed horizontally toward the anterior basal surface of the heart to sense blood flow velocity. The optimal Doppler flow velocity signals were obtained by adjusting the position of the probe and the Doppler range gate depth of 2 mm (for carotid artery) or 2.5–3 mm (for coronary artery), to obtain a maximal velocity signal. A computer-based Doppler signal processor (Model DSPW, Indus Instruments,) was used to store the Doppler signals and for later analysis. For left coronary artery flow, the baseline flow velocity was recorded at 1 % isoflurane concentration. The hyperemic flow velocity was recorded during maximal vasodilatation induced by 2.5 % isoflurane and after three minutes of isoflurane inhalation. Coronary artery flow reserve was calculated as the ratio of hyperemic peak flow velocity to baseline peak flow velocity.

*Echocardiography* Two-dimensional short and long axis views of the left ventricle were obtained by transthoracic echocardiography performed five weeks post-TAC using a 45 MHz probe (770) and the Vevo 770 Imaging System (VisualSonics, Toronto, Canada), under 1.5 % isoflurane inhalation as described previously [1]. M-mode tracings were recorded and used to determine LV end diastolic diameter (LVEDD), LV end systolic diameter (LVESD), and LV posterior wall thickness in diastole (LVPWThD) over three cardiac cycles. LV fractional shortening (FS) was calculated using the formula  $\% FS = (LVEDD - LVESD) / LVEDD$ .

*Histology* Mice were weighed and hearts, lungs, livers and kidneys were dissected at days one, three, seven and five weeks post surgery. Hearts were harvested, washed in PBS, and sectioned at the level of the papillary muscle. The base of the heart was immersed in 4 % PFA for 24 hours, subsequently transferred to 70 % ethanol and embedded in paraffin. Multiple serial 5  $\mu m$  sections (six – 10) were taken every 250  $\mu m$  from the distal region of the heart from the

base to the aorta. Slides (six – 10) were created that contain two sections every 250  $\mu\text{m}$  spanning the base of the heart. Slides from each heart were stained with H&E, Masson's Trichrome and picrosirius Red staining. The remaining slides were archived for later use.

Paraffin embedded IHC was done with a mouse-anti-mouse smooth muscle cell actin- $\alpha$  antibody (Sigma A-5691). In brief, heart sections were first deparaffinized and placed in diluted antigen unmasking solution (Vector, Burlingame, CA) for antigen retrieval using a decloaking chamber (Biocare Medical, Concord, CA). Non-specific sites were blocked using mouse-on-mouse IgG blocking reagent (Vector Labs) for one hour in room temperature. Slides were then incubated with primary antibody for one hour at room temperature, followed by 30 minutes with substrate solution (Vector Red substrate). CAT Hematoxylin (Biocare Medical) was used for counterstaining. Finally, slides were dehydrated, mounted with DPX coverslip (Gallard Schlesinger Industries) and covered by cover glasses. Positive staining was quantified using Metamorph software.

IHC was performed on frozen sections using CD90.2 (1:100, BD Pharmingen<sup>TM</sup>, San Diego, CA, ), CD68 (1:200, Serotec), VCAM-1(1:50, BD Pharmingen<sup>TM</sup>), PECAM-1(1:50, BD Pharmingen<sup>TM</sup>), CD8 (1:50, Serotec), CD19 (1:50, BD Pharmingen<sup>TM</sup>), MPO (1:50, Abcam) and platelet antibody (1:1000, Intercell). Briefly, the heart bases were directly embedded in OCT and frozen at -20 °C. Blocks were cut into 10  $\mu\text{m}$  sections and fixed with chilled acetone in -20 °C. To minimizing the effect of endogenous peroxidases, slides were immersed in 1 %  $\text{H}_2\text{O}_2$  in methanol for two minutes at 40° C. Non-specific sites were blocked using 1.5 % serum from the secondary antibody-derived animal for 15 minutes at 40° C. Slides were then incubated with primary antibodies for 15 minutes at 40° C, the for 15 minutes with biotinylated secondary antibody, and

then for 10 minutes with ABC detector (Vector Labs) at 40 °C. HRP substrate-chromogen (Biomed) was used as the chromogen, and hematoxylin (Accurate Chemical & Scientific Corp.) was used for counterstaining. Frozen slides were fixed with chilled acetone in -20 °C. Non-specific sites were blocked using 1.5 % serum from (the secondary-antibody-derived animals) for 20 minutes at RT. Slides were then incubated with PECAM-1 primary antibody (1:50, BD Pharmingen™) at RT for one hour and a rhodamine-conjugated goat-anti-rat secondary antibody (15 µg/ml, Jackson ImmunoResearch, West Grove, PA) at RT for 30 minutes. Slides were viewed and images were taken using a Leica TCS SP5 laser scanning inverted confocal microscope.

Immunostaining of targeted proteins was quantified in tissue sections from TAC mice and their respective sham controls. For each antibody, isotope-matched non reactive IgG served as the negative control. The percentage of the vessel area occupied by inflammatory cells was measured from digital images using Metamorph software by personnel blinded to treatment. Perivascular and interstitial fibrosis was measured from Masson's Trichrome and picrosirius Red stained slides. Vessel area was quantified using Metamorph software and reported as external elastic lamina (EEL).

*Quantitative PCR* RNA samples were extracted from the apex of the heart (stored in RNA later, -80 °C) using TRIzol (Invitrogen, Grand Island, NY) as described previously [109]. RNA concentration and quality were tested using OD<sub>260 / 280</sub> ratio by Biomet3 (Thermo Electron Corporation, Waltham, MA) and also by examining the product on a 1 % agarose gel. The cDNA synthesis was performed using High-Capacity cDNA Archive kit (Applied Biosystems, Foster City, CA), starting with 1 µg RNA in 20 µl reaction system. Quantitative real-time PCR was done using

Taqman Universal Master Mix and Assays-on Demand primers and probes (Applied Biosystems) and the ABI 7500 system. 18S RNA was used as an endogenous control. An embryo RNA standard was used as a positive control. Results were expressed as mean fold changes of gene expression relative to sham-operated C57Bl/6 mice or control antibody injected TAC mice using  $2^{-\Delta\Delta CT}$  method [109].

*Flow Cytometry* Fifty  $\mu$ l blood was collected in 0.32 % citrate and incubated with anti-Mac-1 antibody (PE conjugated, BD Pharmingen) at a final concentration of 20  $\mu$ g/ml or rat IgG (PE conjugated, Emfret) as an isotype control in the presence of 1  $\mu$ M RGDS peptide to prevent platelet aggregation. CD41 Ab (FITC conjugated, BD Pharmingen™) was added to give a final concentration of 20  $\mu$ g/ml. To activate platelets, 150  $\mu$ M PAR4 activating peptide (Anaspec, Fremont, CA) was added. After 15 minutes of incubation, 1 ml of *Lyse/Fix* solution (BD™ Phosflow) was added to each sample. Platelet-leukocyte aggregates were quantified using FACalibur flow cytometer (Becton Dickinson) and analyzed by CellQuest software.

To measure platelet activation by flow cytometry, blood was collected into 0.32 % citrate and diluted further in Tyrode's Buffer with 0.35 % BSA and 1 mM  $MgCl_2$ . The diluted blood was incubated with 60  $\mu$ g/ml FITC anti-fibrinogen (DAKO) or 20  $\mu$ g/ml FITC anti-P-selectin antibody (BD Sciences) and the indicated agonist, for 10 minutes in the dark. The reaction was stopped by the addition of Tyrode's buffer and paraformaldehyde. Samples were quantified by flow cytometer by gating on platelet populations identified by forward and side-scatter properties.

*Whole Blood Aggregation* Aggregation was studied in whole blood using a Multiplate®, Platelet Function Analyzer (Dynabyte, Munich, Germany). 300  $\mu$ l of whole blood was diluted 1:1 with normal saline (0.91 %) and 1 mM  $MgCl_2$  solution and incubated for 3 minutes at 37 °C, prior to

the addition of 6.5  $\mu$ M ADP. Aggregation units (AU) and the area under the curve (AUC in AU \* minutes) was calculated based on measurements of electric impedance.

*Mouse Plasma Collection.* Mouse blood was collected into EDTA-coated tubes, immediately centrifuged at 2000 g for 10 minutes at RT, and plasma stored at -80 °C.

*Mouse Cardiac Tissue Extraction* The base of the LV was dissected (2 mm  $\times$  2 mm pieces) in 250  $\mu$ l of PBS containing protease inhibitors (Pierce), homogenized using Omni tissue homogenizer, and then sonicated for 10 seconds. Following centrifugation (14,000 rpm for 15 minutes at 4 °C), approx 200  $\mu$ l of supernatant was diluted with 200  $\mu$ l PBS containing protease inhibitors.

*Luminex Assay* Inflammatory cytokine/chemokine levels in mouse plasma and extracts of cardiac tissue were measured by Luminex bead analyte assay using Milliplex MAP Kit according to the manufacturer's instructions (Millipore)

*Culturing and treatment of myocardial fibroblasts* Primary myocardial fibroblasts were isolated from C57BL/6 male mice by mincing hearts in 1ml of dispase solution. After fully mincing, 4 ml dispase solution was added, the sample placed at 37°C, and pipetted up and down at 15 minutes. After 30 minutes, 5ml HBSS+ solution was added to neutralize the dispase. The cell suspension was then centrifuged at 2,200 rpm for eight minutes. The cell pellet was saved and resuspended in plating medium (low glucose DMEM + 10% FBS +Penicillin Streptomycin). Cells from one heart were settled in one, six-well plate over night, washed the next day, and added with fresh media. The attached myocardial fibroblasts were cultured for seven-10 days to reach a 70 % to 80 % confluence before treatment.

Washed platelets were isolated from ACD buffered C57BL/6 male mice blood.  $1.5 \times 10^9$  platelets were stimulated using 1 U/ml of thrombin at 37°C for 10 minutes, neutralized with 1



U/ml hirudin. The suspension was then centrifuged at 3000g at 4°C for 10 minutes and supernatant was collected. Myocardial fibroblasts were treated with 1 ml/well of either platelet releasate or buffer (both diluted 1:5 in medium with 0.1% FBS). Cells were harvested at six hours or 24 hours, and RNA was isolated using RNeasy Plus mini kit (Qiagen). The cDNA synthesis and quantitative PCR were performed as described before.

*Statistical analysis* All results were expressed as mean  $\pm$  standard error of the mean (SEM). Statistical significance within strains was determined using *t*-test or two way ANOVA with multiple pair-wise comparisons as appropriate. The Mann-Whitney test was used for nonparametric analysis. Statistical analysis was performed using Sigma-STAT software, version 3.5 (Systat Software, Inc.). A *p*-value of less than 0.05 was considered significant.

## RESULTS

### **TAC is accompanied by early pericoronary inflammation**

Transverse aortic constriction (TAC) induces an acute and persistent increase in proximal aortic and LV pressure, manifested by an elevation in the ratio of the right to left (R / L) carotid peak flow velocity (Figure 2.1A). Though cellular and molecular events that are not well understood, LV pressure overload in mice elicits significant perivascular and interstitial cardiac fibrosis at five weeks post-surgery [98] (Figure 2.1B). As reported by Hartley and colleagues [95-97], we observed a decline in coronary flow reserve (CFR) after TAC, indicating dysfunction of the coronary arteries (Figures 2.1C and 2.1D). In the present study, we investigated the contribution of early perivascular inflammation to coronary artery remodeling and perivascular fibrosis in the setting of pressure overload. As early as one day post-surgery, inflammatory cells accumulated along the left coronary arteries (Figure 2.2). Both macrophages (CD68<sup>+</sup>; Figures 2.2A and 2.2B) and T-lymphocytes (CD90.2<sup>+</sup>; Figures 2.2A and 2.2C), in the vessels increased by approximately four-fold during the first week post-TAC. The CD8 staining confirmed the presence of T cells. However, B cells stained by CD19 were not detected after TAC (Figure 2A). The expression of vascular cell adhesion molecule 1 (VCAM-1) and myeloperoxidase (MPO) were also increased after TAC (Figure 2.2A). The inflammatory infiltration in the left coronary arteries was accompanied by a perturbation in the endothelium, as evidenced by discontinuous platelet-endothelial cell adhesion molecule-1 (PECAM-1, CD31) staining (Figure 2.3).

To provide insight into the underlying mechanisms for inflammation and remodeling early after TAC we measured RNA or protein levels of candidate cytokine mediators, such as monocyte

chemotactic protein-1 (MCP-1), intercellular adhesion molecule-1 (ICAM-1), tumor necrosis factor- $\alpha$  (TNF- $\alpha$ ), interleukin-6 (IL-6), which were known to contribute in other hypertrophy models [17,18,27,28,30]. We also measured levels of growth factor  $\beta$ -1 (TGF $\beta$ -1) [178,180,183,191] and vascular endothelial growth factor (VEGF), which have demonstrated roles in fibrosis and angiogenesis in the setting of cardiac hypertrophy. Additionally, because our IHC data indicated early T lymphocyte accumulation, we measured RNA or protein levels of IL-1 $\beta$ , IL-10, interferon- $\gamma$  (IFN- $\gamma$ ) in order to define the T lymphocyte subtypes involved. At seven days after TAC, MCP-1 (Figure 2.4A) and VEGF (Figure 2.4B) increased in cardiac tissue. Additionally, IL-10 mRNA expression increased more than three-fold in LV between three and seven days after TAC (Figure 2.4C). In the first several days after TAC, there were no significant changes in TNF- $\alpha$ , ICAM-1, TGF $\beta$ -1 or IFN- $\gamma$  mRNA levels in LV (data not shown). Plasma cytokines, including IL-1 $\beta$ , IL-10, VEGF, IFN- $\gamma$ , TNF- $\alpha$ , and MCP-1, also did not appreciably change early after TAC, although a trend towards higher plasma IL-6 level post-TAC was noted (data not shown).

### **The effects of thrombocytopenia on TAC-induced LV remodeling**

Platelets often contribute to perivascular inflammation [33-40], and enhanced platelet activation is found in patients with cardiac hypertrophy and heart failure [32,41]. Therefore, we investigated the contribution of platelets to the inflammatory response that accompanies TAC. At seven days after surgery, platelet counts in whole blood were higher in TAC animals ( $1299 \pm 226$  / nl) than sham mice ( $803 \pm 191$  / nl;  $P < 0.001$ ). Pressure overload led to platelet deposition along the damaged endothelial layer at three and seven days after TAC surgery

(Figure 2.5A). The platelets appeared to accumulate in association with leukocytes, including macrophages (Figure 2.5B). Systemic platelet activation can be detected in settings of vascular inflammatory diseases, such as atherosclerosis [192-195]. One measure of platelet activation is the presence of circulating platelet-leukocyte aggregates in systemic circulation. In blood collected at seven days after sham surgery,  $25 \pm 3$  % of the leukocytes had attached platelets, whereas  $39 \pm 7$  % of the leukocytes had attached platelets in blood from TAC mice ( $P = 0.106$ ). Interestingly, at three and seven days after surgery, agonist-induced platelet aggregation in whole blood and platelet P-selectin expression were lower in TAC than in sham-treated animals (data not shown), suggesting that the platelets remaining in circulation post-TAC may be less responsive to agonists.

To identify a role for platelets in TAC-induced vascular remodeling, thrombocytopenia was induced by treating mice with a glycoprotein Ib $\alpha$  (GPIb $\alpha$ ) antibody that promotes platelet clearance through an Fc fragment-independent pathway [196]. Following anti-GPIb $\alpha$  IgG treatment, the median platelet count of 70 / nL (25 – 75 % CI: 50 – 101 / nL) was substantially lower than the median platelet count of 1362 / nL observed in mice treated with non-immune IgG (25 – 75 % CI: 1070 – 1567 / nL;  $P < 0.001$ ). White blood cell count was normal, with no lymphopenia noted after administration of anti-GPIb $\alpha$  IgG. The effect of antibody treatment on platelet function was confirmed by measuring tail-bleeding time. The median bleeding time was >600 seconds in mice treated with anti- GPIb $\alpha$  IgG (600 – 660 seconds; 25 – 75 % CI) and 70 seconds (55 – 77 seconds; 25 – 75 % CI) in mice treated with non-immune IgG ( $P < 0.001$ ). Depletion of platelets prior to TAC did not significantly alter macrophage accumulation but

reduced the accumulation of T lymphocytes in the coronary arteries after TAC (from a median of 524  $\mu\text{m}^2$  to 122  $\mu\text{m}^2$ ;  $P = 0.031$ , Figures 2.5C and 2.5D). In association with lower T-cell accumulation in thrombocytopenic mice, IL-10 levels in LV were 50 % lower in mice treated with anti-GPIIb/IIIa IgG (Figure 2.5E).

To determine the long-term consequences of platelet depletion and resultant reductions in T-lymphocytes and IL-10 in the vessel wall, we examined coronary arteries at five weeks after TAC. In thrombocytopenic mice, the large coronary arteries contained significantly more smooth muscle cell (SMC)  $\alpha$ -actin, consistent with an effect on vascular remodeling (Figures 2.6A and 2.6B). In addition, mice treated with anti-GPIIb/IIIa IgG had a trend towards an increase in perivascular fibrosis (Figure 2.6C). These findings were not due to alterations in cardiac size or function since heart weight to body weight ratio (HW: BW) and left ventricular internal diameter in diastole (LVIDd), posterior wall thickness (PWt), and fractional shortening (FS) as measured by echocardiography, were similar in control and thrombocytopenic mice (data not shown).

In addition to recruiting inflammatory cells, platelets may release mediators that directly affect cardiac fibroblasts and thereby influence perivascular fibrosis. Therefore, the effect of platelet releasate on cardiac fibroblasts was investigated. Releasate was prepared from thrombin activated platelets and incubated with primary cultures of murine cardiac fibroblasts. Following 6 hours of exposure to platelet releasate, expression of MMP9 mRNA significantly increased by  $15.5 \pm 0.6$  fold (Figure 2.7) and remained elevated at 24 hours (Figure 2.7). Platelet releasate

also increased  $\alpha$ -SMA expression at 24 hours. In addition, TGF $\beta$ -1 signaling appeared to be enhanced, in that the downstream targets bone morphogenic protein 7 (BMP7) and connective tissue growth factor (CTGF) were  $6.6 \pm 2.4$  and  $3.8 \pm 0.1$  fold higher following exposure to platelet releasate.

### **Absence of lymphocytes exaggerates left coronary remodeling.**

Our results indicated that T (but not B), lymphocytes accrue in the vessel wall as part of the inflammatory response after TAC and that depletion of platelets reduced their perivascular accumulation. To define the impact of lymphocytes on coronary remodeling we used Rag1<sup>-/-</sup> mice. *Rag1* encodes the recombination activation gene 1 that catalyzes V(D)J recombination, an essential step for the generation of immunoglobulins and T lymphocyte receptors. As a consequence, Rag1<sup>-/-</sup> mice lack mature B and T lymphocytes [197]. The absence of lymphocytes in Rag1<sup>-/-</sup> mice did not significantly alter the number of macrophages that accumulated in the coronary arteries seven days after TAC (data not shown). The absence of lymphocytes also did not alter the development of LVH, as HW: BW was not significantly different in wild-type and Rag1<sup>-/-</sup> mice at five weeks post-TAC (Table 2.1). Likewise, overall coronary artery remodeling, as measured by the area of the vessel within the external elastic lamina, was similar in wild-type and Rag1<sup>-/-</sup> mice after TAC (Figures 2.8A and 2.8B). However, lumen area was 1.32-fold smaller in Rag1<sup>-/-</sup> coronary arteries after TAC, with a concomitant increase in collagen content. Quantification of Masson's Trichrome (Figure 2.8C) and picosirius red staining (Figure 2.8E) indicated that Rag1<sup>-/-</sup> mice had less perivascular fibrosis (Figure 2.8D) and collagen content (Figure 2.8F) at baseline but greater levels after TAC than that observed in wild-type mice.

Thus, the fold increase in perivascular fibrosis (11-fold,  $P = 0.031$ , Figure 2.8D) and collagen content (43-fold,  $P = 0.008$ , Figure 2.8F) was significantly higher in Rag1<sup>-/-</sup> mice post-TAC. Interestingly, despite these histological changes, the Rag1<sup>-/-</sup> mice demonstrated preserved CFR after TAC. CFR was  $1.83 \pm 0.15$  in wild-type mice that underwent sham surgery ( $n = 7$ ) and  $1.72 \pm 0.23$  in sham-treated Rag1<sup>-/-</sup> mice ( $n = 3$ ). Following TAC, CFR declined to  $1.22 \pm 0.31$  in wild-type mice ( $n = 13$ ;  $P < 0.05$ ). However, CFR was not significantly different in sham and TAC Rag1<sup>-/-</sup> mice ( $1.57 \pm 0.16$ ;  $n = 7$ ), suggesting that despite the smaller lumen size and greater collagen content, the function of the coronary arteries after TAC was preserved in the absence of lymphocytes. At baseline, in comparison to wild-type mice, Rag1<sup>-/-</sup> mice had reduced LV function which did not decline further following TAC (Table 2.2).

#### **IL-10 may play a protective role in LV remodeling**

Platelets can influence the function of T-cells by eliciting the release of IL-10 from dendritic cells [198]. The finding that thrombocytopenia lowered both T-cell infiltration and IL-10 levels after TAC suggested that platelets may be influencing T-cell-mediated events in an IL-10-dependent manner in this model. Therefore, we sought to determine if IL-10 deficiency recapitulated aspects of the phenotype observed in thrombocytopenic or lymphopenic mice. Cardiac hypertrophy, as assessed by HW: BW ratio, was not significantly different in IL-10<sup>-/-</sup> and wild-type mice after TAC ( $7.7 \pm 2.0$  and  $7.1 \pm 1.3$ , respectively,  $P = 0.596$ , NS). However, IL-10<sup>-/-</sup> LV displayed substantial perivascular fibrosis as detected by Masson's Trichrome staining (Figure 2.9A) with levels ( $11,600 \pm 2000 \mu\text{m}^2$ , mean  $\pm$  sem;  $n = 5$ ) similar to those observed in thrombocytopenic and Rag1<sup>-/-</sup> mice post-TAC and was significantly higher than B6 mice. The IL-

10<sup>-/-</sup> TAC mice also displayed evidence of exaggerated remodeling as measured by SMC  $\alpha$ -actin staining, with a similar level of B6 mice (Figure 2.9B).



Table 2.1 Organ and body weight in WT and Rag1<sup>-/-</sup> mice five weeks after TAC or sham surgery

Genotype	Treatment	n	BW (g)	HW: BW	LiW: BW	LuW: BW	KiW: BW
WT	sham	3	24.8 ± 2.1	5.2 ± 0.84	44.9 ± 3.0	6.1 ± 0.4	13.7 ± 1.2
WT	TAC	7	25.0 ± 1.3	6.9 ± 0.2 <sup>#</sup>	41.8 ± 5.4	6.6 ± 0.5	14.1 ± 0.7
Rag1 <sup>-/-</sup>	sham	3	29.7 ± 1.5	5.6 ± 0.4	52.6 ± 1.7	5.1 ± 0.2	12.7 ± 1.0
Rag1 <sup>-/-</sup>	TAC	7	27.7 ± 1.7	6.7 ± 0.2*	48.7 ± 1.1	5.5 ± 0.2	12.6 ± 0.5

Results are presented as mean ± sd; BW = body weight, HW = heart weight, LW = liver weight, LuW = lung weight, KiW = kidney weight. Two way ANOVA statistics show significant differences in the ration of heart weight to body weight between TAC and sham groups in B6 and Rag1<sup>-/-</sup> mice. <sup>#</sup> P < 0.001, \* P < 0.05 vs sham controls.

Table 2.2 Echocardiographic analysis of heart size and function in WT and Rag1<sup>-/-</sup> mice five weeks after TAC or sham surgery

genotype	treatment	n	FS (%)
WT	sham	3	39 ± 1.8
WT	TAC	7	25.3 ± 1.2*
Rag1 <sup>-/-</sup>	sham	3	32.2 ± 1.8 <sup>#</sup>
Rag1 <sup>-/-</sup>	TAC	7	28.4 ± 1.8

FS = fractional shortening; \* P < 0.05; <sup>#</sup> P < 0.001 vs WT sham control

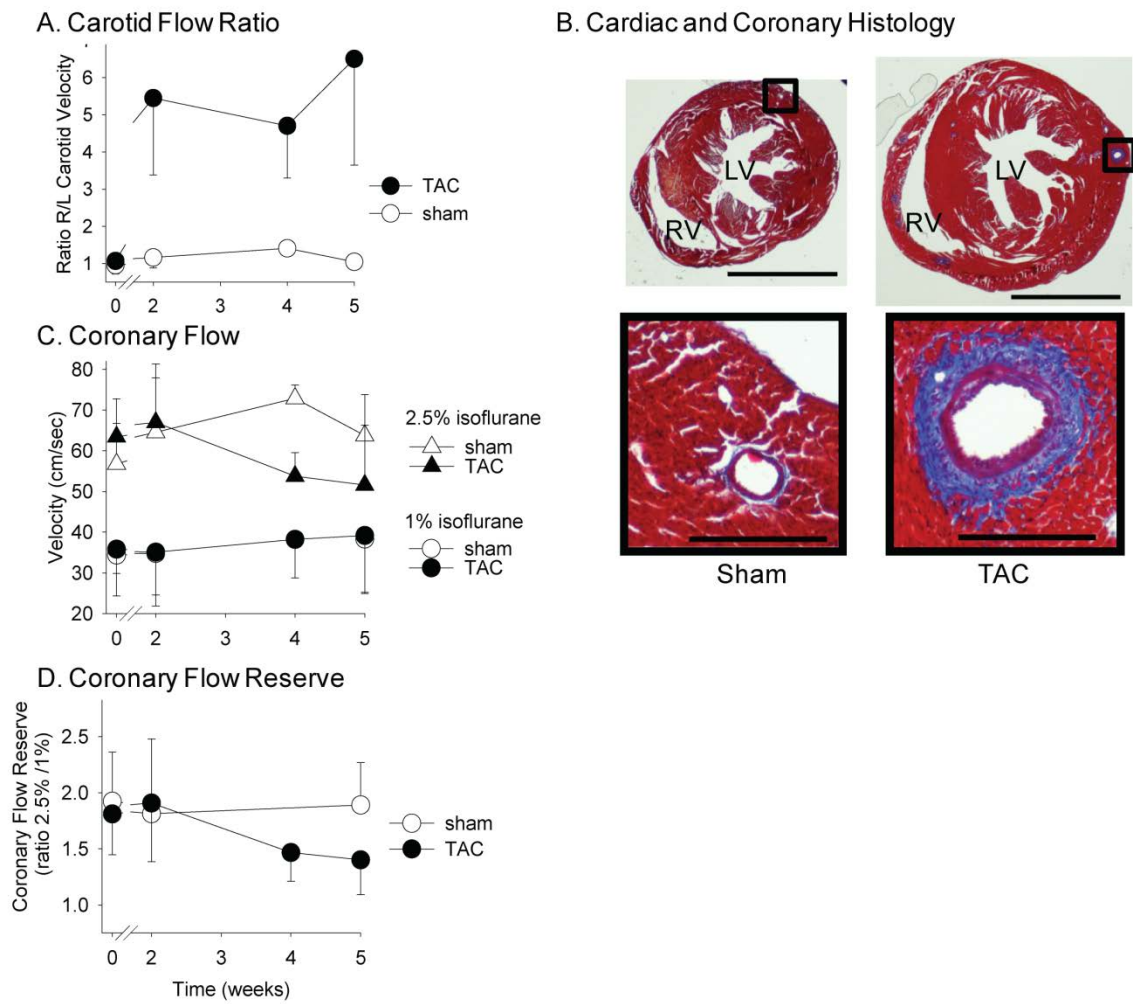


Figure 2.1 TAC-induced LV pressure overload stimulates left coronary remodeling and dysfunction in wild-type C57BL/6 male mice.

A) Ratio of right/left (R / L) peak Doppler flow velocity in carotid arteries before and at indicated times after TAC (closed circle) or sham (open circle) surgery. B) Representative images of Masson's Trichrome stained left ventricle showing left coronary arteries five weeks after sham or TAC surgery. (Top bar = 2323  $\mu\text{m}$ ; bottom bar = 230  $\mu\text{m}$ ). C) Impact of sham (open) and TAC (closed) surgery on coronary flow velocity in mice anesthetized with 1 % (baseline conditions; circles) and 2.5 % (hyperemic conditions; triangles) isoflurane. D) Coronary flow reserve (CFR), measured as the ratio of flow velocity in mice anesthetized with 2.5 % isoflurane to that observed in mice anesthetized with 1 % isoflurane, declines in TAC (closed circle) but not sham (open circle) mice, indicating vascular dysfunction.

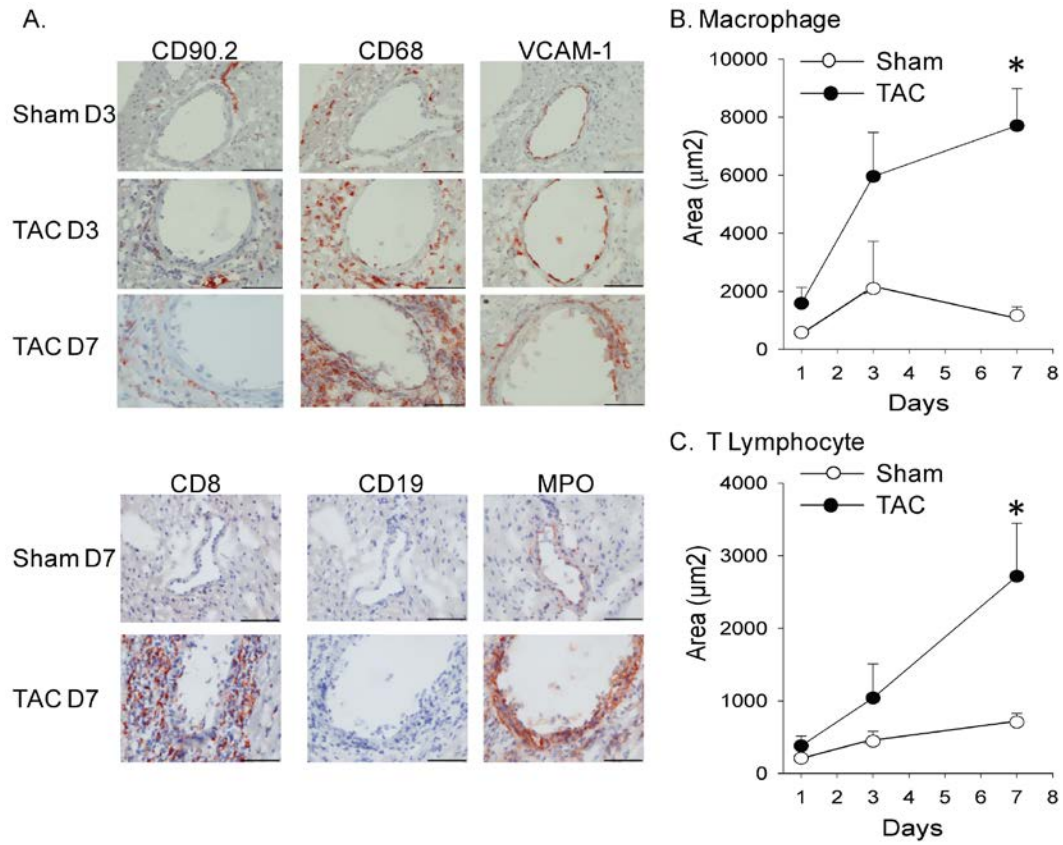


Figure 2.2 TAC elicits an early inflammatory response in wild-type (C57BL/6) male mice.

A) Immunohistochemical staining of inflammatory cells and adhesion molecules in LV sections from wild-type male mice subjected to sham or TAC surgery and sacrificed at different time points (D = days). Positive staining is in red-brown (mag. 40X; Bar = 70  $\mu$ m). T lymphocytes are indicated by CD90.2 and CD8; CD19 is a B lymphocyte marker. VCAM is an endothelial inflammatory marker and myeloperoxidase (MPO) an enzyme stored and released by neutrophils and macrophages. B) and C) Quantification of the accumulation of macrophage (CD68) and T lymphocyte (CD90.2), as measured by area of positive staining in and around the coronary arteries, at different time points following sham (open circles) and TAC (closed circles) surgery. Values are presented as mean  $\pm$  SEM. The images are representative of those obtained in the following numbers. For macrophages: TAC day one, n = 5; TAC day three, n = 7; TAC day seven, n = 9; sham day one, n = 3; sham day three, n = 4; sham day seven, n = 5. For lymphocytes: TAC day one, n = 7; TAC day three, n = 6; TAC day seven, n = 6; sham day one, n = 4; sham day three, n = 5; sham day seven, n = 5. \*P < 0.05 versus same time point in sham.

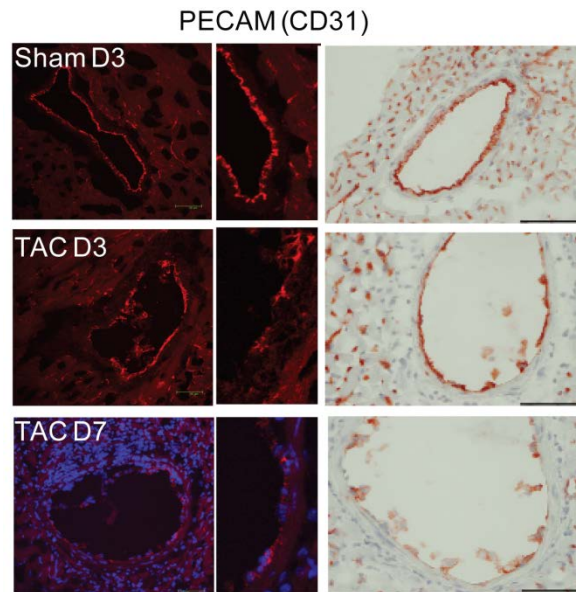


Figure 2.3 Endothelial disruption at three and seven days after TAC surgery.

Confocal (left and middle panel) and IHC (right panel) images of PECAM (CD31) staining along the lumen of left coronary arteries at three days after sham surgery (sham D3) and at three (TAC D3) and seven days (TAC 7D) after TAC surgery. CD31 staining appears continuous along the luminal side in sham mice and discontinuous along similar vessels in TAC mice. Bar = 70  $\mu$ m.

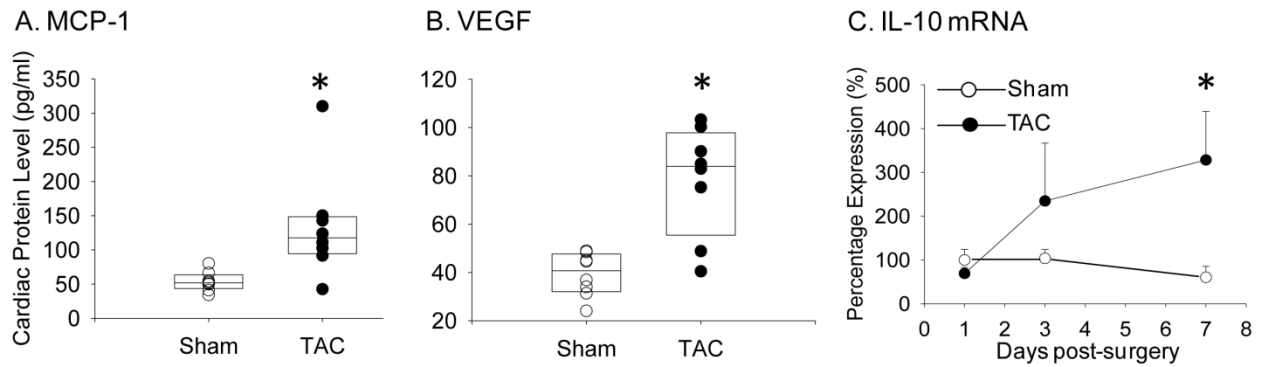


Figure 2.4 Upregulation of inflammatory markers after TAC in wild-type mice.

Levels of MCP-1 (A) and VEGF (B) were measured in homogenized LV at seven days after sham (n = 6) or TAC surgery (n = 8) by Luminex assay. Protein expression (pg / ml) in the homogenate is reported for each individual mouse, and boxes indicated median and 95 % CI. (C) RNA was isolated from LV apex at one to seven days after TAC (n = 3 – 7 per time point). IL-10 mRNA levels were measured by qPCR and values normalized to the sham value at day one, which was set at 100 % expression, and presented as mean  $\pm$  SD. \*P < 0.05 versus sham.



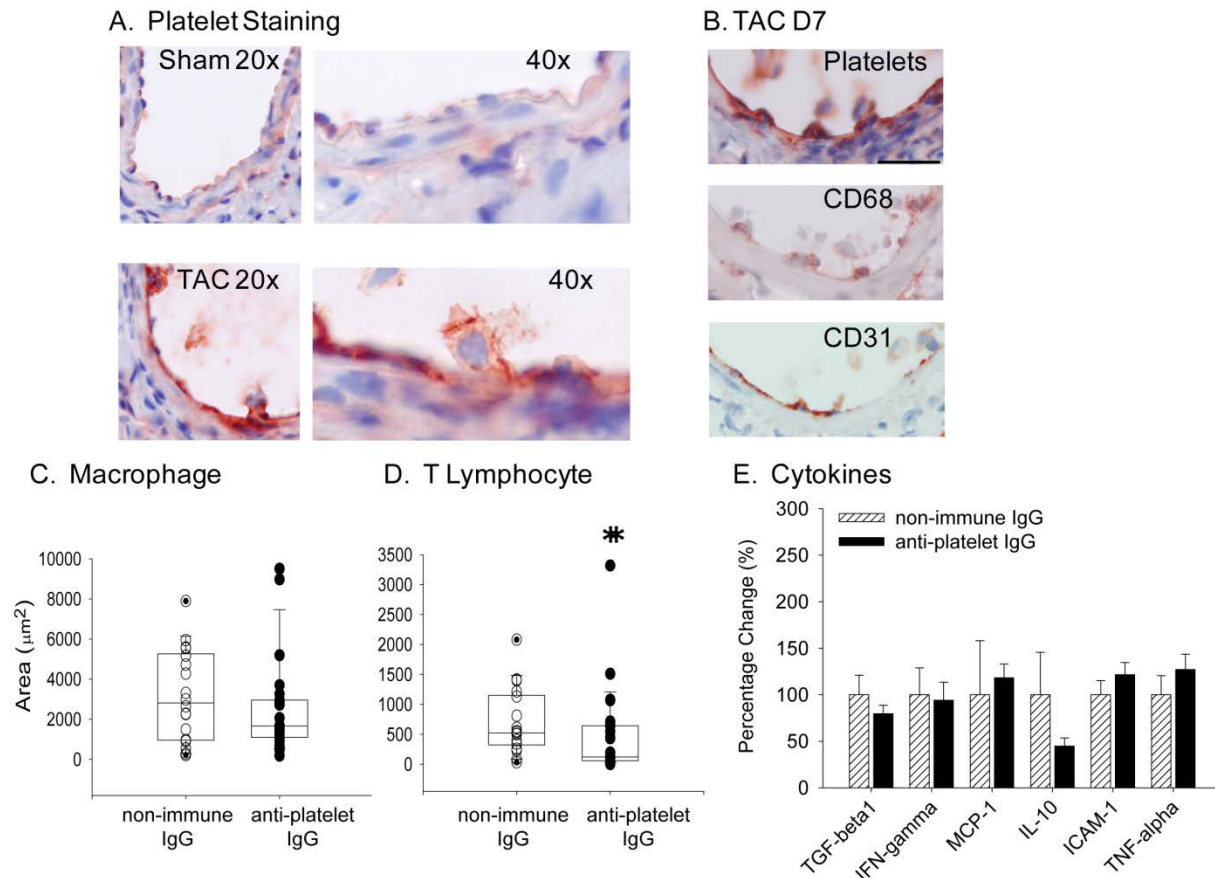


Figure 2.5 Platelet accumulation and effects on perivascular inflammation.

A) Immunohistochemical staining for platelets three days after TAC (mag. 40X). B) Platelet deposition colocalized with macrophages in coronary arteries at seven days after TAC (TAC D7). Serial sections through coronary arteries were stained with antibodies to platelets (top), CD68 (middle) and CD31 (bottom). (mag. 40X; Bar = 70  $\mu\text{m}$ ). Area of positive perivascular staining for C) macrophages (vessel number = n, anti-GPIb $\alpha$  IgG n = 23, non-immune IgG n = 18) and D) T lymphocytes (vessel number = n, anti-GPIb $\alpha$  IgG n = 26, non-immune IgG n = 18) three days after TAC. \*P = 0.05. E) Expression of inflammation markers in LV apex at three days post-TAC was measured by qPCR (mice number = n, anti-GPIb $\alpha$  IgG n = 13, non-immune IgG n = 10) presented as mean  $\pm$  SD.

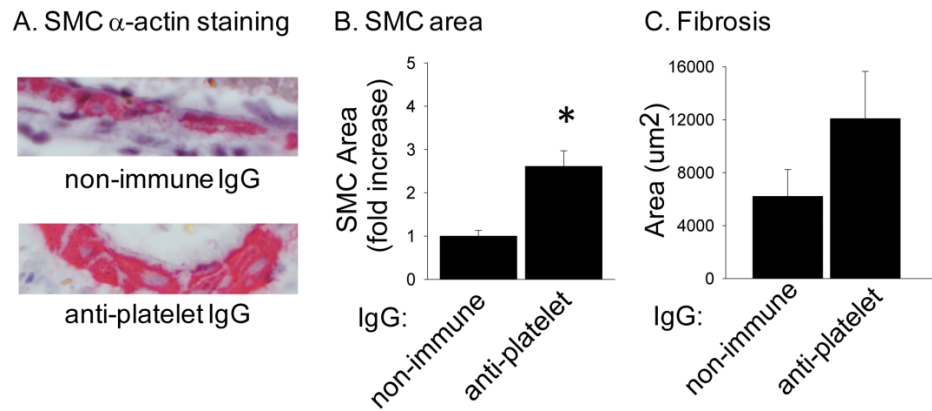


Figure 2.6 Thrombocytopenia promotes coronary vessel remodeling and perivascular fibrosis after TAC.

A) Representative images (mag. 40X) and B) quantification of  $\alpha$ -smooth muscle actin staining in coronary arteries of thrombocytopenic (anti-GPIIb $\alpha$  IgG treated) and control (non-immune IgG injected) mice five weeks after TAC surgery (vessel number = n, anti-GPIIb $\alpha$  IgG n = 11, non-immune IgG n = 5). \*P < 0.05. C) Area of pericoronary fibrosis thrombocytopenic and control mice five weeks after TAC (vessel number = n, anti-GPIIb $\alpha$  IgG n = 10, non-immune IgG n = 5). Fibrosis was identified by Masson's Trichrome stain and reported as area mean  $\pm$  SEM.

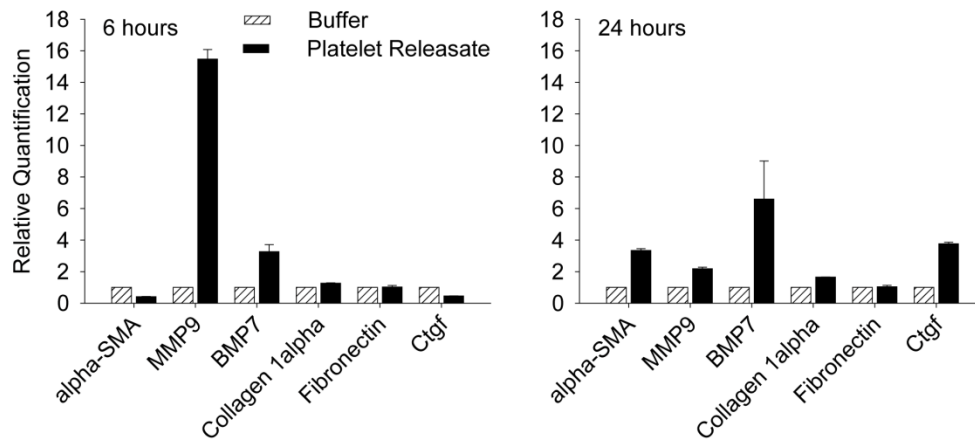


Figure 2.7 The effects of platelet releasate on myocardial fibroblasts.

qPCR was performed to detect the differences of mRNA expression in cardiac fibroblasts exposed to platelet releasate (dark bars) or buffer (open bars) for six (left) or 24 (right) hours. The values were normalized to the buffer-treatment group at the same time point, which was set at fold increase and presented as mean  $\pm$  SD.

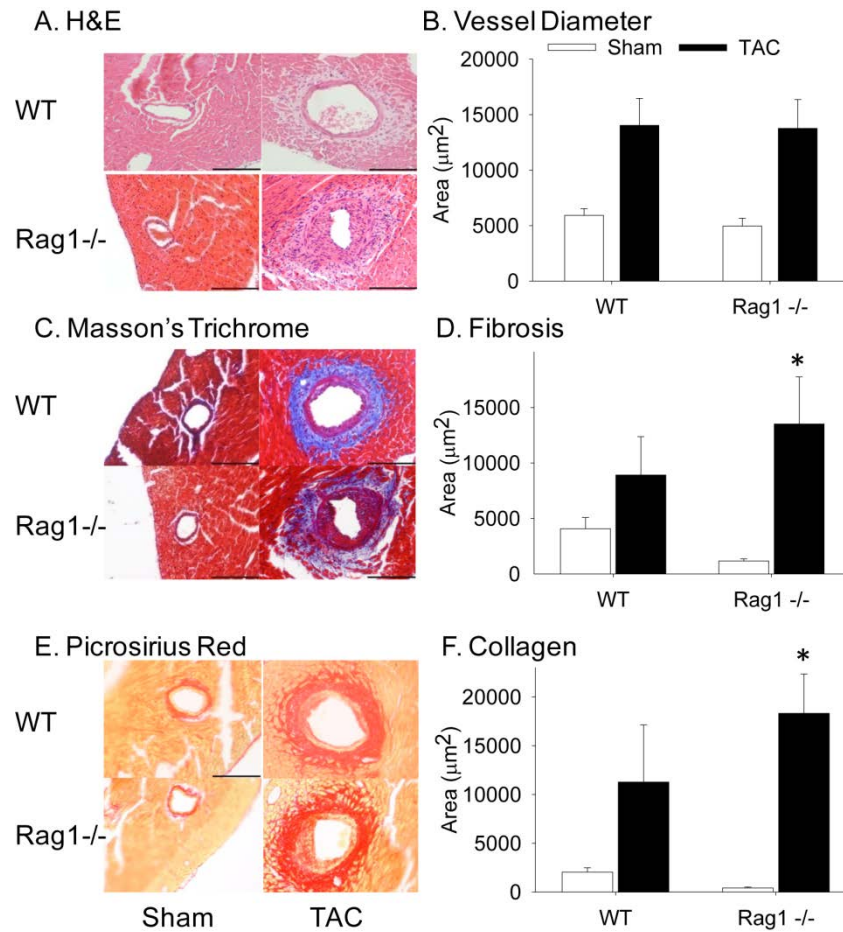


Figure 2.8 Enhanced TAC-induced coronary remodeling in the absence of lymphocytes.

A) H&E staining (mag. 20X) and B) measurement of vessel area inside the external elastic lamina in wild-type (WT) and Rag1<sup>-/-</sup> male mice five weeks after sham or TAC surgery (TAC: WT n = 10, Rag1<sup>-/-</sup> n = 17. Sham: WT n = 9, Rag1<sup>-/-</sup> n = 6). C) Masson's Trichrome staining and D) quantification of pericoronary fibrosis formation in WT and Rag1<sup>-/-</sup> male mice five weeks after surgery reported as area mean ± sem (TAC: WT n = 10, Rag1<sup>-/-</sup> n = 13. Sham: WT n = 9, Rag1<sup>-/-</sup> n = 6). E) Picrosirius red staining and F) quantification of pericoronary collagen deposition in WT and Rag1<sup>-/-</sup> male mice five weeks after surgery reported as area mean ± sem (TAC: WT n = 9, Rag1<sup>-/-</sup> n = 19. Sham: WT n = 7, Rag1<sup>-/-</sup> n = 7). \*P < 0.05. Bar = 145 μm.

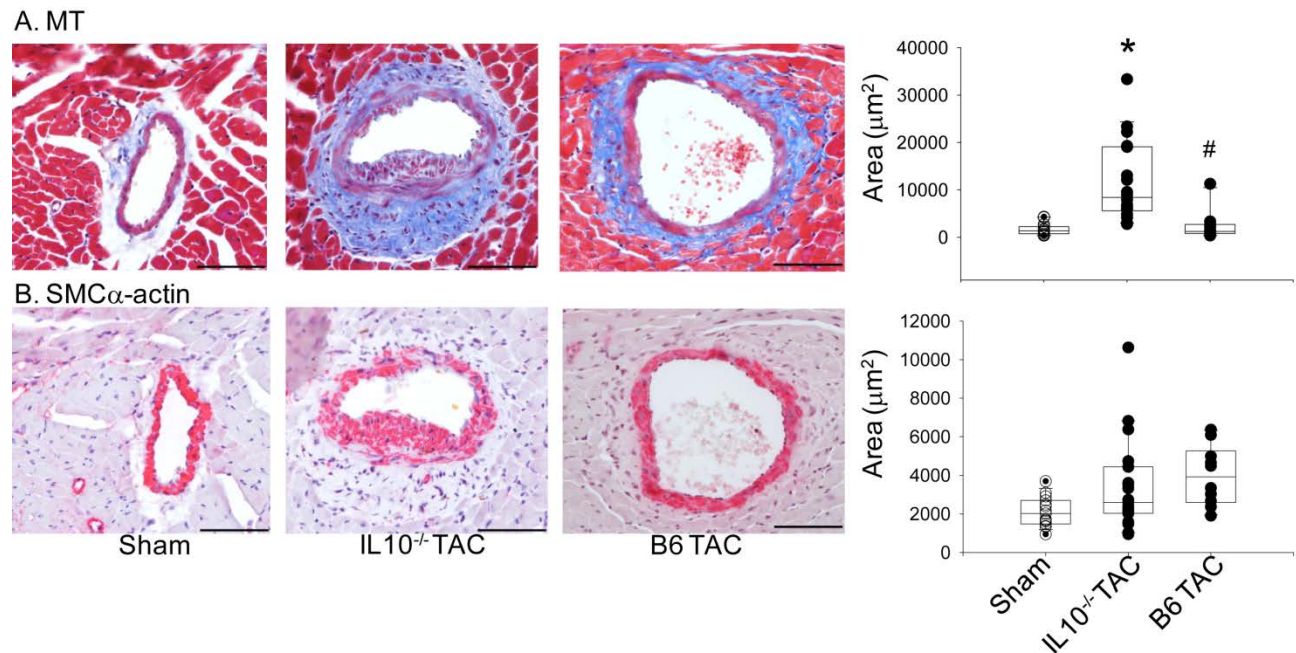


Figure 2.9 TAC-induced coronary remodeling in the absence of IL-10.

A) Representative sections stained with Masson's Trichrome (MT) and visualized at 40X mag. five weeks after sham or TAC surgery (left) and measurements of perivascular fibrosis area (sham n = 5; TAC n = 5). B) SMC  $\alpha$ -actin staining five weeks after sham or TAC surgery (left) and measurements of vessel area occupied by SMC  $\alpha$ -actin (right). \*P < 0.05. Bar = 70  $\mu$ m.

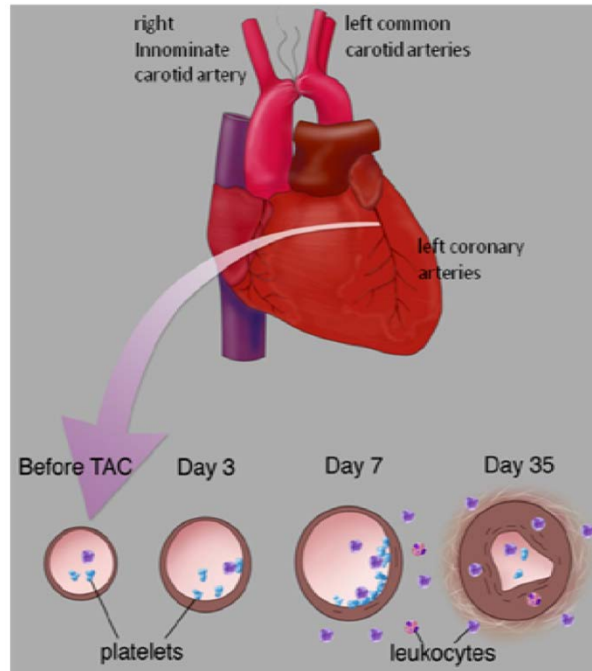
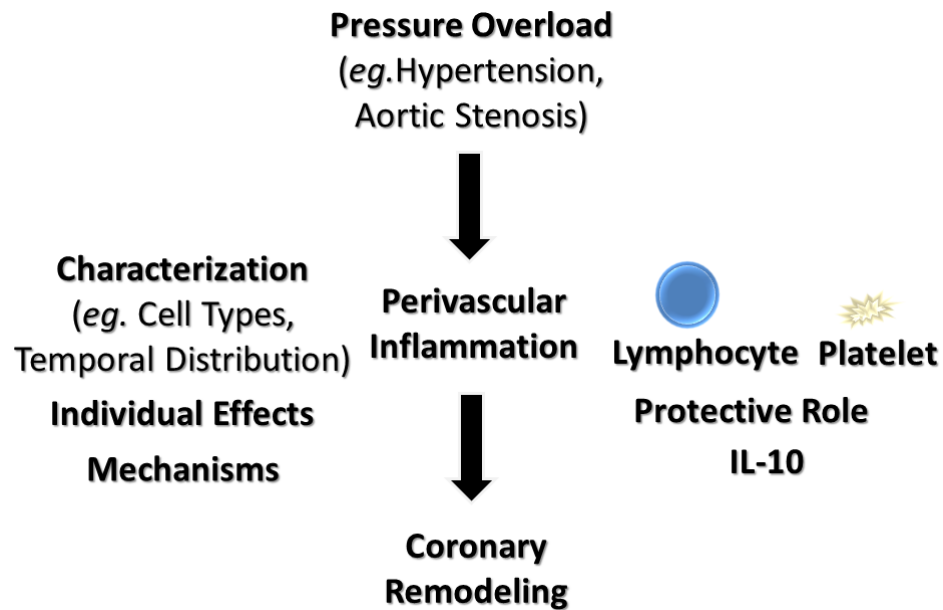


Figure 2.10 Model of TAC-induced early inflammatory responses in which platelets and inflammatory cells are recruited and contribute to the subsequent development of intimal hyperplasia and fibrosis.

## SUMMARY



To summarize the work accomplished in CHAPTER 2: we have observed and characterized the pericoronary accumulation of macrophages, T lymphocytes and platelets early after TAC-induced LV pressure overload. Platelet-depleted mice and lymphocyte-deficient mice revealed both platelets and lymphocyte play a protective role in TAC-induced coronary remodeling, likely, mediated by IL-10.

## **CHAPTER 3: PLATELET RELEASATE PROMOTES CARDIAC HYPERTROPHY FOLLOWING LEFT VENTRICULAR PRESSURE OVERLOAD**

### **INTRODUCTION**

As a consequence of chronically elevated afterload, hypertension stimulates an increase in left ventricular mass or hypertrophy (LVH) and fibrosis, with resultant LV systolic and/or diastolic dysfunction. Hypertensive left ventricular hypertrophy is accompanied by perivascular inflammation, which may contribute to cardiac remodeling. In animals, LV pressure-overload can be modeled by transverse aortic constriction (TAC). We and others have reported that inflammatory cells, including macrophages, T lymphocytes and platelets, accumulated along and within the coronary arteries within days after TAC. The early accumulation of these cells may influence subsequent arterial and ventricular remodeling.

In addition to direct cell-cell interactions, inflammatory cells communicate with the surrounding tissue by releasing cargo stored within granule compartments. Platelets, for example, have three distinct types of secretory vesicles:  $\alpha$ -granules, dense granules and lysosomes, which are a rich source of cytokines, chemokines and growth factors. Components of platelet releasate e.g. serotonin, TGF $\beta$ -1, S1P, have been implicated as regulators of pathologic cardiac remodeling. Thus, it is possible that platelet deposition in the setting of LV pressure overload could influence the tissue response. To investigate the role of granular secretion in LVH and cardiac remodeling, we made use of mice that lack the ability to release cargo from granules.

Platelet granule secretion requires vesicular docking, tethering, priming and membrane fusion. Vesicular fusion is driven by soluble NSF attachment protein receptors (SNARE) complexes,



composed of a VAMP, a Syntaxin, and SNAP-23 proteins [101,119]. Members of the Rab family of Ras GTPases are essential for membrane tethering that occurs prior to fusion [115]. The Rab27 effector protein Munc13-4 appears to play an important role in granular secretion [115,150,154-159]. Several mutations, including a single point mutation in *Munc13-4*, can result in type 3 familial hemophagocytic lymphohistiocytosis (FHL3), which is characterized by hepatosplenomegaly, anemia, and thrombocytopenia [150]. *Unc13d*<sup>jinx</sup> (Jinx) mice carry a mutation in *Unc13d*, the murine homolog of *Munc13-4*, and display secretion defects in natural killer cells, cytotoxic T lymphocytes, neutrophils, mast cells and platelets [153-158] and features of FHL3 [162]. Neutrophils from Jinx mice have alterations in secretion of MMP-9 and MPO, whereas overexpression of Munc13-4 enhances MMP-9 secretion in human neutrophils [156]. Jinx platelets display defects in dense granule,  $\alpha$ -granule and lysosome secretion upon thrombin stimulation in Jinx mice. The addition of Munc13-4 protein restores secretion to mutant platelets and increases secretion in wild-type platelets [154]. The relatively low levels of Munc13-4 in platelets and the partial secretion defects in heterozygous mice have led to the suggestion that the protein may be the rate limiting factor in platelet granular secretion [154]. In this report, we used Jinx mice to determine the contribution of granular secretion to LV remodeling following TAC. Chimeric mice were created by bone marrow transplantation to identify a role for cargo release from bone marrow derived cells. While the loss of Munc13-4 did not affect the initial development of LVH, sustained hypertrophy did not occur in the absence of Munc13-4 in bone marrow derived cells. Cardiac hypertrophy could be restored by administration of platelets or platelet releasate to chimeric mice. These results suggest that

sustained LVH in the setting of pressure overload depends on factor(s) secreted from bone marrow cells, likely from platelets.

## MATERIALS AND METHODS

*Mice.* All procedures conformed to the recommendations of *Guide for the Care and Use of Laboratory Animals* (Department of Health, Education, and Welfare publication number NIH 78-23, 1996) and were approved by the Institutional Animal Care and Use Committee. C57BL/6 mice were purchased from Jackson laboratories. *Unc13-d<sup>Jinx</sup>* (Jinx) mice were generously provided by Dr. Sidney W. Whiteheart. The Jinx mutation was originally identified in a MCMV susceptibility screen performed in offspring of C57BL/6 mice that had been subject to random *N*-ethyl-*N*-nitrosourea (ENU)-induced germline mutagenesis [199]. Mice were housed in cages with HEPA-filtered air in rooms on 12-hour light cycles and fed Purina 5058 rodent chow ad libitum.

*Bone Marrow Transplantation.* Bone marrow cells were isolated from 8-12 week-old donor mice by flushing femurs and tibias with 5 ml ice-cold media (RPMI, 10 mM HEPES, 25 units/ml heparin, 5% FBS) using a 27.5 gauge needle. The cells were washed by centrifugation (453g, at 4 °C for 10 minutes), RBCs lysed in hypotonic saline, and the remainder of the cells suspended in PBS containing 2% heat-inactivated FBS at  $5 \times 10^7$  cells / ml. Six to 8 week-old recipient mice were irradiated twice (450 rad) 3 hours apart, and then injected with  $5 \times 10^6$  cells within 4 hours after the second irradiation.

*Transverse Aortic Constriction (TAC):* TAC and sham surgery was performed as previously described [200].

*Washed Platelet Preparation.* Blood was collect into ACD (2.5% sodium citrate, 0.4% citric Acid, 1.5% D-glucose) anticoagulant supplement with 1  $\mu$ M PGE<sub>1</sub> and diluted with normal saline prior to centrifugation (201 x g for 10 minutes at room temperature) to obtain platelet-rich

plasma/saline. After washing red blood cells an additional time, supernatants were pooled, supplemented with 1  $\mu$ M PGE<sub>1</sub>, and centrifuged to pellet the platelets (974g for 10 minutes at room temperature). The platelet pellet was washed by resuspension in citrate-glucose-saline buffer, pH 6.5, and centrifugation. Washed platelets were resuspended at  $1 \times 10^9$ /mL in Tyrode's buffer (NaHCO<sub>3</sub> 12mM, NaCl 138mM, D-glucose 5.5mM, KCl 2.9mM, MgCl<sub>2</sub>.6H<sub>2</sub>O 2mM, NaH<sub>2</sub>PO<sub>4</sub>.H<sub>2</sub>O 0.42mM, HEPES 10mM), pH 7.4.

*Platelet Aggregation.* Platelets were diluted to  $1 - 3 \times 10^8$ /mL in Tyrodes buffer and allowed to rest for at least 30 min. Aggregation was performed at 37 °C in a Chronolog dual chamber lumiaggregometer in silicon-coated cuvettes with stir bars.

*Platelet Releasate.* Washed platelets ( $1 \times 10^9$ /mL) suspended in Tyrode's buffer were pre-incubated at 37 °C for 10 minutes and stimulated with thrombin (0.125 U/mL) for 10 minutes at 37 °C. To measure TGF $\beta$ -1, the suspension was centrifuged (14,000 g for 20 minutes in 4 °C) to collect supernatant and platelet pellets. Releasate to inject into mice was obtained by centrifugation at 3,000 x g for 10 minutes at 4 °C.

*Lipid Extraction and S1P Determinations* were performed as described previously [201]. 2 mL methanol, 1 mL of chloroform and 450  $\mu$ L of 0.1 M HCl was added into 8 mL borosilicate glass tube with addition of 50  $\mu$ L plasma sample from each mouse. 50  $\mu$ L of C17 S1P was also added as internal standard. The mixture was vortexed for 5 minutes and placed in 4 °C overnight. 1 mL chloroform and 1.3 mL 0.1 M HCl were added and the mixture was vortex for 5 minutes to separate phases. The tubes were centrifuged at  $>3,000 \times g$  for 10 minutes. The lower phase was transferred to 4 mL screwed-cap tube using a Pasteur pipette. Samples were evaporated to dryness under N<sub>2</sub> using N-evap in fume hood. 100  $\mu$ L of methanol was added to each tube

which was then vortexed and stand for 10-15 minutes at room temperature before transferred to autosampler insert vial for mass spectrometry study. Analysis of S1P, sphingosine and hexadecenal (as its semicarbazone derivative) were accomplished using a Shimadzu UFLC (ultra-fast liquid chromatography) coupled with an ABI 4000-Qtrap hybrid linear ion trap triple quadrupole mass spectrometer in MRM (multiple reaction monitoring) mode using C17-S1P.

*Statistical Analysis* All results were expressed as mean  $\pm$  standard deviation (SD). Statistical significance within strains was determined using *t*-test or two-way ANOVA with multiple pairwise comparisons as appropriate. In *t*-test, if samples failed the normality test, Rank *t*-test were used. In some cases of two-way ANOVA, data was Log-transformed to be normally distributed. Statistical analysis was performed using Sigma-STAT software, version 3.5 (Systat Software, Inc.). A *p*-value of less than 0.05 was considered significant.

## RESULTS

To create animals with impaired cargo release from hematopoietic cells, wild-type C57BL/6 (WT) male mice were lethally irradiated and reconstituted with bone marrow isolated from Jinx mice, which lack functional Munc13-4 (Jinx>WT). WT mice that received WT marrow (WT>WT) were used as the controls. Immunoblot analysis confirmed the absence of Munc13-4 in platelets from WT mice reconstituted with Jinx cells (Jinx>WT) (Figure 3.1). No difference in blood cell counts was observed in the chimeric mice (Table 3.1).

### **Lack of Munc13-4 does not alter early response to pressure overload.**

At 6 – 7 weeks after bone marrow transplantation, mice were subjected to sham or TAC surgery. Prior to surgery, cardiac function was similar in WT mice that had received WT marrow (WT>WT) and Jinx marrow (Jinx>WT) (Table 3.2). Our previous findings indicated that inflammatory cells and platelets accumulate along coronary vessels and within ventricular tissue within days after pressure overload. Both cell types have been implicated by us and others as modulating cardiac remodeling, and release of granule contents is one mechanism by which these cells could influence the response to pressure overload. Therefore, we examined the consequences of lack of Munc13-4 in bone marrow derived cells early after TAC. Bone marrow transplant did not affect the initial hypertrophic responses at Day 7 after TAC. The heart weight : body weight (HW: BW) ratio in WT>WT mice was  $6.67 \pm 0.69$  mg/g following TAC which is higher than the  $5.48 \pm 0.31$  mg/g observed in sham-operated controls ( $P < 0.001$ ) and similar to that previously reported for WT not subjected to irradiation and transplantation [98]. Jinx>WT chimeric mice that underwent TAC also had significantly higher HW: BW ratios than did

sham counterparts. ( $6.38 \pm 0.85$  versus  $5.21 \pm 0.27$ ;  $P < 0.001$ ). The extent of early cardiac hypertrophy in the Jinx chimers was similar to that observed in WT>WT mice (Figure 3.2A). The development of cardiac hypertrophy in the setting of pressure overload is accompanied by fetal gene reprogramming and increased mRNA expression of *Nppa*, *Nppb*, *Myh7* and *Acta1*. Both WT>WT and Jinx>WT mice exhibited increases of fetal gene expression at 7 days after TAC (Figure 3.2B). Early inflammatory cell accumulation was unaffected by the loss of Munc13-4 in hematopoietic cells (Figure 3.2C). These results indicate that the initial response to pressure overload does not require Munc13-4-dependent events in bone marrow cells.

**Attenuated cardiac hypertrophy 5 weeks after TAC in mice with defects in granule cargo release from hematopoietic cells.**

To determine if granule secretion contributed to the progression of cardiac hypertrophy, the response in mice with WT or Jinx marrow was examined at five weeks after surgery. Blood counts for the mice at this time point are presented in Table 3.3. As expected, WT>WT mice had a significantly higher HW: BW ratio than did sham-operated WT>WT animals ( $7.6 \pm 2.3$  vs.  $5.3 \pm 0.3$ ;  $P = 0.044$ ; Table 3.4). WT>WT mice also had a significant increase in their LV posterior wall thickness following TAC ( $1.3 \pm 0.2$  vs.  $0.8 \pm 0.1$  mm in sham-operated controls;  $P = 0.004$ ; Table 3.4). In contrast, WT mice that were reconstituted with Jinx marrow displayed a less robust increase in cardiac mass at 5 weeks after TAC. While the absolute HW: BW ratio was higher in Jinx>WT that underwent TAC surgery than in sham controls, the difference did not reach statistical significance ( $6.7 \pm 1.0$  vs.  $5.6 \pm 0.6$ ;  $P = 0.32$ ). The same was observed with LV posterior wall thickness ( $0.9 \pm 0.3$  vs.  $0.8 \pm 0.1$  mm;  $P = 0.685$ ) (Table 3.4). There was a

statistically significant difference in HW: BW ratio in the WT>WT and Jinx>WT mice after TAC, indicating more robust development of cardiac hypertrophy in mice expressing Munc13-4 in marrow cells. Masson trichrome staining of heart sections confirmed smaller left ventricular size in WT mice with Jinx marrow cells as compared to WT mice that received WT marrow (Figure 3.3A). These results suggest that the absence of Munc13-4 in hematopoietic cells protects from cardiac hypertrophy at late times after pressure overload.

To determine if absence of hypertrophy at 5 weeks after TAC in Jinx>B6 mice was due to a lack of cardiomyocyte hypertrophy, histomorphometric analysis was performed on LV sections stained with PAS. In comparison to cell size in hearts from B6>B6 mice after TAC, the cardiomyocytes in Jinx>WT mice were 3-fold smaller after TAC (Figure 3.3B). As was observed at 7 days post-TAC, upregulation of *Nppa*, *Nppb*, *Myh7* and *Acta1* occurred in both WT>WT and Jinx>WT mice at 5 weeks after TAC (Figure 3.3C), in the face of lower cardiac mass in Jinx>WT mice. Perivascular fibrosis (Figure 3.4A and 3.4B) and interstitial fibrosis (data not shown) were similar in the two groups as was expression of *Mmp9* and *Col 1a* (Figure 3.4C).

#### **Platelets and platelet releasate partially restores cardiac hypertrophy after TAC in mice lacking Munc13-4 in hematopoietic cells.**

Lack of Munc13-4 impairs degranulation of NK cells, cytotoxic T lymphocytes, and platelets. Platelets, by storing and releasing granule content with activation, may be an important source for proteins and small molecules, such as transforming growth factor  $\beta$ -1 (TGF $\beta$ -1) found in  $\alpha$ -granules and sphingosine-1-phosphate (S1P) that influence cardiac hypertrophy. Jinx platelets do not release contents from dense granules and have severely impaired release of  $\alpha$ -granules



[154]. To test whether the phenotype observed in irradiated WT mice that had been reconstituted with Jinx marrow was due to a defect in platelet secretion, a pilot study was done by administering Jinx>WT chimers with platelets from wild-type WT mice or releasate from thrombin-stimulated WT platelets. The administration of platelets to Jinx>WT mice partially increased the HW: BW ratio after TAC to  $8.2 \pm 1.9$  mg/g versus  $6.9 \pm 0.1$  mg/g observed in control Jinx>WT mice. The HW: BW ratios observed in Jinx>WT mice treated with platelets were similar to those observed in WT>WT mice post-TAC ( $7.4 \pm 0.4$  mg/g versus  $6.8 \pm 0.8$  mg/g). The effect was not solely dependent on intact platelets, as cardiac hypertrophy following TAC was slightly although not significantly increased by administering platelet releasate to Jinx>WT chimers. HW: BW ratio was  $7.4 \pm 0.4$  mg/g in Jinx>WT mice that received releasate from thrombin-stimulated platelets and  $6.8 \pm 0.8$  mg/g in animals that received buffer control (containing thrombin and hirudin). Cardiomyocyte size was slightly higher in the chimeric mice that received platelets ( $301 \pm 98 \mu\text{m}^2$ ) than those that received vehicle ( $289 \pm 26 \mu\text{m}^2$ ). Likewise, injection of platelet releasate leads to a numerical increase of cardiomyocyte size of chimeric mice ( $297 \pm 51 \mu\text{m}^2$  versus  $244 \pm 48 \mu\text{m}^2$ ). Together these results support a role for Munc13-4-mediated platelet secretion in pressure-induced cardiac hypertrophy. In order to detect the possible-existing significance, experiments need to be done with a large number of animals.

TGF $\beta$ -1, which is secreted by a variety of cells, has been implicated in the development of cardiac hypertrophy and fibrosis. Platelets store TGF $\beta$ -1 in  $\alpha$ -granules and therefore serve as a major source for TGF $\beta$ -1. Platelet-derived TGF $\beta$ -1 has been implicated in LVH [179]. We established a role for Munc13-4 in the release of TGF $\beta$ -1 from platelets by measuring its release

from isolated WT and Jinx platelets following thrombin stimulation. Thrombin but not PGE<sub>1</sub> triggered release of TGFβ-1 from WT platelets (Figure 3.5A). TGFβ-1 in releasate from thrombin-stimulated Jinx platelets was 4-fold lower than WT platelets and no different than levels observed after PGE<sub>1</sub> treatment (Figure 3.5A). Despite the observation that Munc13-4 was important for the release of TGFβ-1 from activated platelets *in vitro*, no differences in plasma or serum level of TGFβ-1 were noted in WT and Jinx mice (Figure 3.5B). Furthermore, plasma TGFβ-1 level were similar in WT>WT and Jinx>WT mice (Table 3.5). No difference in plasma TGFβ-1 was observed in sham or TAC mice. Plasma levels were  $1.5 \pm 0.2$  and  $1.7 \pm 0.4$  ng/ml in WT>WT TAC and sham groups and  $1.6 \pm 0.8$  and  $1.3 \pm 0.2$  ng/ml in Jinx>WT TAC and sham groups. Although no differences were observed in plasma levels, TGFβ-1 downstream signaling, as evidence by *Ctgf* expression, was also significantly higher in Jinx>WT than in WT>WT mice at 7 days after TAC (Figure 3.7). Apart from TGFβ-1, S1P is also shown to induce hypertrophic response in cardiomyocyte. Similarly, no difference in plasma S1P level was observed between Jinx>WT and WT>WT mice (Figure 3.6).

Table 3.1 Echocardiography parameters in before surgery

	WT>WT (n=6)	Jinx>WT (n=6)
LVIDd (mm)	4.2 ± 0.2	4.2 ± 0.1
LVPW;d (mm)	0.7 ± 0.2	0.7 ± 0.2
EF (%)	52 ± 5	54 ± 5

LVID;d: left ventricular internal diameter in diastole. LVPW;d: left ventricular posterior wall thickness in diastole. No significant differences were observed between the two groups by Student t-test. ( $P \leq 0.05$  is considered significant.)

Table 3.2 Complete blood count (CBC) 7-day after surgery

	WT>WT Sham (n=3)	WT>WT TAC (n=6)	Jinx>WT Sham (n=3)	Jinx>WT TAC (n=7)
WBC (K/ $\mu$ l)	5.5 $\pm$ 0.6	6.0 $\pm$ 1.5	4.1 $\pm$ 0.7	7.3 $\pm$ 1.7 *
NE (K/ $\mu$ l)	0.7 $\pm$ 0.2	1.4 $\pm$ 0.6	0.5 $\pm$ 0.1	2.2 $\pm$ 1.1 *
LY (K/ $\mu$ l)	4.5 $\pm$ 0.4	4.4 $\pm$ 1.4	3.5 $\pm$ 0.5	4.9 $\pm$ 1.5
MO (K/ $\mu$ l)	0.2 $\pm$ 0.1	0.2 $\pm$ 0.1	0.1 $\pm$ 0.0	0.2 $\pm$ 0.1
HCT (%)	39.1 $\pm$ 1.1	38.9 $\pm$ 2.0	36.0 $\pm$ 2.0 ♦	38.1 $\pm$ 1.5
MCV (fL)	45.6 $\pm$ 1.7	40.7 $\pm$ 1.2 ♦	41.1 $\pm$ 0.5 ♦	41.3 $\pm$ 0.6
PLT (K/ $\mu$ l)	774 $\pm$ 51	794 $\pm$ 103	964 $\pm$ 64 ♦	914 $\pm$ 94 #

WBC: white blood cell; NE: neutrophil; LY: lymphocyte; MO: monocyte; HCT: hematocrit; MCV: mean cell volume; PLT: platelet. ♦ P<0.05 compared to WT>WT Sham; # P<0.05 compared to WT>WT TAC by Two-Way ANOVA.

Table 3.3 Complete blood count (CBC) data of chimeric mice 5-week after surgery

	WT>WT Sham (n=3)	WT>WT TAC (n=3)	Jinx>WT Sham (n=3)	Jinx>WT TAC (n=9)
WBC (K/ $\mu$ l)	14.2 $\pm$ 2.8	7.9 $\pm$ 2.6	8.2 $\pm$ 2.1	8.9 $\pm$ 3.7
NE (K/ $\mu$ l)	1.1 $\pm$ 0.2	1.0 $\pm$ 0.6	0.6 $\pm$ 0.3	1.9 $\pm$ 1.6
LY (K/ $\mu$ l)	11.9 $\pm$ 2.4	6.5 $\pm$ 2.2 $\blacklozenge$	6.7 $\pm$ 1.3 $\blacklozenge$	6.7 $\pm$ 2.3
MO (K/ $\mu$ l)	0.8 $\pm$ 0.1	0.3 $\pm$ 0.2 $\blacklozenge$	0.7 $\pm$ 0.3	0.4 $\pm$ 0.3
HCT (%)	40.7 $\pm$ 1.6	41.6 $\pm$ 1.2	39.7 $\pm$ 1.2	38.4 $\pm$ 4.1
Hbg (g/dL)	10.5 $\pm$ 0.2	11.2 $\pm$ 0.7	10.5 $\pm$ 0.3	11.5 $\pm$ 1.5
PLT (K/ $\mu$ l)	792 $\pm$ 73	846 $\pm$ 121	791 $\pm$ 144	1020 $\pm$ 252

WBC: white blood cell; NE: neutrophil; LY: lymphocyte; MO: monocyte; HCT: hematocrit; MCV: mean cell volume; PLT: platelet.  $\blacklozenge$  P value  $\leq$ 0.05 compared to WT>WT Sham as determined by Two-Way ANOVA.

Table 3.4 WT mice with Jinx marrow are partially protected from LVH at five weeks after TAC

	WT>WT Sham	WT>WT TAC	Jinx>WT Sham	Jinx>WT TAC
HW/BW (mg/g)	5.3 ± 0.3	7.6 ± 2.3 ♦	5.6 ± 0.6	6.7 ± 1.0
LVPW;d (mm)	0.8 ± 0.1	1.3 ± 0.2 ♦	0.8 ± 0.1	0.9 ± 0.3*

HW/BW: heart weight to body weight ratio; LVPW;d: left ventricular posterior wall thickness in diastole. n = 3-9, ♦ P<0.05 compared to WT>WT Sham; \* P<0.05 compared to WT>WT TAC by Two-Way ANOVA.

Table 3.5 Plasma TGF $\beta$ -1 in chimeric mice

	WT>WT Sham	WT>WT TAC	Jinx>WT Sham	Jinx>WT TAC
TGF $\beta$ -1 (ng/ml)	1.5 $\pm$ 0.2	1.7 $\pm$ 0.4	1.6 $\pm$ 0.8	1.3 $\pm$ 0.2

No difference between groups by Two-Way ANOVA. (P value  $\leq$ 0.05 is considered to be significant.)

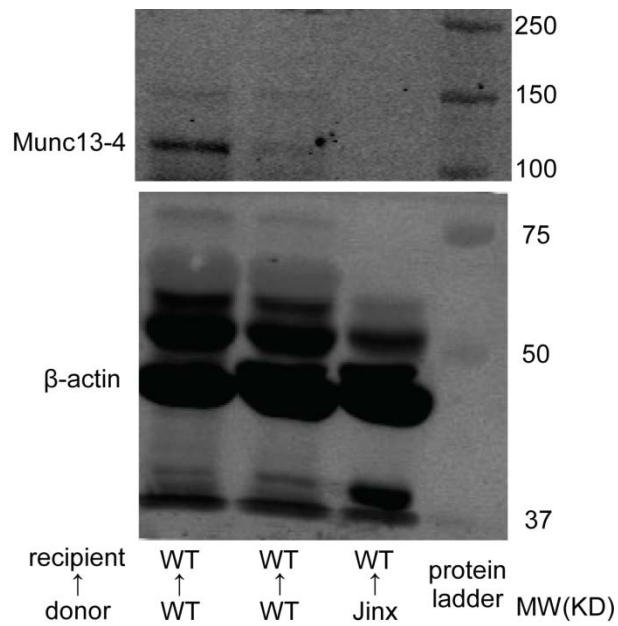


Figure 3.1 Lack of Munc13-4 in irradiated B6 WT mice reconstituted with Jinx marrow cells.

Representative immunoblotting images demonstrate that Munc13-4 protein (120 KD) was present in platelet lysate of WT>WT mice, but absent in Jinx>WT BMT mice.  $\beta$ -actin (45 KD) was used as a loading control.



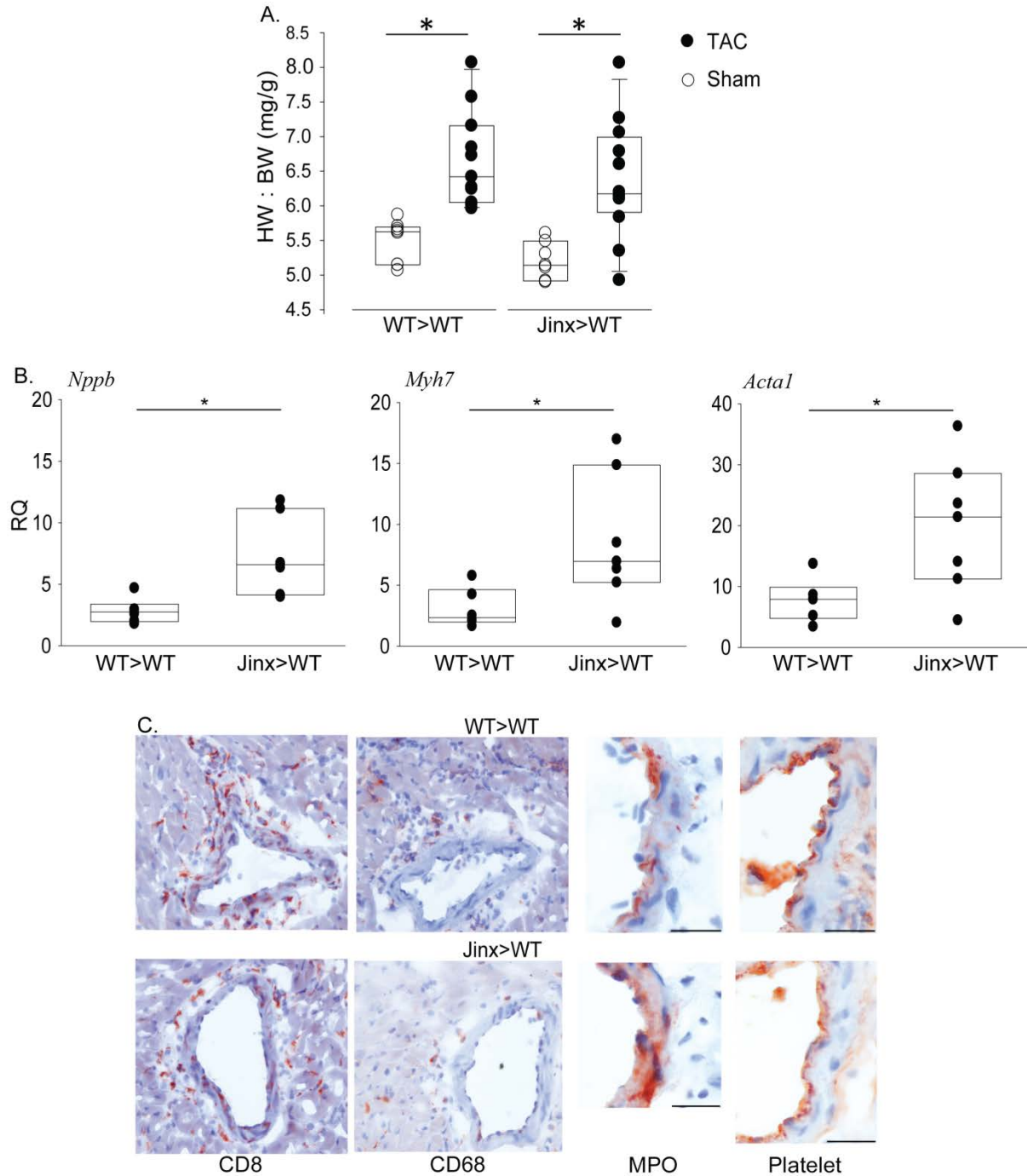


Figure 3.2 TAC-induced cardiac hypertrophy and perivascular inflammation 7 days after surgery.

A) Heart weight to body weight ratio (HW: BW) of chimeric mice. In box-plot, the median with 10<sup>th</sup>, 25<sup>th</sup>, 75<sup>th</sup> and 90<sup>th</sup> percentiles are shown as vertical boxes with error bars. Error bars values are column means. Animal number / group: WT>WT Sham = 8, WT>WT TAC = 11, Jinx>WT

Sham = 7, Jinx>WT TAC = 12 \*P < 0.001 by Two-Way ANOVA. B) Real-time quantitative PCR was performed to measure mRNA of fetal genes in hearts from chimeric mice. *Nppb* (brain natriuretic peptide), *Myh7* ( $\beta$ -myosin heavy chain), and *Acta1* (skeletal muscle  $\alpha$ -actin). Values are reports as normalized to those observed in WT>WT sham mice (set at 1). N per group: WT>WT TAC = 6, Jinx>WT TAC = 7. \*P < 0.05 by Student t-test. C) Representative images (40 $\times$ ) of perivascular accumulation of T lymphocytes (CD8), macrophages (CD68), as well as deposition of MPO and platelets. (bar = 70  $\mu$ m)

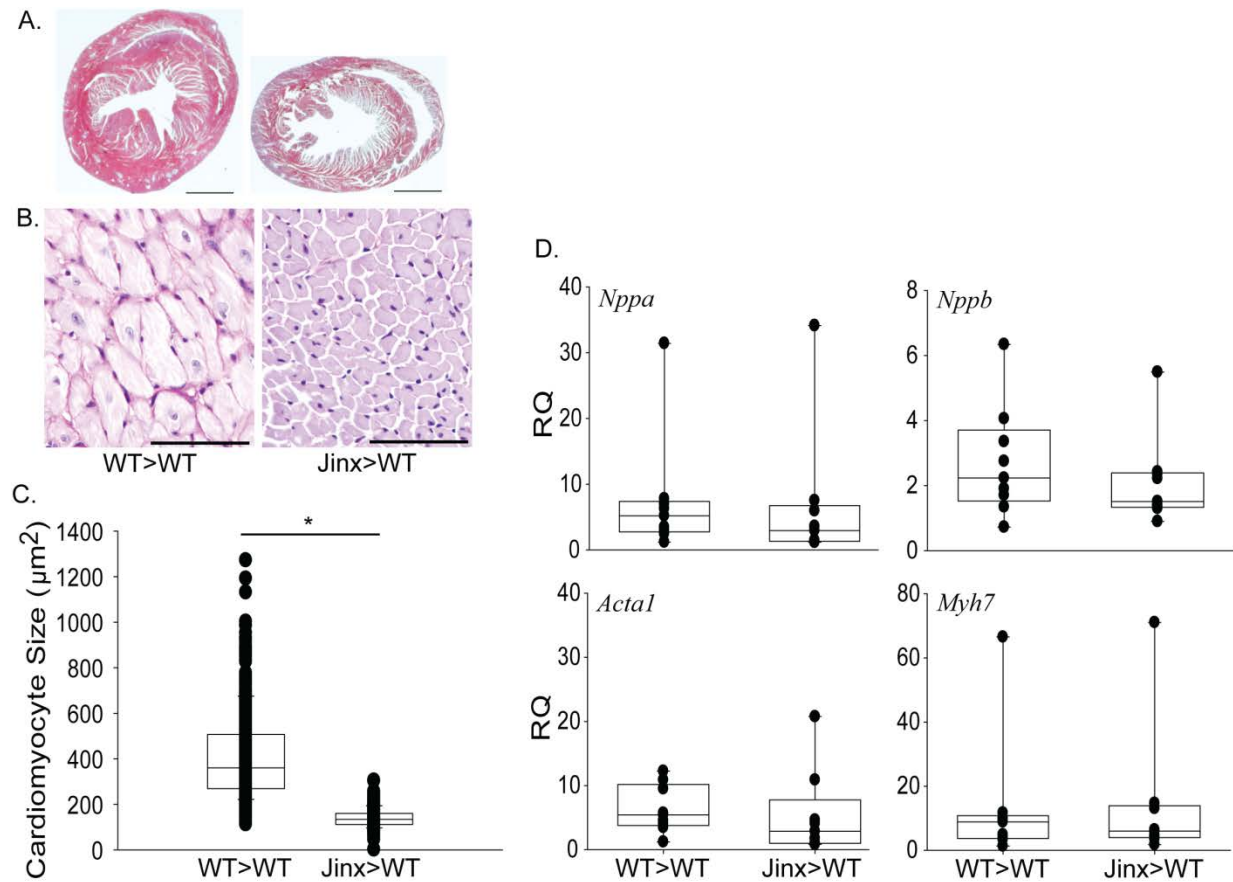


Figure 3.3 Jinx chimeric mice are protected from cardiac hypertrophy 5 weeks after TAC.

A) Representative images of heart sections stained with Masson's trichrome from WT>WT and Jinx>WT mice (1×, Bar = 4083 μm). B) Representative images from periodic acid-Schiff (PAS) stained sections (40×, Bar = 70 μm). C) Quantification of cardiomyocyte area demonstrated reduced cardiomyocyte size in Jinx>WT mice compared to WT>WT mice. Histology quantification was done by Metamorph software. n = 4 mice / group. \*P < 0.001 by Student *t*-test. D) Real-time quantitative PCR was performed to measure mRNA of fetal genes in hearts from chimeric mice. *Nppa* (atrial natriuretic peptide), *Nppb* (brain natriuretic peptide), *Acta1* (skeletal muscle α-actin) and *Myh7* (β-myosin heavy chain). Values are reports as normalized to those observed in WT>WT sham mice (set at 1). n = 9 mice / group. No difference were

observed between WT>WT and Jinx>WT values after TAC by Student *t*-test, with  $P < 0.05$  was considered significant.

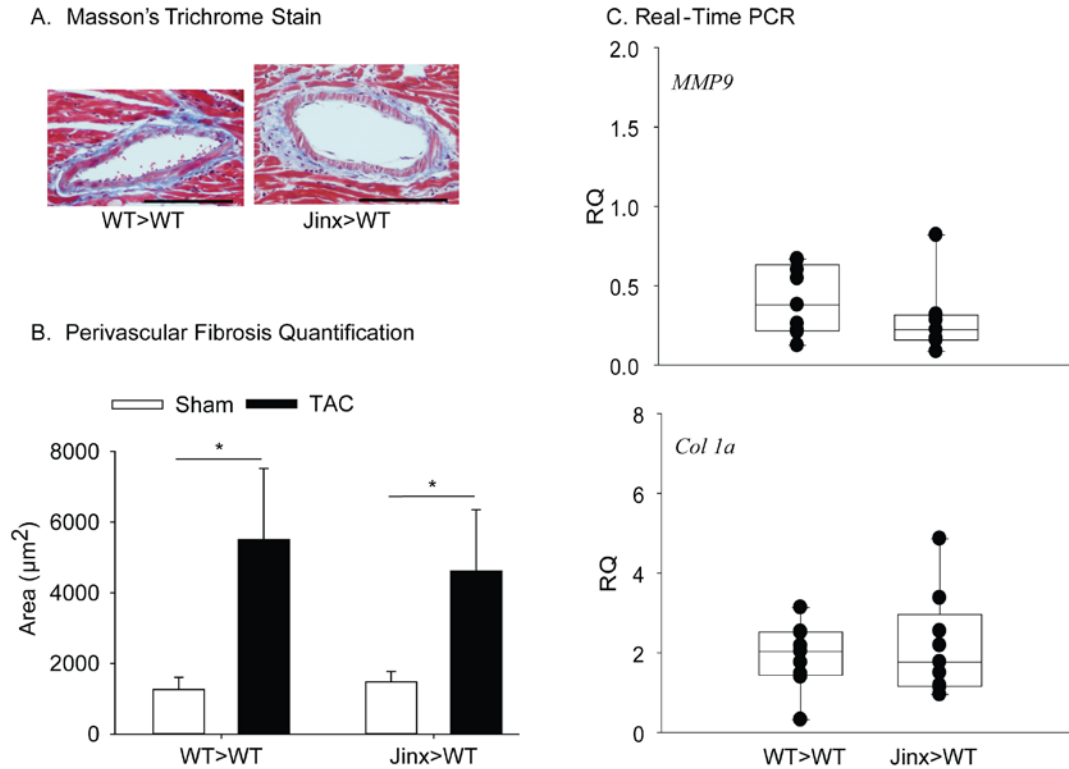


Figure 3.4 Cardiac fibrosis 5 weeks after TAC.

A) Representative images of Masson's trichrome staining (20 $\times$ , Bar = 145  $\mu$ m) and B) quantification of peri-vascular fibrosis in mice 5 weeks after surgery. N / group: WT>WT Sham = 3, WT>WT TAC = 9, Jinx>WT Sham = 3, Jinx>WT TAC = 9. Data were presented as Mean (bar) with SEM (error bar). Data were Log-transformed for Two-Way ANOVA, \* $p < 0.001$ . C) Real-time quantitative PCR of *MMP9* (Matrix Metalloproteinase 9) and *Col 1a* (Collagen 1). Values are reports as normalized to those observed in WT>WT sham mice (set at 1). n= 9 mice / group. No significant difference was observed by Student *t*-test.

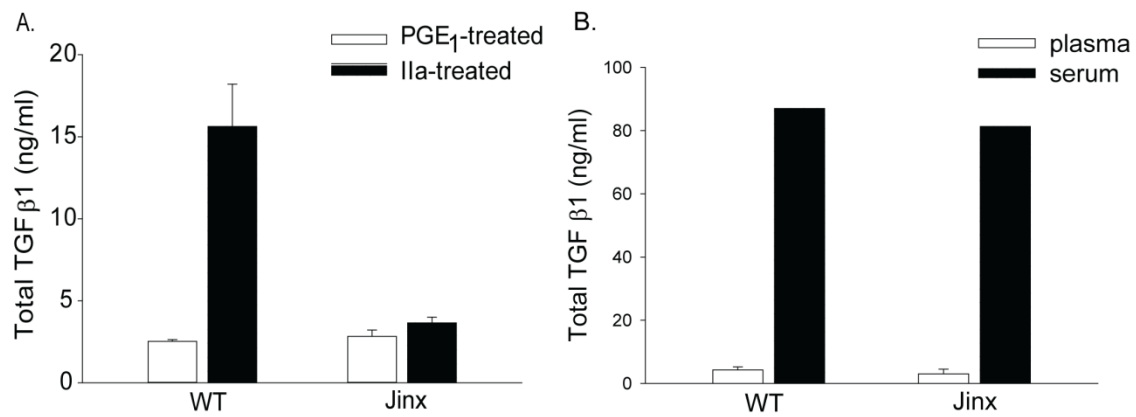


Figure 3.5 TGF-β1 plasma and serum levels in Jinx and B6 WT mice.

A) Platelets were isolated from WT or Jinx mice, treated with PGE<sub>1</sub> or thrombin (IIa). Total TGF-β1 in the releasate was measured as described in Methods. B) TGF-β1 levels measured in plasma or serum from WT and Jinx mice. No significant difference was observed between genotypes by Student *t*-test, *n* = 3 mice / group.

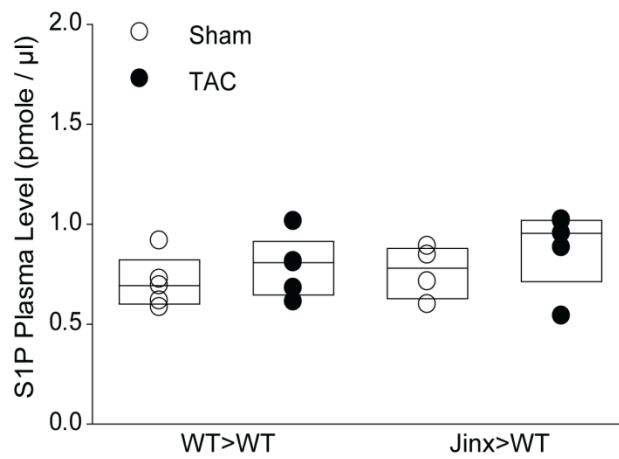


Figure 3.6 Plasma S1P levels in 7 days after TAC.

S1P plasma level was measured by mass spectrometry. Number/ group: WT>WT Sham = 5, WT>WT TAC = 5, Jinx>WT Sham = 4, Jinx>WT TAC = 5. No difference was detected between WT>WT and Jinx>WT mice after TAC by Two-Way ANOVA.

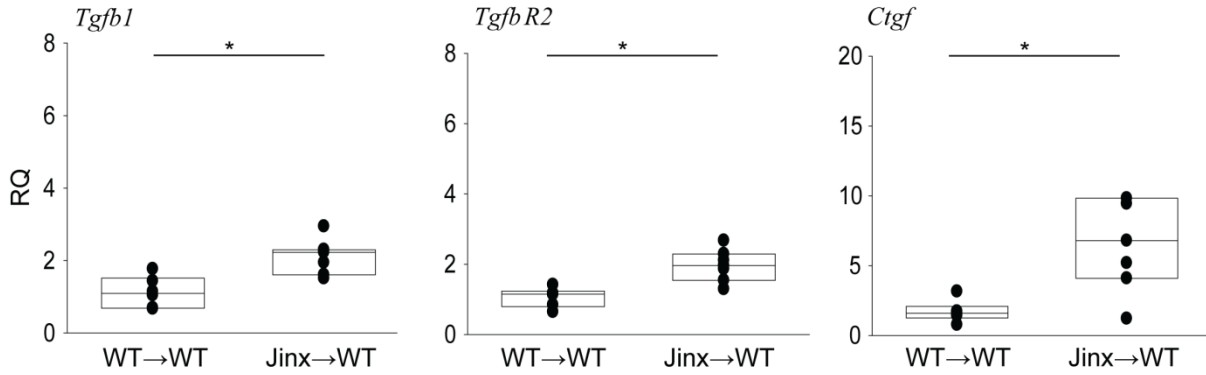
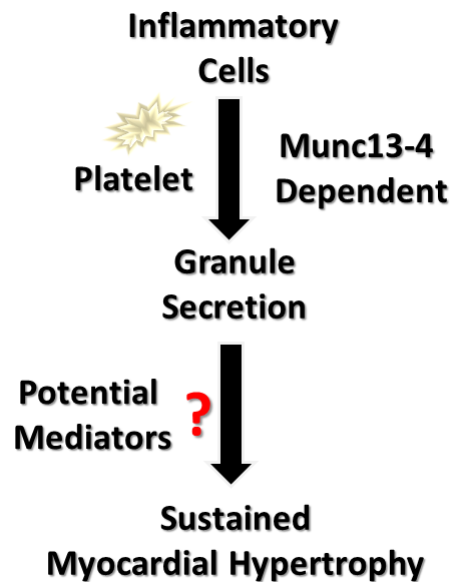


Figure 3.7 TGF $\beta$ -1 signaling 7 days after TAC.

Real-time quantitative PCR was performed to measure mRNA of TGF $\beta$ -1 signaling in hearts from chimeric mice. *Tgfb1* (transforming growth factor  $\beta$ -1), *Tgfb R2* (TGF $\beta$ -1 receptor 2) and *Ctgf* (connective tissue growth factor). Values are reports as normalized to those observed in WT>WT sham mice (set at 1). N per group: WT>WT TAC = 6, Jinx>WT TAC = 7. \*P < 0.05 by Student *t*-test.



## SUMMARY



To summarize the work accomplished in CHAPTER 3: Granule contents secreted in a Munc13-4-dependent pathway, likely from platelets, are required for the sustained myocardial hypertrophy induced by pressure overload. Munc13-4-dependent secretory deficiency affects neither early inflammatory and hypertrophic response, nor later fibrotic responses.

## CHAPTER 4: DISCUSSION AND FUTURE DIRECTIONS

### SECTION 1

**TAC Model** We reported previously that LV pressure overload in mice elicited significant perivascular and interstitial cardiac fibrosis at five weeks post-surgery [98]. As reported by Hartley and colleagues, we observed impaired coronary artery function, as measured by CFR, after TAC [95-97]. In the present study, we expanded our findings by examining the contribution of early perivascular inflammation to coronary artery remodeling in the setting of pressure overload. A striking and rapid accumulation of platelets, macrophages, and T lymphocytes occurred around the left coronary vessels early post-TAC. In detail, macrophage and T-lymphocyte accumulation was observed as early as one day after TAC and peaked at day seven. In our previous study, late leukocyte infiltration was detected in cardiac tissue at times up to five weeks [98]. Consistent with our data, Ying Xia et al. observed macrophage and neutrophil infiltration at day seven after TAC and a gradual decline until day 28, at which time levels were still higher than those in the sham group [99]. We observed platelet deposition at three and seven days post-TAC, with no significant difference between the time points. Based on the time course of peak inflammatory cell infiltration, we concentrated on understanding of the events that occur early after TAC. Therefore, the effects on coronary arteries are dependent on the early accumulation, rather than a chronic accumulation of these cells.

**Suprarenal Aortic Constriction (AC):** As described previously by our group and Kuwahara et al [18,98], both transverse aortic constriction (TAC) and suprarenal aortic constriction (AC) induce leukocyte infiltration (e.g. macrophage) in the setting of cardiac hypertrophy and fibrosis at four to five weeks, post surgery. However, TAC does not affect peripheral blood pressure, while

AC increases mean arterial blood pressure as early as one day post surgery. Also, most investigators report a decline in fractional shortening (FS) at five to eight weeks after TAC; whereas AC has been reported not to affect FS. Therefore, AC may impair diastolic dysfunction in the setting of preserved systolic function.

**Shear-Stress and Perivascular Inflammation** Quantification of coronary vessel size revealed that TAC mice had a significant increase in vessel size as compared to sham-operated animals. In parallel, perivascular fibrosis formation significantly increased. Although the precise mechanism(s) by which changes in flow may affect the coronary remodeling after TAC are unknown, numerous studies have shown that flow-induced changes in shear stress can contribute to perivascular inflammatory responses in coronary atherosclerosis and in-stent restenosis [202,203]. In particular, PECAM-1 (CD31) serves as part of the mechanical sensor complex regulating flow-induced vascular inflammation and remodeling [204-208]. In our model, endothelial disturbance, as evidenced by discontinuous PECAM staining, occurred within three days after TAC. Therefore, we hypothesize that pressure overload in the left ventricle alters coronary flow, shear stress, and endothelial function, which subsequently triggers platelet deposition and perivascular accumulation of inflammatory cells. The precise molecular mechanism(s) responsible for the changes are presently not understood. Future studies will investigate whether PECAM-1 expression or phosphorylation is altered by flow changes resulting from TAC.

**Coronary Flow Regulation** In our TAC model, Coronary dilatory dysfunction induced by LV pressure-overload was shown by reduced coronary flow reserve (CFR). Coronary flow is tightly regulated under physiology condition through different mechanisms. Metabolic stimulation is one major regulator. When increased cardiac output needed, more O<sub>2</sub> is consumed, leading to increased CO<sub>2</sub> production. Increased pCO<sub>2</sub> results in more protons (eg. H<sup>+</sup>, HCO<sub>3</sub><sup>-</sup>) which in turn stimulate coronary vasodilation [209]. The vasodilation induced by metabolic products increases blood flow and O<sub>2</sub> supply and therefore is critical for maintaining the normal function of the heart [209]. The metabolic products, such as reactive oxygen species (ROS) and adenosine, also have vasodilatory effects [209]. Further, the decreased pO<sub>2</sub> also serves as a director vasodilator [209]. Another regulation mechanism is called flow-mediated regulation which is based on the endothelium. Vascular endothelium may sense the shear alteration through the mechanical sensors on the lumen surface, which leads to endothelial production of either vasodilators (eg. NO, H<sub>2</sub>O<sub>2</sub>) or vasoconstrictors (eg. endothelin), working on smooth muscle cells to elicit vasodilation or vasoconstriction [210]. Coronary flow is also regulated by sympathetic and parasympathetic nervous systems [211]. Apart from these, recently perivascular inflammation is also shown to be involved in the regulation of coronary blood flow in cardiac diseases, such as myocardial ischemia reperfusion [212]. In brief, inflammatory cells and their secretion will reduce level of the vasodilators and increase the level of vasoconstrictors, which will lead to impaired coronary dilatory function [212]. Early perivascular accumulation and tissue infiltration of inflammatory cells were also observed in our model, which might be an additional factor contributing to the impaired coronary dilation.

**Platelets and Leukocyte Interaction** The appearance of platelet positive staining on the luminal surface of left coronary vessels and co-localization with leukocytes, suggested a role for platelets in coronary artery remodeling in response to pressure overload. Previous literature has reported that platelets dynamically influence the immune system through CD154 (CD40L) mediated interactions with CD40 on T and B lymphocytes [88,213,214]. Moreover, platelets enhance IL-10 expression by immature dendritic cells which in turn promotes the proliferation of naive T-cells [198]. We report that pericoronary T lymphocytes accumulation was significantly reduced in thrombocytopenic mice, suggesting a potential role for platelets in T lymphocytes recruitment, either through direct contact or indirectly through mediators. Our immunodepletion protocol resulted in thrombocytopenia for up to one week, supporting a role for platelets in this time frame. Because platelet deposition and lymphocyte accumulation appeared as early as 24 hours after TAC (data not shown and Figure 2.2A), we are unable to establish whether platelet deposition is the initiating event or whether it occurs in response to inflammatory changes and serves to perpetuate the inflammatory response.

**Induced-Thrombocytopenia** Exposure to high shear stress enables platelets to elicit IL-10 production from dendritic cells [198]. The change in flow following TAC may trigger a similar response from platelets and contribute to IL-10 expression and T cell accumulation, which would account for lower levels of IL-10 and T cells in thrombocytopenic animals. The subsequent increase in SMC  $\alpha$ -actin in thrombocytopenic animals could reflect an impact of these events on either the proliferative or inflammatory profile of SMC. Immune-mediated thrombocytopenia is followed by reactive thrombocytosis. Therefore, in the anti-GPIIb/IIIa IgG-

treated mice, it is possible that a subsequent increase in platelet count is influencing subsequent events, although given the propensity for platelet surfaces to passivate over time; this seems less likely than an effect of the initial thrombocytopenia. However, it is still not known how reactive thrombocytosis may contribute. TAC-induced platelet accumulation was observed at three and seven days and thrombocytopenia elicited by the GPIIb- $\alpha$  antibody is sustained for up to one week. We do not know if reactive thrombocytosis promotes late platelet events, although we do not detect differences in inflammatory cells at the late time points. In addition, reactive thrombocytosis can be accompanied by platelet dysfunction, and the impact of either elevated platelet counts or platelet dysfunction is not elucidated in this model.

**The Role of T lymphocytes in Cardiac Remodeling** Previous reports have implicated T lymphocytes in hypertensive cardiovascular diseases [81]. Our observations in Rag1<sup>-/-</sup> mice additionally suggest a role for lymphocytes in influencing remodeling by limiting neointima formation and perivascular fibrosis following TAC. Interestingly, despite the increase in fibrosis, CFR was improved in the absence of lymphocytes. These effects are likely mediated largely by T-cells, as we were unable to detect changes in B-cell accumulation in cardiac tissue post-TAC. In addition, at baseline, the collagen content in Rag1<sup>-/-</sup> mice was lower, supporting a role for lymphocytes in extracellular matrix dynamics under basal conditions. Others have reported lower basal vascular superoxide levels in Rag1<sup>-/-</sup> mice [81]. Vascular superoxide correlates with and may influence fibrotic remodeling, and may underlie the differences in the perivascular collagen content we observed in the sham-operated Rag1<sup>-/-</sup> mice.

The subsets of T cells involved in TAC-induced remodeling responses are presently unknown. Subsets of T lymphocytes appear to differentially influence pathological remodeling. For example, whereas CD1d-positive natural killer cells seem to promote the development of neointima after vascular injury in a carotid collar model [69], CD4<sup>+</sup>CD25<sup>+</sup> regulatory T cells adoptive transfer not only reduces angiotensin-induced early infiltration of inflammatory cells in cardiac tissue, but also blunts the subsequent development of cardiac hypertrophy, fibrosis formation, and arrhythmogenic potential [74]. Moreover, a balance between T helper 1 (Th1) and Th2 cells has been proposed to contribute to coronary and myocardial inflammation, and may be essential for cardiac extracellular matrix remodeling [70,71,215]. In an immune modulation mouse model, induction of Th1 responses led to increased collagen deposition, more LV stiffness, and down-regulation of MMP-9 and MMP-13 gene expression [71].

**The Role of IL-10 in TAC** In the TAC model, we observed a significant increase in expression of IL-10 in cardiac tissue between days one and seven post-TAC. IL-10 is a Th2 cytokine produced by many cell types, including macrophages and T helper 2 cells. IL-10 signals through the JAK/STAT3 pathway to modulate the expression of certain pro-inflammatory molecules and usually plays an important role in anti-inflammatory responses. For example, IL-10 is able to attenuate the NF- $\kappa$ B pathway through inhibition of IKK or NF- $\kappa$ B nuclear translocation [216]. Also, IL-10 can suppress vascular smooth muscle cell activation and proliferation and thereby attenuate neointima formation [35,217,218]. Recently, Krishnamurthy et al. reported that IL-10 treatment reduced macrophage accumulation and inflammatory cytokine expression, leading to attenuated left ventricular remodeling after myocardial infarction [219]. In keeping with these observations, bone marrow, mononuclear cell-derived IL-10 attenuates T cell infiltration

and cardiac remodeling after myocardial infarction, which prevents cardiac dysfunction [220]. In our model, increased expression of IL-10 parallels T lymphocyte infiltration early after TAC and may serve to attenuate the inflammatory responses and suppress SMC proliferation. Indeed, lower IL-10 levels correlate with increased medial hypertrophy in thrombocytopenic mice after TAC. Likewise, IL-10<sup>-/-</sup> mice display normal cardiac hypertrophy, but exaggerated vascular fibrotic remodeling post-TAC.

The results presented above indicate that platelets may influence coronary remodeling and perivascular fibrosis after TAC through recruitment of T-lymphocytes and stimulating IL-10-dependent signaling. In addition, platelets may have direct effects on coronary fibroblast function by releasing mediators that phenotypically modify fibroblasts. Indeed, we found that platelet releasate directly stimulates cardiac fibroblasts to increase the MMP9 expression and upregulate TGFβ-1 signaling. Platelets contain large storage of TGFβ-1 in their α-granules that could potentially activate fibroblasts and increase MMP production. Whether platelet-triggered MMP9 production attenuates or otherwise affects fibrosis remains to be established.

In summary, perivascular inflammation proceeds and accompanies coronary remodeling in the setting of pressure overload. Platelets, macrophages and lymphocytes accumulate along and around the coronary arteries early after TAC, accompanied by up-regulation of IL-10 expression in the myocardial tissue. Following TAC, the vessels undergo positive remodeling that is accompanied by extensive perivascular fibrosis. Surprisingly, both platelets and lymphocytes appear to play a protective role in minimizing remodeling and fibrosis. Our data are consistent



with a model in which platelets influence lymphocyte recruitment -- either by direct interaction or indirectly through stimulation of IL-10 (and/or other mediators) -- by recruited or resident cells. The IL-10 may act to suppress ongoing inflammation and limit perivascular fibrosis. Similar mechanisms may occur in settings of hypertension and our model may have particular relevance to hypertensive urgency, in which acute and dramatic elevations in blood pressure may be associated with a disruption in endothelial function and a pro-inflammatory state in coronary arteries. The optimal strategy for minimizing coronary artery damage in the setting of acute elevations in pressure remains to be determined.

## SECTION 2

We found that mice lacking the Rab27 effector protein Munc13-4 in bone marrow cells (Jinx>WT) were partially protected from the development of LVH at five weeks after pressure overload. The lack of hypertrophy was due to smaller cardiomyocyte size in mice with Jinx bone marrow cells, indicating protection from cardiomyocyte hypertrophy. The initial response to pressure overload at seven days was not detectably different from mice with normal bone marrow (WT>WT), in that the mice developed cardiac hypertrophy, an inflammatory response, and upregulation of cardiac fetal gene expression in response to the mechanical stress of pressure. Our results imply that there is a role for granule secretion in propagating the hypertrophy response that is initiated by pressure overload.

**Cardiac Endogenous Negative Regulators of Hypertrophy** Granules in hematopoietic cells contain a variety of cytokines, with many functions including promoting and inhibiting angiogenesis, fibrosis, thrombosis, and migration that could affect cardiac remodeling. The reduced hypertrophy in the Jinx chimeric mice could be due to loss of positive regulators from hematopoietic cells. Alternatively, factors that suppress endogenous negative regulators of cardiac hypertrophy may not be released. Two major types of endogenous negative regulators have been reported [221]: group I negative regulators (i.e. glycogen synthase kinase - 3) which are constitutively active during physiological conditions and inhibited by hypertrophic stimuli and promote hypertrophy; group II (i.e. ICER) regulators that are upregulated upon hypertrophic stimuli and counteract the response. Negative regulators belonging to both groups, such as thioredoxin (Trx1), have also been reported. It has been shown that Trx1 is upregulated in pressure-overload [222]. It is possible that component of hematopoietic cell

releasate influences cardiomyocyte expression of a group 2 regulator. Whether interaction between inflammatory cells and cardiomyocytes inhibits the expression of cardiac endogenous regulators remains to be determined. It is also unclear which factors they are. Still, in terms of the identified pathways through which the endogenous regulators play their roles, the potential suppressors secreted by hematopoietic cells, if they exist, may directly interact with endogenous negative regulators, or work by influencing PKA pathway or the intracellular oxidative stress [221].

**Platelet-Derived Potential Mediators of Cardiac Hypertrophy** Platelets and to a lesser extent platelet releasate were able to promote cardiac hypertrophy mice lacking the Rab27 effector protein Munc13-4 in bone marrow cells. These findings indicate that factors present in platelet granules and likely secreted in a Munc13-4-dependent manner influence cardiomyocyte hypertrophy. The loss of Munc13-4 results in defects in platelet  $\alpha$ -granules, dense granules and lysosomes. Several possible candidate mediators that are released from platelets and reportedly promote cardiac hypertrophy include TGF $\beta$ 1 [179], sphingosine-1-phosphate, and serotonin. Platelets contribute to plasma TGF $\beta$ -1 and platelet-derived TGF $\beta$ 1 influences cardiac remodeling after TAC [179]. Our findings indicate that Munc13-4 is important for thrombin-mediated release of TGF $\beta$ -1 from platelets. In response to thrombin, isolated WT but not Jinx platelets release substantial TGF $\beta$ -1. However, no differences were observed in TGF $\beta$ -1 levels in serum or plasma levels from Jinx and B6 mice. TGF $\beta$ -1 secretion from platelets may occur through multiple pathways. Platelet  $\alpha$ -granules, where TGF $\beta$ -1 is stored, may be heterogeneous subpopulations that can be differentially released [105,223]. Thus, stimuli other than thrombin may have less dependency on Munc13-4. We were unable to detect an

effect of TAC on plasma levels of TGF $\beta$ -1 at 7 days after surgery. Likewise no difference in plasma levels of S1P, another putative regulator of cardiomyocytes, was detected in Jinx and B6 chimeric mice 7 days after surgery. It is possible that there are differences at early time points, because peri-coronary deposition of platelets occurs as early as 24 hours after TAC (previous published data). Additionally, local microenvironmental effects of those mediators, rather than the systemic circulating ones, may be important for the hypertrophic response. Finally, while our studies implicate platelets as regulators of cardiac hypertrophy, the phenotype observed in mice lacking Munc13-4 could be due to a lack of cargo release from other hematopoietic cells, which influence cardiomyocytes.

As I have mentioned in Chapter 1 Section 1, elevated platelet activation has been observed in series of cardiovascular diseases. Therefore, the **anti-thrombotic therapies**, in particular the **anti-platelet therapy**, might not only benefit the patients through preventing blood clot formation but also through reducing the secretion of hypertrophy-promoting factors from platelets.

**Reprogramming of Fetal Genes**, such as ANP, BNP,  $\beta$ -MHC,  $\alpha$ -skeletal actin, occurs during cardiac hypertrophy. Seven days after TAC, fetal gene expression was upregulated in both Jinx>WT and WT>WT mice. Intriguingly, the fetal gene expression profile persisted in mice with Jinx marrow at 5 weeks, under conditions where they did not display progression of cardiac hypertrophy. Previous studies of unloaded hypertrophic hearts reported that the unloading did not alter fetal gene expression, leading to speculation that opposite stimuli may elicit similar patterns of gene expression [224]. In our study, the continued presence of pressure overload may be triggering fetal gene expression, but is not sufficient to promote continued

hypertrophy, which requires factors released from hematopoietic cells. In keeping with these observations, no difference in either inflammatory cell infiltration or the fibrotic responses was observed in mice lacking Munc13-4 in marrow cells. These findings suggest that fibrosis and myocardial hypertrophy are distinctly regulated, at least later in the course of the disease.

In summary, factors secreted from marrow-derived cells in a Munc13-4-dependent manner are important for maintaining the hypertrophic response of cardiomyocytes in response to pressure-overload. Platelet cargo release accounts for at least some of the effect. Thus, inhibition of platelet granule secretion might represent an effective way to reduce cardiac hypertrophy.

**Future Directions** In terms of our data, further study to discover the potential mediators or signaling pathways accounting for the phenotype we observed is very important. We would replace the complicated animal models we used in our preliminary study by a cultured cardiomyocyte cell line (H9C2). As positive control, cells will be treated with the proposed mediators (TGF $\beta$ -1, S1P and serotonin) individually thus generating hypertrophy phenotype. The cells will then be treated with the properly titrated WT platelet releasate to see if it can induce hypertrophic responses, or with Jinx platelet releasate to see if the hypertrophic response is absent due to Munc13-4 deficiency.

Hypertrophic responses will be studied by immunostaining (cardiomyocyte morphology) and quantitative PCR (fetal genes' expression). If we see attenuated myocyte hypertrophy in response to Jinx platelet releasate compared to WT releasate, we will further elucidate the potential mediators using platelets deficient of those mediators either through genetical modification (i.e. platelets from TGF $\beta$ -1<sup>-/-</sup> mice or sphingosine kinase 1(SphK1)<sup>-/-</sup> mice) or

pharmacological manipulation (i.e. neutralizing antibody to TGF $\beta$ -1). If we see less hypertrophy in treatment of platelet releasate deficient of certain proposed mediator, we will repeat the experiment *in vivo* by injecting these platelets or their releasate into Jinx chimeric mice to see whether Munc13-4 deficiency diminishes the recovered hypertrophy induced by WT platelet reinjection.

If we do not see hypertrophic response with treatment of WT platelet releasate, it might suggest the restored cardiac hypertrophy *in vivo* is due to indirect effects of other inflammatory cells which can be influenced by platelet secretion. To address this question, we can quantify the blood cell components of Jinx chimeric mice with platelet injection at different time points by complete blood count. To be more accurate, flow cytometry can be used to identify specific inflammatory cell groups. If we still see hypertrophic responses with treatment of Jinx platelet releasate, it might indicate that secretion of hypertrophic mediators from platelets is not prevented by Munc13-4 deficiency. Therefore, attenuated cardiac hypertrophy observed in Jinx chimeric mice could be due to secretion defects from other cell types which are regulated by platelet secretion.

More mediators need to be explored if we did not see less hypertrophy in groups treated with platelet releasate deficient of the proposed mediators. Luminex assay could be performed to measure plasma or cardiac level of potential pro-hypertrophic factors in chimeric mice which could be secreted from platelets and other hematopoietic cells. Gene microarray could also be performed to measure the expression of cardiac endogenous negative regulators. Due to the distinct temporal distribution of gene expression, several representative time points need to be chosen.

Copyright © Fanmuyi Yang 2012

## BIBLIOGRAPHY

1. Nadal-Ginard B, Kajstura J, Leri A, Anversa P (2003) Myocyte death, growth, and regeneration in cardiac hypertrophy and failure. *Circ Res* 92: 139-150.
2. Raman SV (2010) The hypertensive heart. An integrated understanding informed by imaging. *J Am Coll Cardiol* 55: 91-96.
3. Gradman AH, Alfayoumi F (2006) From left ventricular hypertrophy to congestive heart failure: management of hypertensive heart disease. *Prog Cardiovasc Dis* 48: 326-341.
4. Ruilope LM, Schmieder RE (2008) Left ventricular hypertrophy and clinical outcomes in hypertensive patients. *Am J Hypertens* 21: 500-508.
5. Balakumar P, Jagadeesh G (2010) Multifarious molecular signaling cascades of cardiac hypertrophy: can the muddy waters be cleared? *Pharmacol Res* 62: 365-383.
6. Wright JW, Mizutani S, Harding JW (2008) Pathways involved in the transition from hypertension to hypertrophy to heart failure. Treatment strategies. *Heart Fail Rev* 13: 367-375.
7. Vakili BA, Okin PM, Devereux RB (2001) Prognostic implications of left ventricular hypertrophy. *Am Heart J* 141: 334-341.
8. Bikkina M, Levy D, Evans JC, Larson MG, Benjamin EJ, et al. (1994) Left ventricular mass and risk of stroke in an elderly cohort. The Framingham Heart Study. *JAMA* 272: 33-36.
9. Beache GM, Herzka DA, Boxerman JL, Post WS, Gupta SN, et al. (2001) Attenuated myocardial vasodilator response in patients with hypertensive hypertrophy



- revealed by oxygenation-dependent magnetic resonance imaging. *Circulation* 104: 1214-1217.
10. Kaplan NM et al (2010) Clinical implications and treatment of left ventricular hypertrophy in hypertension. UpToDate.
  11. Rohini A, Agrawal N, Koyani CN, Singh R (2010) Molecular targets and regulators of cardiac hypertrophy. *Pharmacol Res* 61: 269-280.
  12. Rosenkranz S (2004) TGF-beta1 and angiotensin networking in cardiac remodeling. *Cardiovasc Res* 63: 423-432.
  13. Rohr S (2009) Myofibroblasts in diseased hearts: new players in cardiac arrhythmias? *Heart Rhythm* 6: 848-856.
  14. Berk BC, Fujiwara K, Lehoux S (2007) ECM remodeling in hypertensive heart disease. *J Clin Invest* 117: 568-575.
  15. Nicoletti A, Michel JB (1999) Cardiac fibrosis and inflammation: interaction with hemodynamic and hormonal factors. *Cardiovasc Res* 41: 532-543.
  16. Janicki JS, Brower GL (2002) The role of myocardial fibrillar collagen in ventricular remodeling and function. *J Card Fail* 8: S319-325.
  17. Kuwahara F, Kai H, Tokuda K, Takeya M, Takeshita A, et al. (2004) Hypertensive myocardial fibrosis and diastolic dysfunction: another model of inflammation? *Hypertension* 43: 739-745.
  18. Kai H, Kuwahara F, Tokuda K, Imaizumi T (2005) Diastolic dysfunction in hypertensive hearts: roles of perivascular inflammation and reactive myocardial fibrosis. *Hypertens Res* 28: 483-490.

19. Kwon DH, Smedira NG, Rodriguez ER, Tan C, Setser R, et al. (2009) Cardiac magnetic resonance detection of myocardial scarring in hypertrophic cardiomyopathy: correlation with histopathology and prevalence of ventricular tachycardia. *J Am Coll Cardiol* 54: 242-249.
20. Dellsperger KC, Marcus ML (1990) Effects of left ventricular hypertrophy on the coronary circulation. *Am J Cardiol* 65: 1504-1510.
21. Bache RJ (1988) Effects of hypertrophy on the coronary circulation. *Prog Cardiovasc Dis* 30: 403-440.
22. Dellsperger KC, Marcus ML (1988) The effects of pressure-induced cardiac hypertrophy on the functional capacity of the coronary circulation. *Am J Hypertens* 1: 200-207.
23. Marcus ML, Gascho JA, Mueller TM, Eastham C, Wright CB, et al. (1981) The effects of ventricular hypertrophy on the coronary circulation. *Basic Res Cardiol* 76: 575-581.
24. Marcus ML, Mueller TM, Gascho JA, Kerber RE (1979) Effects of cardiac hypertrophy secondary to hypertension on the coronary circulation. *Am J Cardiol* 44: 1023-1028.
25. Bache RJ, Wright L, Laxson DD, Dai XZ (1990) Effect of coronary stenosis on myocardial blood flow during exercise in the chronically pressure-overloaded hypertrophied left ventricle. *Circulation* 81: 1967-1973.
26. Harrison DG, Guzik TJ, Goronzy J, Weyand C (2008) Is hypertension an immunologic disease? *Curr Cardiol Rep* 10: 464-469.
27. Kagitani S, Ueno H, Hirade S, Takahashi T, Takata M, et al. (2004) Tranilast attenuates myocardial fibrosis in association with suppression of monocyte/macrophage infiltration in DOCA/salt hypertensive rats. *J Hypertens* 22: 1007-1015.

28. Kuwahara F, Kai H, Tokuda K, Niiyama H, Tahara N, et al. (2003) Roles of intercellular adhesion molecule-1 in hypertensive cardiac remodeling. *Hypertension* 41: 819-823.
29. Gonzalez A, Ravassa S, Beaumont J, Lopez B, Diez J (2011) New targets to treat the structural remodeling of the myocardium. *J Am Coll Cardiol* 58: 1833-1843.
30. Ishimaru K, Ueno H, Kagitani S, Takabayashi D, Takata M, et al. (2007) Fasudil attenuates myocardial fibrosis in association with inhibition of monocyte/macrophage infiltration in the heart of DOCA/salt hypertensive rats. *J Cardiovasc Pharmacol* 50: 187-194.
31. Yin H, Zhang J, Lin H, Wang R, Qiao Y, et al. (2008) p38 mitogen-activated protein kinase inhibition decreases TNF $\alpha$  secretion and protects against left ventricular remodeling in rats with myocardial ischemia. *Inflammation* 31: 65-73.
32. Gawaz M (2004) Role of platelets in coronary thrombosis and reperfusion of ischemic myocardium. *Cardiovasc Res* 61: 498-511.
33. Kleinschnitz C, Pozgajova M, Pham M, Bendszus M, Nieswandt B, et al. (2007) Targeting platelets in acute experimental stroke: impact of glycoprotein Ib, VI, and IIb/IIIa blockade on infarct size, functional outcome, and intracranial bleeding. *circulation* 115: 2323-2330.
34. Nieswandt B, Aktas B, Moers A, Sachs UJ (2005) Platelets in atherothrombosis: lessons from mouse models. *J Thromb Haemost* 3: 1725-1736.
35. Zernecke A, Liehn EA, Gao JL, Kuziel WA, Murphy PM, et al. (2006) Deficiency in CCR5 but not CCR1 protects against neointima formation in atherosclerosis-prone mice: involvement of IL-10. *Blood* 107: 4240-4243.

36. Klinger MH (1997) Platelets and inflammation. *Anat Embryol (Berl)* 196: 1-11.
37. McNicol A, Israels SJ (2008) Beyond hemostasis: the role of platelets in inflammation, malignancy and infection. *Cardiovasc Hematol Disord Drug Targets* 8: 99-117.
38. Schmitt-Sody M, Metz P, Gottschalk O, Zysk S, Birkenmaier C, et al. (2007) Selective inhibition of platelets by the GPIIb/IIIa receptor antagonist Tirofiban reduces leukocyte-endothelial cell interaction in murine antigen-induced arthritis. *Inflamm Res* 56: 414-420.
39. Zago AC, Simon DI, Wang Y, Sakuma M, Chen Z, et al. (2008) The importance of the interaction between leukocyte integrin Mac-1 and platelet glycoprotein Ib-a for leukocyte recruitment by platelets and for the inflammatory response to vascular injury. *Arq Bras Cardiol* 90: 54-63.
40. Wagner DD, Frenette PS (2008) The vessel wall and its interactions. *Blood* 111: 5271-5281.
41. van Gils JM, Zwaginga JJ, Hordijk PL (2008) Molecular and functional interactions among monocytes, platelets, and endothelial cells and their relevance for cardiovascular diseases. *J Leukoc Biol*.
42. Galkina E, Ley K (2007) Vascular adhesion molecules in atherosclerosis. *Arterioscler Thromb Vasc Biol* 27: 2292-2301.
43. Gleissner CA, von Hundelshausen P, Ley K (2008) Platelet chemokines in vascular disease. *Arterioscler Thromb Vasc Biol* 28: 1920-1927.
44. von Hundelshausen P, Koenen RR, Sack M, Mause SF, Adriaens W, et al. (2005) Heterophilic interactions of platelet factor 4 and RANTES promote monocyte arrest on endothelium. *Blood* 105: 924-930.

45. Koenen RR, von Hundelshausen P, Nesmelova IV, Zerneck A, Liehn EA, et al. (2009) Disrupting functional interactions between platelet chemokines inhibits atherosclerosis in hyperlipidemic mice. *Nat Med* 15: 97-103.
46. Stumpf C, Lehner C, Raaz D, Yilmaz A, Anger T, et al. (2008) Platelets contribute to enhanced MCP-1 levels in patients with chronic heart failure. *Heart* 94: 65-69.
47. Dimitrow PP, Undas A, Bober M, Tracz W, Dubiel JS (2008) Obstructive hypertrophic cardiomyopathy is associated with enhanced thrombin generation and platelet activation. *Heart* 94: e21.
48. Xu Y, Huo Y, Toufektsian MC, Ramos SI, Ma Y, et al. (2006) Activated platelets contribute importantly to myocardial reperfusion injury. *Am J Physiol Heart Circ Physiol* 290: H692-699.
49. Wang K, Zhou X, Zhou Z, Mal N, Fan L, et al. (2005) Platelet, not endothelial, P-selectin is required for neointimal formation after vascular injury. *Arterioscler Thromb Vasc Biol* 25: 1584-1589.
50. Cloutier N, Pare A, Farndale RW, Schumacher HR, Nigrovic PA, et al. (2012) Platelets can enhance vascular permeability. *Blood*.
51. Iannaccone M, Sitia G, Isogawa M, Marchese P, Castro MG, et al. (2005) Platelets mediate cytotoxic T lymphocyte-induced liver damage. *Nat Med* 11: 1167-1169.
52. Hu W, Jin R, Zhang J, You T, Peng Z, et al. (2010) The critical roles of platelet activation and reduced NO bioavailability in fatal pulmonary arterial hypertension in a murine hemolysis model. *Blood* 116: 1613-1622.

53. Langer HF, Choi EY, Zhou H, Schleicher R, Chung KJ, et al. (2012) Platelets contribute to the pathogenesis of experimental autoimmune encephalomyelitis. *Circ Res* 110: 1202-1210.
54. Serebruany VL (2010) Clopidogrel and heart failure survival: missed opportunity or wrong turn? *J Am Coll Cardiol* 55: 1308-1309.
55. Bonde L, Sorensen R, Fosbol EL, Abildstrom SZ, Hansen PR, et al. (2010) Increased mortality associated with low use of clopidogrel in patients with heart failure and acute myocardial infarction not undergoing percutaneous coronary intervention: a nationwide study. *J Am Coll Cardiol* 55: 1300-1307.
56. Tsuchikane E, Fukuhara A, Kobayashi T, Kirino M, Yamasaki K, et al. (1999) Impact of cilostazol on restenosis after percutaneous coronary balloon angioplasty. *Circulation* 100: 21-26.
57. Erlich JM, Talmor DS, Cartin-Ceba R, Gajic O, Kor DJ (2011) Prehospitalization antiplatelet therapy is associated with a reduced incidence of acute lung injury: a population-based cohort study. *Chest* 139: 289-295.
58. Ho-Tin-Noe B, Goerge T, Cifuni SM, Duerschmied D, Wagner DD (2008) Platelet granule secretion continuously prevents intratumor hemorrhage. *Cancer Res* 68: 6851-6858.
59. Goerge T, Ho-Tin-Noe B, Carbo C, Benarafa C, Remold-O'Donnell E, et al. (2008) Inflammation induces hemorrhage in thrombocytopenia. *Blood* 111: 4958-4964.
60. Cheng K, Malliaras K, Shen D, Tseliou E, Ionta V, et al. (2012) Intramyocardial injection of platelet gel promotes endogenous repair and augments cardiac function in rats with myocardial infarction. *J Am Coll Cardiol* 59: 256-264.

61. Poplawski A, Skorulska M, Niewiarowski S (1968) Increased platelet adhesiveness in hypertensive cardiovascular disease. *J Atheroscler Res* 8: 721-723.
62. Nadar SK, Blann AD, Kamath S, Beevers DG, Lip GY (2004) Platelet indexes in relation to target organ damage in high-risk hypertensive patients: a substudy of the Anglo-Scandinavian Cardiac Outcomes Trial (ASCOT). *J Am Coll Cardiol* 44: 415-422.
63. Cao X, Xie X, Zhou J, Yang P, Wang Y, et al. (2012) Increased platelet volume in a general population with prehypertension: a cross-sectional study of 80 545 participants from China. *Hypertens Res*.
64. Varol E, Akcay S, Icli A, Yucel H, Ozkan E, et al. (2010) Mean platelet volume in patients with prehypertension and hypertension. *Clin Hemorheol Microcirc* 45: 67-72.
65. Gkaliagkousi E, Passacquale G, Douma S, Zamboulis C, Ferro A (2010) Platelet activation in essential hypertension: implications for antiplatelet treatment. *Am J Hypertens* 23: 229-236.
66. Riondino S, Pignatelli P, Pulcinelli FM, Lenti L, Di Veroli C, et al. (1999) Platelet hyperactivity in hypertensive older patients is controlled by lowering blood pressure. *J Am Geriatr Soc* 47: 943-947.
67. Nomura S, Shouzu A, Omoto S, Nishikawa M, Fukuhara S, et al. (2004) Losartan and simvastatin inhibit platelet activation in hypertensive patients. *J Thromb Thrombolysis* 18: 177-185.
68. Shinohara Y, Gotoh F, Tohgi H, Hirai S, Terashi A, et al. (2008) Antiplatelet cilostazol is beneficial in diabetic and/or hypertensive ischemic stroke patients. Subgroup analysis of the cilostazol stroke prevention study. *Cerebrovasc Dis* 26: 63-70.

69. Strom A, Wigren M, Hultgardh-Nilsson A, Saxena A, Gomez MF, et al. (2007)  
Involvement of the CD1d-natural killer T cell pathway in neointima formation after  
vascular injury. *Circ Res* 101: e83-89.
70. Yu Q, Horak K, Larson DF (2006) Role of T lymphocytes in hypertension-induced  
cardiac extracellular matrix remodeling. *Hypertension* 48: 98-104.
71. Yu Q, Watson RR, Marchalonis JJ, Larson DF (2005) A role for T lymphocytes in  
mediating cardiac diastolic function. *Am J Physiol Heart Circ Physiol* 289: H643-651.
72. Song L, Leung C, Schindler C (2001) Lymphocytes are important in early  
atherosclerosis. *J Clin Invest* 108: 251-259.
73. Chow LH, Huh S, Jiang J, Zhong R, Pickering JG (1996) Intimal thickening develops  
without humoral immunity in a mouse aortic allograft model of chronic vascular  
rejection. *Circulation* 94: 3079-3082.
74. Kvakan H, Kleinewietfeld M, Qadri F, Park JK, Fischer R, et al. (2009) Regulatory T cells  
ameliorate angiotensin II-induced cardiac damage. *Circulation* 119: 2904-2912.
75. Kim JH, Kim HY, Kim S, Chung JH, Park WS, et al. (2005) Natural killer T (NKT) cells  
attenuate bleomycin-induced pulmonary fibrosis by producing interferon-gamma.  
*Am J Pathol* 167: 1231-1241.
76. Hansson GK, Holm J, Holm S, Fotev Z, Hedrich HJ, et al. (1991) T lymphocytes inhibit the  
vascular response to injury. *Proc Natl Acad Sci U S A* 88: 10530-10534.
77. Remskar M, Li H, Chyu KY, Shah PK, Cercek B (2001) Absence of CD40 signaling is  
associated with an increase in intimal thickening after arterial injury. *Circ Res* 88:  
390-394.



78. Dimayuga P, Cercek B, Oguchi S, Fredrikson GN, Yano J, et al. (2002) Inhibitory effect on arterial injury-induced neointimal formation by adoptive B-cell transfer in Rag-1 knockout mice. *Arterioscler Thromb Vasc Biol* 22: 644-649.
79. Moyssakis I, Lionakis N, Votteas V (2009) Hypertrophic obstructive cardiomyopathy in rheumatoid arthritis - coincidence or association? A case report. *Exp Clin Cardiol* 14: e21-22.
80. Moyssakis I, Papadopoulos DP, Anastasiadis G, Vlachoyannopoulos P (2006) Hypertrophic cardiomyopathy in systemic sclerosis. A report of two cases. *Clin Rheumatol* 25: 404-406.
81. Guzik TJ, Hoch NE, Brown KA, McCann LA, Rahman A, et al. (2007) Role of the T cell in the genesis of angiotensin II induced hypertension and vascular dysfunction. *J Exp Med* 204: 2449-2460.
82. Hoch NE, Guzik TJ, Chen W, Deans T, Maalouf SA, et al. (2009) Regulation of T-cell function by endogenously produced angiotensin II. *Am J Physiol Regul Integr Comp Physiol* 296: R208-216.
83. Marvar PJ, Thabet SR, Guzik TJ, Lob HE, McCann LA, et al. (2010) Central and peripheral mechanisms of T-lymphocyte activation and vascular inflammation produced by angiotensin II-induced hypertension. *Circ Res* 107: 263-270.
84. Crowley SD, Song YS, Lin EE, Griffiths R, Kim HS, et al. (2010) Lymphocyte responses exacerbate angiotensin II-dependent hypertension. *Am J Physiol Regul Integr Comp Physiol* 298: R1089-1097.
85. Li N (2008) Platelet-lymphocyte cross-talk. *J Leukoc Biol* 83: 1069-1078.

86. Pitchford SC, Momi S, Giannini S, Casali L, Spina D, et al. (2005) Platelet P-selectin is required for pulmonary eosinophil and lymphocyte recruitment in a murine model of allergic inflammation. *Blood* 105: 2074-2081.
87. Khandoga A, Hanschen M, Kessler JS, Krombach F (2006) CD4+ T cells contribute to postischemic liver injury in mice by interacting with sinusoidal endothelium and platelets. *Hepatology* 43: 306-315.
88. Sowa JM, Crist SA, Ratliff TL, Elzey BD (2009) Platelet influence on T- and B-cell responses. *Arch Immunol Ther Exp (Warsz)* 57: 235-241.
89. Renshaw BR, Fanslow WC, 3rd, Armitage RJ, Campbell KA, Liggitt D, et al. (1994) Humoral immune responses in CD40 ligand-deficient mice. *J Exp Med* 180: 1889-1900.
90. Khan SY, Kelher MR, Heal JM, Blumberg N, Boshkov LK, et al. (2006) Soluble CD40 ligand accumulates in stored blood components, primes neutrophils through CD40, and is a potential cofactor in the development of transfusion-related acute lung injury. *Blood* 108: 2455-2462.
91. Osman M, Russell J, Granger DN (2009) Lymphocyte-derived interferon-gamma mediates ischemia-reperfusion-induced leukocyte and platelet adhesion in intestinal microcirculation. *Am J Physiol Gastrointest Liver Physiol* 296: G659-663.
92. Danese S, de la Motte C, Reyes BM, Sans M, Levine AD, et al. (2004) Cutting edge: T cells trigger CD40-dependent platelet activation and granular RANTES release: a novel pathway for immune response amplification. *J Immunol* 172: 2011-2015.

93. Nakamura A, Rokosh DG, Paccanaro M, Yee RR, Simpson PC, et al. (2001) LV systolic performance improves with development of hypertrophy after transverse aortic constriction in mice. *Am J Physiol Heart Circ Physiol* 281: H1104-1112.
94. Kwon JS, Lee SJ, Kim YG, Bae JW, Hwang KK, et al. (2006) Effect of pressure overload and its recovery on the rat carotid artery: change of vascular reactivity and remodeling process. *Heart Vessels* 21: 48-55.
95. Hartley CJ, Reddy AK, Michael LH, Entman ML, Taffet GE (2009) Coronary flow reserve as an index of cardiac function in mice with cardiovascular abnormalities. *Conf Proc IEEE Eng Med Biol Soc* 2009: 1094-1097.
96. Hartley CJ, Reddy AK, Madala S, Michael LH, Entman ML, et al. (2008) Doppler estimation of reduced coronary flow reserve in mice with pressure overload cardiac hypertrophy. *Ultrasound Med Biol* 34: 892-901.
97. Hartley CJ, Reddy AK, Madala S, Michael LH, Entman ML, et al. (2007) Effects of isoflurane on coronary blood flow velocity in young, old and ApoE(-/-) mice measured by Doppler ultrasound. *Ultrasound Med Biol* 33: 512-521.
98. Barrick CJ, Rojas M, Schoonhoven R, Smyth SS, Threadgill DW (2007) Cardiac response to pressure overload in 129S1/SvImJ and C57BL/6J mice: temporal- and background-dependent development of concentric left ventricular hypertrophy. *Am J Physiol Heart Circ Physiol* 292: H2119-2130.
99. Xia Y, Lee K, Li N, Corbett D, Mendoza L, et al. (2009) Characterization of the inflammatory and fibrotic response in a mouse model of cardiac pressure overload. *Histochem Cell Biol* 131: 471-481.

100. Logan MR, Odemuyiwa SO, Moqbel R (2003) Understanding exocytosis in immune and inflammatory cells: the molecular basis of mediator secretion. *J Allergy Clin Immunol* 111: 923-932; quiz 933.
101. Burgoyne RD, Morgan A (2003) Secretory granule exocytosis. *Physiol Rev* 83: 581-632.
102. Smyth S.S. WS, Italiano J.E., Collier B.S. (2010) Platelet Morphology, Biochemistry, and Function. . Williams Hematology. 8e ed.
103. King SM, Reed GL (2002) Development of platelet secretory granules. *Semin Cell Dev Biol* 13: 293-302.
104. Heijnen HF, Schiel AE, Fijnheer R, Geuze HJ, Sixma JJ (1999) Activated platelets release two types of membrane vesicles: microvesicles by surface shedding and exosomes derived from exocytosis of multivesicular bodies and alpha-granules. *Blood* 94: 3791-3799.
105. Blair P, Flaumenhaft R (2009) Platelet alpha-granules: basic biology and clinical correlates. *Blood Rev* 23: 177-189.
106. Kahr WH, Hinckley J, Li L, Schwertz H, Christensen H, et al. (2011) Mutations in NBEAL2, encoding a BEACH protein, cause gray platelet syndrome. *Nat Genet* 43: 738-740.
107. Gunay-Aygun M, Falik-Zaccai TC, Vilboux T, Zivony-Elboum Y, Gumruk F, et al. (2011) NBEAL2 is mutated in gray platelet syndrome and is required for biogenesis of platelet alpha-granules. *Nat Genet* 43: 732-734.

108. Albers CA, Cvejic A, Favier R, Bouwmans EE, Alessi MC, et al. (2011) Exome sequencing identifies NBEAL2 as the causative gene for gray platelet syndrome. *Nat Genet* 43: 735-737.
109. Livak KJ, Schmittgen TD (2001) Analysis of relative gene expression data using real-time quantitative PCR and the 2<sup>(-Delta Delta C(T))</sup> Method. *Methods* 25: 402-408.
110. Zhang ZG, Zhang L, Tsang W, Goussev A, Powers C, et al. (2001) Dynamic platelet accumulation at the site of the occluded middle cerebral artery and in downstream microvessels is associated with loss of microvascular integrity after embolic middle cerebral artery occlusion. *Brain Res* 912: 181-194.
111. Sanchez-Yague J, Llanillo M (1986) Lipid composition of subcellular particles from sheep platelets. Location of phosphatidylethanolamine and phosphatidylserine in plasma membranes and platelet liposomes. *Biochim Biophys Acta* 856: 193-201.
112. Coorssen JR, Haslam RJ (1993) GTP gamma S and phorbol ester act synergistically to stimulate both Ca<sup>(2+)</sup>-independent secretion and phospholipase D activity in permeabilized human platelets. Inhibition by BAPTA and analogues. *FEBS Lett* 316: 170-174.
113. Coorssen JR (1996) Phospholipase activation and secretion: evidence that PLA2, PLC, and PLD are not essential to exocytosis. *Am J Physiol* 270: C1153-1163.
114. Zeniou-Meyer M, Zabari N, Ashery U, Chasserot-Golaz S, Haeberle AM, et al. (2007) Phospholipase D1 production of phosphatidic acid at the plasma membrane promotes exocytosis of large dense-core granules at a late stage. *J Biol Chem* 282: 21746-21757.

115. Flaumenhaft R (2003) Molecular basis of platelet granule secretion. *Arterioscler Thromb Vasc Biol* 23: 1152-1160.
116. Rozenvayn N, Flaumenhaft R (2001) Phosphatidylinositol 4,5-bisphosphate mediates  $\text{Ca}^{2+}$ -induced platelet alpha-granule secretion: evidence for type II phosphatidylinositol 5-phosphate 4-kinase function. *J Biol Chem* 276: 22410-22419.
117. James DJ, Khodthong C, Kowalchuk JA, Martin TF (2008) Phosphatidylinositol 4,5-bisphosphate regulates SNARE-dependent membrane fusion. *J Cell Biol* 182: 355-366.
118. Capuano C, Paolini R, Molfetta R, Frati L, Santoni A, et al. (2012) PIP2-dependent regulation of Munc13-4 endocytic recycling: impact on the cytolytic secretory pathway. *Blood* 119: 2252-2262.
119. Graf CT, Riedel D, Schmitt HD, Jahn R (2005) Identification of functionally interacting SNAREs by using complementary substitutions in the conserved '0' layer. *Mol Biol Cell* 16: 2263-2274.
120. Flaumenhaft R, Croce K, Chen E, Furie B, Furie BC (1999) Proteins of the exocytotic core complex mediate platelet alpha-granule secretion. Roles of vesicle-associated membrane protein, SNAP-23, and syntaxin 4. *J Biol Chem* 274: 2492-2501.
121. Lemons PP, Chen D, Whiteheart SW (2000) Molecular mechanisms of platelet exocytosis: requirements for alpha-granule release. *Biochem Biophys Res Commun* 267: 875-880.
122. Woronowicz K, Dilks JR, Rozenvayn N, Dowal L, Blair PS, et al. (2010) The platelet actin cytoskeleton associates with SNAREs and participates in alpha-granule secretion. *Biochemistry* 49: 4533-4542.

123. Bernstein AM, Whiteheart SW (1999) Identification of a cellubrevin/vesicle associated membrane protein 3 homologue in human platelets. *Blood* 93: 571-579.
124. Ren Q, Barber HK, Crawford GL, Karim ZA, Zhao C, et al. (2007) Endobrevin/VAMP-8 is the primary v-SNARE for the platelet release reaction. *Mol Biol Cell* 18: 24-33.
125. Polgar J, Chung SH, Reed GL (2002) Vesicle-associated membrane protein 3 (VAMP-3) and VAMP-8 are present in human platelets and are required for granule secretion. *Blood* 100: 1081-1083.
126. Schraw TD, Rutledge TW, Crawford GL, Bernstein AM, Kalen AL, et al. (2003) Granule stores from cellubrevin/VAMP-3 null mouse platelets exhibit normal stimulus-induced release. *Blood* 102: 1716-1722.
127. Chen D, Lemons PP, Schraw T, Whiteheart SW (2000) Molecular mechanisms of platelet exocytosis: role of SNAP-23 and syntaxin 2 and 4 in lysosome release. *Blood* 96: 1782-1788.
128. Chen D, Bernstein AM, Lemons PP, Whiteheart SW (2000) Molecular mechanisms of platelet exocytosis: role of SNAP-23 and syntaxin 2 in dense core granule release. *Blood* 95: 921-929.
129. Gillitzer A, Peluso M, Bultmann A, Munch G, Gawaz M, et al. (2008) Effect of dominant negative SNAP-23 expression on platelet function. *J Thromb Haemost* 6: 1757-1763.
130. Rutledge TW, Whiteheart SW (2002) SNAP-23 is a target for calpain cleavage in activated platelets. *J Biol Chem* 277: 37009-37015.
131. Lai KC, Flaumenhaft R (2003) SNARE protein degradation upon platelet activation: calpain cleaves SNAP-23. *J Cell Physiol* 194: 206-214.

132. Ye S, Karim ZA, Al Hawas R, Pessin JE, Filipovich AH, et al. (2012) Syntaxin-11, but not syntaxin-2 or syntaxin-4, is required for platelet secretion. *Blood* 120: 2484-2492.
133. Polgar J, Reed GL (1999) A critical role for N-ethylmaleimide-sensitive fusion protein (NSF) in platelet granule secretion. *Blood* 94: 1313-1318.
134. Al Hawas R, Ren Q, Ye S, Karim ZA, Filipovich AH, et al. (2012) Munc18b/STXBP2 is required for platelet secretion. *Blood* 120: 2493-2500.
135. Pfeffer SR (1999) Transport-vesicle targeting: tethers before SNAREs. *Nat Cell Biol* 1: E17-22.
136. Karniguian A, Zahraoui A, Tavitian A (1993) Identification of small GTP-binding rab proteins in human platelets: thrombin-induced phosphorylation of rab3B, rab6, and rab8 proteins. *Proc Natl Acad Sci U S A* 90: 7647-7651.
137. Chen D, Guo J, Miki T, Tachibana M, Gahl WA (1997) Molecular cloning and characterization of rab27a and rab27b, novel human rab proteins shared by melanocytes and platelets. *Biochem Mol Med* 60: 27-37.
138. Richards-Smith B, Novak EK, Jang EK, He P, Haslam RJ, et al. (1999) Analyses of proteins involved in vesicular trafficking in platelets of mouse models of Hermansky Pudlak syndrome. *Mol Genet Metab* 68: 14-23.
139. Ninkovic I, White JG, Rangel-Filho A, Datta YH (2008) The role of Rab38 in platelet dense granule defects. *J Thromb Haemost* 6: 2143-2151.
140. Tolmachova T, Anders R, Stinchcombe J, Bossi G, Griffiths GM, et al. (2004) A general role for Rab27a in secretory cells. *Mol Biol Cell* 15: 332-344.
141. Haddad EK, Wu X, Hammer JA, 3rd, Henkart PA (2001) Defective granule exocytosis in Rab27a-deficient lymphocytes from Ashen mice. *J Cell Biol* 152: 835-842.



142. Bahadoran P, Aberdam E, Mantoux F, Busca R, Bille K, et al. (2001) Rab27a: A key to melanosome transport in human melanocytes. *J Cell Biol* 152: 843-850.
143. Stinchcombe JC, Barral DC, Mules EH, Booth S, Hume AN, et al. (2001) Rab27a is required for regulated secretion in cytotoxic T lymphocytes. *J Cell Biol* 152: 825-834.
144. Hume AN, Collinson LM, Rapak A, Gomes AQ, Hopkins CR, et al. (2001) Rab27a regulates the peripheral distribution of melanosomes in melanocytes. *J Cell Biol* 152: 795-808.
145. Novak EK, Gautam R, Reddington M, Collinson LM, Copeland NG, et al. (2002) The regulation of platelet-dense granules by Rab27a in the ashen mouse, a model of Hermansky-Pudlak and Griscelli syndromes, is granule-specific and dependent on genetic background. *Blood* 100: 128-135.
146. Wilson SM, Yip R, Swing DA, O'Sullivan TN, Zhang Y, et al. (2000) A mutation in Rab27a causes the vesicle transport defects observed in ashen mice. *Proc Natl Acad Sci U S A* 97: 7933-7938.
147. Barral DC, Ramalho JS, Anders R, Hume AN, Knapton HJ, et al. (2002) Functional redundancy of Rab27 proteins and the pathogenesis of Griscelli syndrome. *J Clin Invest* 110: 247-257.
148. Tolmachova T, Abrink M, Futter CE, Authi KS, Seabra MC (2007) Rab27b regulates number and secretion of platelet dense granules. *Proc Natl Acad Sci U S A* 104: 5872-5877.

149. Koch H, Hofmann K, Brose N (2000) Definition of Munc13-homology-domains and characterization of a novel ubiquitously expressed Munc13 isoform. *Biochem J* 349: 247-253.
150. Feldmann J, Callebaut I, Raposo G, Certain S, Bacq D, et al. (2003) Munc13-4 is essential for cytolytic granules fusion and is mutated in a form of familial hemophagocytic lymphohistiocytosis (FHL3). *Cell* 115: 461-473.
151. Augustin I, Betz A, Herrmann C, Jo T, Brose N (1999) Differential expression of two novel Munc13 proteins in rat brain. *Biochem J* 337 ( Pt 3): 363-371.
152. Brose N, Hofmann K, Hata Y, Sudhof TC (1995) Mammalian homologues of *Caenorhabditis elegans* unc-13 gene define novel family of C2-domain proteins. *J Biol Chem* 270: 25273-25280.
153. Chang TY, Jaffray J, Woda B, Newburger PE, Usmani GN (2011) Hemophagocytic lymphohistiocytosis with MUNC13-4 gene mutation or reduced natural killer cell function prior to onset of childhood leukemia. *Pediatr Blood Cancer* 56: 856-858.
154. Ren Q, Wimmer C, Chicka MC, Ye S, Ren Y, et al. (2010) Munc13-4 is a limiting factor in the pathway required for platelet granule release and hemostasis. *Blood* 116: 869-877.
155. Brzezinska AA, Johnson JL, Munafo DB, Crozat K, Beutler B, et al. (2008) The Rab27a effectors JFC1/Slp1 and Munc13-4 regulate exocytosis of neutrophil granules. *Traffic* 9: 2151-2164.
156. Pivot-Pajot C, Varoquaux F, de Saint Basile G, Bourgoin SG (2008) Munc13-4 regulates granule secretion in human neutrophils. *J Immunol* 180: 6786-6797.

157. Higashio H, Nishimura N, Ishizaki H, Miyoshi J, Orita S, et al. (2008) Doc2 alpha and Munc13-4 regulate Ca(2+) -dependent secretory lysosome exocytosis in mast cells. *J Immunol* 180: 4774-4784.
158. Neeft M, Wieffer M, de Jong AS, Negroiu G, Metz CH, et al. (2005) Munc13-4 is an effector of rab27a and controls secretion of lysosomes in hematopoietic cells. *Mol Biol Cell* 16: 731-741.
159. Shirakawa R, Higashi T, Tabuchi A, Yoshioka A, Nishioka H, et al. (2004) Munc13-4 is a GTP-Rab27-binding protein regulating dense core granule secretion in platelets. *J Biol Chem* 279: 10730-10737.
160. Menager MM, Menasche G, Romao M, Knapnougel P, Ho CH, et al. (2007) Secretory cytotoxic granule maturation and exocytosis require the effector protein hMunc13-4. *Nat Immunol* 8: 257-267.
161. Yamamoto K, Ishii E, Sako M, Ohga S, Furuno K, et al. (2004) Identification of novel MUNC13-4 mutations in familial haemophagocytic lymphohistiocytosis and functional analysis of MUNC13-4-deficient cytotoxic T lymphocytes. *J Med Genet* 41: 763-767.
162. Crozat K, Hoebe K, Ugolini S, Hong NA, Janssen E, et al. (2007) Jinx, an MCMV susceptibility phenotype caused by disruption of Unc13d: a mouse model of type 3 familial hemophagocytic lymphohistiocytosis. *J Exp Med* 204: 853-863.
163. Berger M, Gray JA, Roth BL (2009) The expanded biology of serotonin. *Annu Rev Med* 60: 355-366.
164. Roth BL (1994) Multiple serotonin receptors: clinical and experimental aspects. *Ann Clin Psychiatry* 6: 67-78.

165. Monassier L, Laplante MA, Ayadi T, Doly S, Maroteaux L (2010) Contribution of gene-modified mice and rats to our understanding of the cardiovascular pharmacology of serotonin. *Pharmacol Ther* 128: 559-567.
166. Papadimas GK, Tzirogiannis KN, Mykoniatis MG, Grypioti AD, Manta GA, et al. (2012) The emerging role of serotonin in liver regeneration. *Swiss Med Wkly* 142: w13548.
167. Nebigil CG, Choi DS, Dierich A, Hickel P, Le Meur M, et al. (2000) Serotonin 2B receptor is required for heart development. *Proc Natl Acad Sci U S A* 97: 9508-9513.
168. Nebigil CG, Jaffre F, Messaddeq N, Hickel P, Monassier L, et al. (2003) Overexpression of the serotonin 5-HT<sub>2B</sub> receptor in heart leads to abnormal mitochondrial function and cardiac hypertrophy. *Circulation* 107: 3223-3229.
169. Bai CF, Liu JC, Zhao R, Cao W, Liu SB, et al. (2010) Role of 5-HT<sub>2B</sub> receptors in cardiomyocyte apoptosis in noradrenaline-induced cardiomyopathy in rats. *Clin Exp Pharmacol Physiol* 37: e145-151.
170. Liang YJ, Lai LP, Wang BW, Juang SJ, Chang CM, et al. (2006) Mechanical stress enhances serotonin 2B receptor modulating brain natriuretic peptide through nuclear factor-kappaB in cardiomyocytes. *Cardiovasc Res* 72: 303-312.
171. Jaffre F, Callebort J, Sarre A, Etienne N, Nebigil CG, et al. (2004) Involvement of the serotonin 5-HT<sub>2B</sub> receptor in cardiac hypertrophy linked to sympathetic stimulation: control of interleukin-6, interleukin-1beta, and tumor necrosis factor-alpha cytokine production by ventricular fibroblasts. *Circulation* 110: 969-974.
172. Monassier L, Laplante MA, Jaffre F, Bousquet P, Maroteaux L, et al. (2008) Serotonin 5-HT<sub>2B</sub> receptor blockade prevents reactive oxygen species-induced cardiac hypertrophy in mice. *Hypertension* 52: 301-307.

173. Bianchi P, Pimentel DR, Murphy MP, Colucci WS, Parini A (2005) A new hypertrophic mechanism of serotonin in cardiac myocytes: receptor-independent ROS generation. *FASEB J* 19: 641-643.
174. Tachibana H, Cheng HJ, Ukai T, Igawa A, Zhang ZS, et al. (2005) Levosimendan improves LV systolic and diastolic performance at rest and during exercise after heart failure. *Am J Physiol Heart Circ Physiol* 288: H914-922.
175. Tu DN, Zou AR, Liao YH, Du YM, Wang XP, et al. (2008) Blockade of the human ether-a-go-go-related gene potassium channel by ketanserin. *Sheng Li Xue Bao* 60: 525-534.
176. Lim H, Zhu YZ (2006) Role of transforming growth factor-beta in the progression of heart failure. *Cell Mol Life Sci* 63: 2584-2596.
177. Koitabashi N, Danner T, Zaiman AL, Pinto YM, Rowell J, et al. (2011) Pivotal role of cardiomyocyte TGF-beta signaling in the murine pathological response to sustained pressure overload. *J Clin Invest* 121: 2301-2312.
178. Teekakirikul P, Eminaga S, Toka O, Alcalai R, Wang L, et al. (2010) Cardiac fibrosis in mice with hypertrophic cardiomyopathy is mediated by non-myocyte proliferation and requires Tgf-beta. *J Clin Invest* 120: 3520-3529.
179. Meyer A, Wang W, Qu J, Croft L, Degen JL, et al. (2012) Platelet TGF-beta1 contributions to plasma TGF-beta1, cardiac fibrosis, and systolic dysfunction in a mouse model of pressure overload. *Blood* 119: 1064-1074.
180. Schultz Jel J, Witt SA, Glascock BJ, Nieman ML, Reiser PJ, et al. (2002) TGF-beta1 mediates the hypertrophic cardiomyocyte growth induced by angiotensin II. *J Clin Invest* 109: 787-796.

181. Dickson MC, Martin JS, Cousins FM, Kulkarni AB, Karlsson S, et al. (1995) Defective haematopoiesis and vasculogenesis in transforming growth factor-beta 1 knock out mice. *Development* 121: 1845-1854.
182. Kulkarni AB, Ward JM, Yaswen L, Mackall CL, Bauer SR, et al. (1995) Transforming growth factor-beta 1 null mice. An animal model for inflammatory disorders. *Am J Pathol* 146: 264-275.
183. Rosenkranz S, Flesch M, Amann K, Haeuseler C, Kilter H, et al. (2002) Alterations of beta-adrenergic signaling and cardiac hypertrophy in transgenic mice overexpressing TGF-beta(1). *Am J Physiol Heart Circ Physiol* 283: H1253-1262.
184. Kuwahara F, Kai H, Tokuda K, Kai M, Takeshita A, et al. (2002) Transforming growth factor-beta function blocking prevents myocardial fibrosis and diastolic dysfunction in pressure-overloaded rats. *Circulation* 106: 130-135.
185. Lucas JA, Zhang Y, Li P, Gong K, Miller AP, et al. (2010) Inhibition of transforming growth factor-beta signaling induces left ventricular dilation and dysfunction in the pressure-overloaded heart. *Am J Physiol Heart Circ Physiol* 298: H424-432.
186. Rosen H, Gonzalez-Cabrera PJ, Sanna MG, Brown S (2009) Sphingosine 1-phosphate receptor signaling. *Annu Rev Biochem* 78: 743-768.
187. Means CK, Brown JH (2009) Sphingosine-1-phosphate receptor signalling in the heart. *Cardiovasc Res* 82: 193-200.
188. Means CK, Xiao CY, Li Z, Zhang T, Omens JH, et al. (2007) Sphingosine 1-phosphate S1P2 and S1P3 receptor-mediated Akt activation protects against in vivo myocardial ischemia-reperfusion injury. *Am J Physiol Heart Circ Physiol* 292: H2944-2951.

189. Robert P, Tsui P, Laville MP, Livi GP, Sarau HM, et al. (2001) EDG1 receptor stimulation leads to cardiac hypertrophy in rat neonatal myocytes. *J Mol Cell Cardiol* 33: 1589-1606.
190. Brakch N, Dormond O, Bekri S, Golshayan D, Correvon M, et al. (2010) Evidence for a role of sphingosine-1 phosphate in cardiovascular remodelling in Fabry disease. *Eur Heart J* 31: 67-76.
191. He K, Fu Y, Zhang W, Yuan J, Li Z, et al. (2011) Single-molecule imaging revealed enhanced dimerization of transforming growth factor beta type II receptors in hypertrophic cardiomyocytes. *Biochem Biophys Res Commun* 407: 313-317.
192. von Hundelshausen P, Weber KS, Huo Y, Proudfoot AE, Nelson PJ, et al. (2001) RANTES deposition by platelets triggers monocyte arrest on inflamed and atherosclerotic endothelium. *Circulation* 103: 1772-1777.
193. Schafer A, Bauersachs J (2008) Endothelial dysfunction, impaired endogenous platelet inhibition and platelet activation in diabetes and atherosclerosis. *Curr Vasc Pharmacol* 6: 52-60.
194. Shoji T, Koyama H, Fukumoto S, Maeno T, Yokoyama H, et al. (2006) Platelet activation is associated with hypoadiponectinemia and carotid atherosclerosis. *Atherosclerosis* 188: 190-195.
195. Cyrus T, Tang LX, Rokach J, FitzGerald GA, Pratico D (2001) Lipid peroxidation and platelet activation in murine atherosclerosis. *Circulation* 104: 1940-1945.
196. Nieswandt B, Bergmeier W, Rackebrandt K, Gessner JE, Zirngibl H (2000) Identification of critical antigen-specific mechanisms in the development of immune thrombocytopenic purpura in mice. *Blood* 96: 2520-2527.

197. Mombaerts P, Iacomini J, Johnson RS, Herrup K, Tonegawa S, et al. (1992) RAG-1-deficient mice have no mature B and T lymphocytes. *Cell* 68: 869-877.
198. Hagihara M, Higuchi A, Tamura N, Ueda Y, Hirabayashi K, et al. (2004) Platelets, after exposure to a high shear stress, induce IL-10-producing, mature dendritic cells in vitro. *J Immunol* 172: 5297-5303.
199. Crozat K, Georgel P, Rutschmann S, Mann N, Du X, et al. (2006) Analysis of the MCMV resistome by ENU mutagenesis. *Mamm Genome* 17: 398-406.
200. Yang F, Dong A, Mueller P, Caicedo J, Sutton AM, et al. (2012) Coronary artery remodeling in a model of left ventricular pressure overload is influenced by platelets and inflammatory cells. *PLoS One* 7: e40196.
201. Selim S, Sunkara M, Salous AK, Leung SW, Berdyshev EV, et al. (2011) Plasma levels of sphingosine 1-phosphate are strongly correlated with haematocrit, but variably restored by red blood cell transfusions. *Clin Sci (Lond)* 121: 565-572.
202. Chatzizisis YS, Coskun AU, Jonas M, Edelman ER, Feldman CL, et al. (2007) Role of endothelial shear stress in the natural history of coronary atherosclerosis and vascular remodeling: molecular, cellular, and vascular behavior. *J Am Coll Cardiol* 49: 2379-2393.
203. Stone PH, Coskun AU, Kinlay S, Clark ME, Sonka M, et al. (2003) Effect of endothelial shear stress on the progression of coronary artery disease, vascular remodeling, and in-stent restenosis in humans: in vivo 6-month follow-up study. *Circulation* 108: 438-444.



204. Harry BL, Sanders JM, Feaver RE, Lansey M, Deem TL, et al. (2008) Endothelial cell PECAM-1 promotes atherosclerotic lesions in areas of disturbed flow in ApoE-deficient mice. *Arterioscler Thromb Vasc Biol* 28: 2003-2008.
205. Tzima E, Irani-Tehrani M, Kiosses WB, Dejana E, Schultz DA, et al. (2005) A mechanosensory complex that mediates the endothelial cell response to fluid shear stress. *Nature* 437: 426-431.
206. Chen Z, Tzima E (2009) PECAM-1 is necessary for flow-induced vascular remodeling. *Arterioscler Thromb Vasc Biol* 29: 1067-1073.
207. Liu Y, Sweet DT, Irani-Tehrani M, Maeda N, Tzima E (2008) Shc coordinates signals from intercellular junctions and integrins to regulate flow-induced inflammation. *J Cell Biol* 182: 185-196.
208. Goel R, Schrank BR, Arora S, Boylan B, Fleming B, et al. (2008) Site-specific effects of PECAM-1 on atherosclerosis in LDL receptor-deficient mice. *Arterioscler Thromb Vasc Biol* 28: 1996-2002.
209. Deussen A, Ohanyan V, Jannasch A, Yin L, Chilian W (2012) Mechanisms of metabolic coronary flow regulation. *J Mol Cell Cardiol* 52: 794-801.
210. Beyer AM, Gutterman DD (2012) Regulation of the human coronary microcirculation. *J Mol Cell Cardiol* 52: 814-821.
211. Duncker DJ, Bache RJ, Merkus D (2012) Regulation of coronary resistance vessel tone in response to exercise. *J Mol Cell Cardiol* 52: 802-813.
212. Li J, Zhang H, Zhang C (2012) Role of inflammation in the regulation of coronary blood flow in ischemia and reperfusion: mechanisms and therapeutic implications. *J Mol Cell Cardiol* 52: 865-872.

213. Elzey BD, Sprague DL, Ratliff TL (2005) The emerging role of platelets in adaptive immunity. *Cell Immunol* 238: 1-9.
214. Wang Y, Niu J (2008) Platelets inhibit in vitro response of lymphocytes to mitogens. *Immunol Lett* 119: 57-61.
215. Cheng X, Liao YH, Ge H, Li B, Zhang J, et al. (2005) TH1/TH2 functional imbalance after acute myocardial infarction: coronary arterial inflammation or myocardial inflammation. *J Clin Immunol* 25: 246-253.
216. Schottelius AJ, Mayo MW, Sartor RB, Baldwin AS, Jr. (1999) Interleukin-10 signaling blocks inhibitor of kappaB kinase activity and nuclear factor kappaB DNA binding. *J Biol Chem* 274: 31868-31874.
217. Mazighi M, Pelle A, Gonzalez W, Mtairag el M, Philippe M, et al. (2004) IL-10 inhibits vascular smooth muscle cell activation in vitro and in vivo. *Am J Physiol Heart Circ Physiol* 287: H866-871.
218. Selzman CH, Meldrum DR, Cain BS, Meng X, Shames BD, et al. (1998) Interleukin-10 inhibits postinjury tumor necrosis factor-mediated human vascular smooth muscle proliferation. *J Surg Res* 80: 352-356.
219. Krishnamurthy P, Rajasingh J, Lambers E, Qin G, Losordo DW, et al. (2009) IL-10 inhibits inflammation and attenuates left ventricular remodeling after myocardial infarction via activation of STAT3 and suppression of HuR. *Circ Res* 104: e9-18.
220. Burchfield JS, Iwasaki M, Koyanagi M, Urbich C, Rosenthal N, et al. (2008) Interleukin-10 from transplanted bone marrow mononuclear cells contributes to cardiac protection after myocardial infarction. *Circ Res* 103: 203-211.

221. Hardt SE, Sadoshima J (2004) Negative regulators of cardiac hypertrophy. *Cardiovasc Res* 63: 500-509.
222. Yamamoto M, Yang G, Hong C, Liu J, Holle E, et al. (2003) Inhibition of endogenous thioredoxin in the heart increases oxidative stress and cardiac hypertrophy. *J Clin Invest* 112: 1395-1406.
223. Johnston GI, Pickett EB, McEver RP, George JN (1987) Heterogeneity of platelet secretion in response to thrombin demonstrated by fluorescence flow cytometry. *Blood* 69: 1401-1403.
224. Depre C, Shipley GL, Chen W, Han Q, Doenst T, et al. (1998) Unloaded heart in vivo replicates fetal gene expression of cardiac hypertrophy. *Nat Med* 4: 1269-1275.

## VITA

Fanmuyi Yang

### Date of Birth

04/05/1984, Huainan, Anhui Province, China

### Education

Bachelor of Science in Biotechnology

Biology Department of Xiamen University (XMU),

Xiamen, Fujian, China (07/2006)

### Publications

Panchatcharam M, Miriyala S, **Yang F**, Rojas M, End C, Vallant C, Dong A, Lynch K, Chun J, Morris AJ, Smyth SS. Lysophosphatidic acid receptors 1 and 2 play roles in regulation of vascular injury responses but not blood pressure. *Circulation Research* 2008

Barrick CJ, Dong A, Waikel R, Corn D, **Yang F**, Threadgill DW, Smyth SS. Parent-of-origin effects on cardiac response to pressure overload in mice. *Am J Physiol Heart Circ Physiol* 2009

Panchatcharam M, Miriyala S, **Yang F**, Leitges M, Chrzanowska-Wodnicka M, Quilliam LA, Anaya P, Morris AJ, Smyth SS. Enhanced proliferation and migration of vascular smooth muscle cells in response to vascular injury under hyperglycemic conditions is controlled by beta3 integrin signaling. *Int J Biochem Cell Biol* 2010

Li Z, **Yang F**, Dunn S, Gross AK, Smyth SS. Platelets as immune mediators: Their role in host defense responses and sepsis. *Thromb Res* 2011

Cheng HY, Dong A, Panchatcharam M, Mueller P, **Yang F**, Li Z, Mills G, Chun J, Morris AJ, Smyth SS. Lysophosphatidic acid signaling protects pulmonary vasculature from hypoxia-induced remodeling. *Arterioscler Thromb Vasc Biol* 2012

**Yang F**, Dong A, Mueller P, Caicedo J, Moore A, Odetunde J, Barrick CJ, Smyth SS. Coronary artery remodeling in a model of left ventricular pressure overload is influenced by platelets and inflammatory cells. *PLoS ONE* 2012

### Attended National and International Meetings

Arteriosclerosis, Thrombosis and Vascular Biology Conference 2008. Atlanta, GA, USA

Mid-West Platelet Conference 2008. Lexington, KY, USA, *poster presentation*

Arteriosclerosis, Thrombosis and Vascular Biology Conference 2009. Washington, DC, USA, *poster presentation*

Mid-West Platelet Conference 2010. Chapel Hill, NC, USA, *poster presentation*

Arteriosclerosis, Thrombosis and Vascular Biology Conference 2011. Washington, DC, USA, *poster presentation*

Arteriosclerosis, Thrombosis and Vascular Biology Conference 2012. Washington, DC, USA, *poster presentation*

Vasculata 2012. Nashville, TN, USA, *poster presentation*

Mid-West Platelet Conference 2012. Cleveland, OH, USA, *poster presentation*

### **Honors and Awards**

XMU Fellowship-First Prize (2002-2003)

XMU Fellowship-Third Prize (2003-2004)

UK Travel Award (2011)

American Heart Association Pre-Doctoral Fellowship – “The Role of Platelets in Early Pericoronary Inflammation Induced by Transverse Aortic Constriction (TAC)” (2011-2012)

UK Travel Award (2012)

Vasculata Travel Award (2012)

### **Funding**

American Heart Association Pre-Doctoral Fellowship – “The Role of Platelets in Early Pericoronary Inflammation Induced by Transverse Aortic Constriction (TAC)” (2011-2012)